LuftBlick Report 2016011

ESA Ground-Based Air-Quality Spectrometer Validation Network and Uncertainties Study

Validation Reports

	Name	Company	Date
prepared by	Moritz Müller	LuftBlick	15 Jan 2017
	Martin Tiefengraber	LuftBlick	15 Jan 2017
	Alexander Cede	LuftBlick	15 Jan 2017
checked by	Katherine Cede	LuftBlick	15 Jan 2017
approved by			

Contents

Document Change Record

Issue	Date	Section	Observations
0.1	4 Jul 2016	All	First draft version
1.0	13 Jul 2016	All	Minor addenda.
1.1	19 Aug 2016	1 (p.5), 2 (p.7), 2.1.4 (p.10), 2.2.5 (p.18), 2.3 (p.21), 3.1 (p.22), 3.2.1 (p.23), 3.2.2 (p.23), 3.3 (p.25), 4.2 (p.114)	Minor addenda, typo corrections, clarifications. All in response to ESA comments.
2.0	15 Jan 2017	1 (p.5), 2 (p.7), 2.2.5 (p.18), 2.3 (p.21), 3.2 (p.22)	Satellite data set OMINO2 v2.1 is replaced by v3.0 and compared. Extended description of the climatological correction and the footprint correction method.

Acronyms and Abbreviations

AVDC	Aura Validation Data Center
CC	Correlation coefficient
ClimCor	Climatological footprint correction
CTP	Cross track position
DNO_2R	Approximated diurnal range of $TotNO_2$
dLAT	Latitudinal distance of the footprint center to Pandora.
dLON	Longitudinal distance of the footprint center to Pandora.
DQ0	Pandora High Quality Data
EffLoc	Effective validation location
GeoFilt	OMI pixel geolocation filters
GSFC	Goddard Space Flight Center
MEDD	Median difference = medianTotGAS(OMI - Pandora)
MKT	Mann-Kendall test
NASA	National Aeronautics and Space Administration
OMI	Ozone monitoring instrument
PanAVG	Pandora data averaging time around the OMI overpass time.
Pandonia	ESA Ground-Based Air-Quality Spectrometer Validation Network
RMS	Root mean square error to a linear fit
SatCF	Satellite footprint cloud fraction
SatFPT	Satellite footprint size
SatUncNO2	Uncertainty in $TotNO_2$ for OMI
SLP	Slope of linear fit Pandora vs. OMI
SZA	Solar Zenith Angle
TempO3	Effective ozone temperature
TotNO2	Total column nitrogen dioxide
TotO3	Total column ozone
ValPars	Validation parameters
ValSite	Validation site
VZA	Viewing zenith angle

1 Introduction

This report is version 2 of the deliverable D19 of the Pandonia project [2, 1]. The Pandonia network is being established in order to validate satellite trace gas retrievals with ground based remote sensing measurements. In this report we use total column ozone (TotO3) and total column nitrogen dioxide (TotNO2) from the entire Pandora database to validate retrievals from the ozone monitoring instrument (OMI). We used OMI data since they are the closest match to the specifications of the future Sentinel-5p mission.

The major difference to the version 1 of this deliverable D19 [13] is the change in the OMINO2 data version. Namely from OMNO2 v2.1 to OMNO2 v3.0 [8]. The data version for OMTO3 is the same as for version 1 of this report, but the time series for some incomplete stations have been rectified. Further, we outline our latest advances in terms of enhancing the representativeness of satellite versus ground-based data sets.

The outcome of this study and the conclusions we draw from it are condensed in section 2 with details about O_3 validation in section 2.1 and NO_2 validation in section 2.2. In this section the entire data base as an ensemble is emphasized. Section 2.2 is extended by a comparison between the two OMINO2 data versions. The underlying data sets and the validation sites considered are described in section 3.1. In section 3.2 we feature two already applied methods and one planned method to reduce the effects of the different viewing geometries from ground-based (direct sun) and satellite (near nadir) observations. A sensitivity study on data filter parameters is further outlined in 3.3. The detailed validation results for each station are finally presented in section 4, where both scatter plots with statistics (section 4.1) and long term stability estimations (section 4.2) for selected stations are presented.

1.1 Applicable Documents

[1] Ground-Based Air-Quality Spectrometer Validation Network and Uncertainties Study [Proposal], LuftBlick Proposal 201309A, Issue 2, 2013.

[2] ESA Ground-Based Air-Quality Spectrometer Validation Network and Uncertainties Study [Statement of Work], ENVI-SPPA-EOPG-SW-13-0003, Issue 1, Revision 3, 2013.

[3] A. Cede. *Manual for Blick Software Suite Version 5*, 2016. URL `http://pandonia.net/docs/manuals_reports_notes/BlickSoftwareSuite_Manual_v5.pdf`.

1.2 Reference Documents

[4] G. Bernhard, R. D. Evans, G. J. Labow, and S. J. Oltmans. Bias in Dobson total ozone measurements at high latitudes due to approximations in calculations of ozone absorption coefficients and air mass. *Journal of Geophysical Research: Atmospheres*, 110(D10), 2005.

[5] A. Cede, M. Tiefengraber, and A. Redondas. ESA Ground-Based Air-Quality Spectrometer Validation Network and Uncertainties Study, LuftBlick Report 2014001: Network Intercalibration Procedure, 2014.

[6] J. D. Cryer and Kung-Sik Chan. *Time series analysis with applications in R*. Springer, 2008.

[7] Richard O. Gilbert. *Statistical methods for environmental pollution monitoring*. John Wiley & Sons, 1987.

[8] S. Marchenko, N. A. Krotkov, L. N. Lamsal, E. A. Celarier, W. H. Swartz, and E. J. Bucsela. Revising the slant column density retrieval of nitrogen dioxide observed by the ozone monitoring instrument. *Journal of Geophysical Research: Atmospheres*, 120(11):5670–5692, 2015. ISSN 2169-8996. doi: 10.1002/2014JD022913. URL `http://dx.doi.org/10.1002/2014JD022913`. 2014JD022913.

[9] OMI Team. *Ozone Monitoring Intrument (OMI) - Data User´s Guide*. NASA. URL `https://disc.gsfc.nasa.gov/Aura/data-holdings/additional/documentation/README.OMI_DUG.pdf`.

[10] M. Tiefengraber and A. Cede. Inter-calibration of ground-based spectrometers and Lidars – Minispectrometer Intercalibration and Satellite Validation, LuftBlick Report 2013004: Minispectrometer Data Quality Report, 2013.

[11] M. Tiefengraber and A. Cede. OMI validation support, LuftBlick Report 2015003: List of Pandoras to be considered for OMI validation, 2015.

[12] M. Tiefengraber and M. Müller. OMI validation support, LuftBlick Report 2015010: Pandora validation data, 2015.

[13] Müller M. Tiefengraber, M. and A. Cede. ESA Ground-Based Air-Quality Spectrometer Validation Network and Uncertainties Study, LuftBlick Report 2016011: Validation reports, 2016.

[14] S. Vandenbussche, C. De Clercq, and J.-C. Lambert. EC FP6 GEOmon Technical note D4.2.1 – Multi-dimensional characterisation of remotely sensed data – Chapter 3: Satellite measurements of nadir-scattered ultraviolet-visible light. Technical report, BIRA-IASB, 8 2009. GEOmon TN-IASBOBSOP/Chapter 3.

2 Summary and Conclusion

This report presents the validation results of the OMTO3 product version 8.5 and OMNO2 product version 3.0 to the ground-based, direct-sun retrievals of Pandora (v002). The validation period covers a maximum time range of about 6 years (2009 to 2015) and considers a maximum possible number of 81 validation sites (ValSite). For convenience we refer to the short names of the ValSites throughout this entire document. For "translation", please look up *Tiefengraber and Cede* [11].
We chose a set of parameters where the validation quality is assessed on (ValPars). These are:

Validation parameter	**Abbreviation**
Correlation coefficient between OMI and Pandora data	CC
Root mean square error to a linear fit for Pandora vs. OMI data	RMS
Slope of a linear fit in Pandora vs. OMI	SLP
Median difference (= medianTotGAS(OMI - Pandora)) between OMI and Pandora data	MEDD

Table 1: Validation parameters used in this study to assess the validation quality.

CC (in relative units) and RMS (in absolute units) give us an estimate about the linear correlation or "scattering" between OMI and Pandora data points. Beside the common SLP parameter, MEDD tangibly expresses the disagreement between both data sets.

To ensure that only data of high quality are included in the validation study, data filtering is utilized (details see section 3.3). For Pandora we allowed only data passing the highest quality criteria. A sensitivity study is carried out to assess the impact of selected filter parameter thresholds on OMI pixels. By this means we tested the impact of the pixel location and size (geolocation filters, GeoFilt) as well as the cloud fraction, and in the case of TotNO2, the OMI retrieval uncertainty on the ValPars in Table 1. Additionally, favorable Pandora data averaging time around the OMI overpass time is deduced.

Beside the data filtering two further correction steps are tested on the data. For Pandora the physical validation location (= geolocation) of the instruments are shifted to take into account the effective absorber height of O_3 and NO_2, respectively, for direct-sun data (details see section 3.2.1). We denote this adapted location effective validation location (EffLoc). OMI pixels are further corrected based on a high resolution, time averaged climatological footprint map (ClimCor) of TotO3 and TotNO2 (details see section 3.2.2). By this means the varying position of the footprint pixels for different overpasses are taken into account and help to mitigate the errors introduced when significant gradients of TotGAS are seen across a OMI pixel.

An other option would be to use this type of information as an additional filter criteria, for example not including all pixels where ClimCor exceeds a certain threshold. Nevertheless we have chosen to not apply further filter ot the data, because most of our time series are rather short and we prefer to conserve as many data points as possible.

Since we assume EffLoc, ClimCor and GeoFilt to have a particular influence on the validation outcome, they are considered in the results in terms of combined scenarios like

- **E1 or E0** means EffLoc considered or not, and
- **C1 or C0** means ClimCor applied or not, and
- **G1 or G0** means GeoFilt applied or not.

To further get an idea about the long term stability of TotO3 and TotNO2 retrieved from the ground-based instrument, time series of the difference to OMI TotO3 and TotNO2 are studied and statistically analyzed (we avoid "trend" analysis to not tempt to think in terms of O_3 or NO_2 trends.).

2.1 O_3 Validation

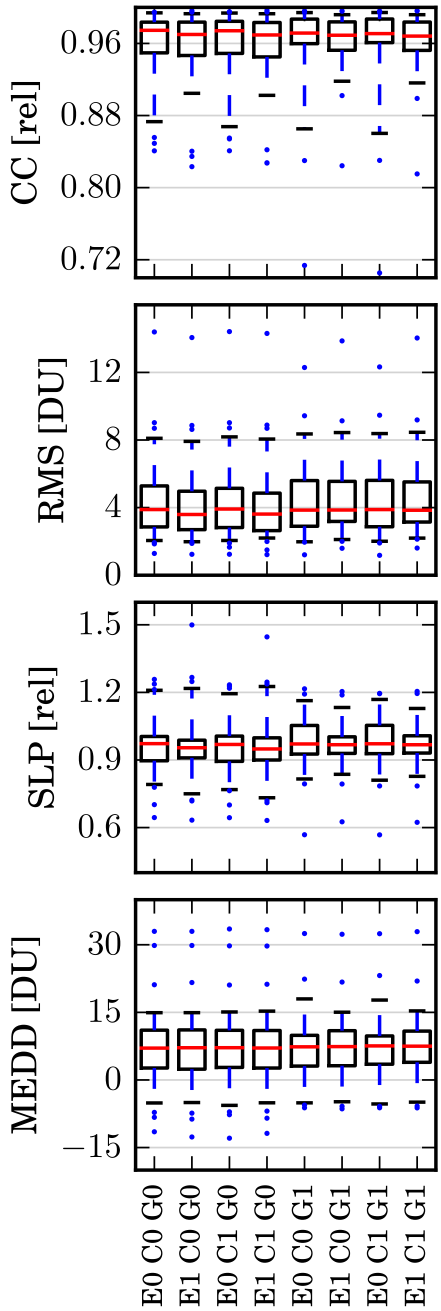

Figure 1: Network validation results for TotO3. The validation parameters for different validation scenarios are shown for the entire network as an ensemble. Applied (not applied) EffLoc is indicated by E1(0), applied (not applied) ClimCor is indicated by C1(0) and applied (not applied) GeoFilt is indicated with G1(0). The box plots depict the median values by a the red bar and the 25 to 75 percentiles are embraced by the black box. The 5 to 95 percentiles are marked by the black bars. Values outside this range are given as blue dots.

2.1.1 Data Filter Thresholds

The sensitivity study for TotO3 validation suggests to include only OMI pixels with cloud fractions < 0.1 and also emphasizes to average Pandora data $\pm$ 90 minutes around the OMI overpass time. Applying cloud fraction filtering to OMI data and filtering Pandora data reduce the number of available ValSites from 81 to 57. The sensitivity study reveals also a significant improvement in the validation quality when applying GeoFilt to the OMI pixels. Since this strongly drops the number of data points, the available number of ValSites reduces to

41. This emphasizes the necessity of long, continuous time series of ground based validation data.

2.1.2 Network Validation

The TotO3 validation assessment is condensed in Figure 1 featuring the entire data set as an ensemble. All ValSites are included in each box plot and are analyzed for all ValPars for different scenarios. The median value of each ValPar is depicted as red bar, the black box comprises the 25 to 75 percentile range and the black bars define the 5 to 95 percentile range. The blue dots indicate ValSites lying outside this range.

The differences between the individual scenarios for the ValPars is not very pronounced, however we can still reveal three findings: First, applying GeoFilt reduces the number of outliers in the ValPars between all ValSites. Second, utilizing EffLoc instead of the physical Pandora location further narrows the spread in the ValPars between all ValSites. Especially high latitude ValSites during mid latitude winter experience the mismatch between EffLoc and the physical position. Third, whether ClimCor is applied or not does not have any significant impact on the validation outcome. This seems reasonably, since usually no strong TotO3 gradients are expected across an OMI pixel.

To quantify the final validation result for TotO3, we utilize the scenario yielding the best overall validation quality (compare Figure 1). This is scenario E1 C0 G1, meaning applied EffLoc and GeoFilt but no ClimCor. The 25, 50 and 75 percentile values for the ValPars are given in Table 2.

ValPar	**Value: 25 perc | 50 perc | 75 perc**
CC	0.95 | 0.97 | 0.98
RMS [DU]	3.18 | 3.86 | 5.55
SLP	0.93 | 0.97 | 1.00
MEDD [DU]	3.16 | 7.40 | 10.93

Table 2: ValPars for validation scenario E1 C0 G1. Shown are the 25, 50 and 75 percentiles.

High CC can be expected for TotO3 validation. 75 percent of all ValSites show a better CC than 0.95. Expressed in an absolute number, the median RMS is near 4 DU. The vast majority of the data show SLP < 1, which would imply an underestimation of the OMI TotO3 data compared to Pandora. However, since different seasons show different SLP values (as mentioned before) and we have included all kind of time periods, we can not extract a conclusion from that.

Rather surprisingly though, MEDD is positive with a median value of about 7 DU. This would suggest Pandora underestimating TotO3 compared to OMI. This difference could be attributed to the type of cross sections used, difference in the wavelength range, or the specific way Pandora instruments are calibrated, where the spectral sensitivity is not included at this moment and also no elaborated spectral stray light correction is applied. When looking at the data on a seasonal basis, also the impact of assuming a constant TempO3 in the Pandora TotO3 retrieval (more in the next section) is seen. This is summarized in Table, 3, where the median value for each ValPar is given for all seasons (WI=winter, SP=spring, SU=summer, AU=autumn). The seasonal difference is clearly demonstrated by MEDD, showing SP and AU to be approximately equal, while WI (SU) TotO3 shows a negative (positive) bias.

ValPar	**WI**	**SP**	**SU**	**AU**
CC	0.98	0.97	0.95	0.96
RMS [DU]	4.82	4.86	3.53	3.39
SLP	0.97	0.95	0.90	1.00
MEDD [DU]	-2.55	5.95	9.12	6.46

Table 3: Seasonal median for ValPars for validation scenario E0 C0 G0 (that is no correction and geolocation filtering is applied).

2.1.3 Station Validation

The results for each ValSite separately are shown in Figure 2 (3) for data with no (with) GeoFilt applied. The different scenarios, the same abbreviations as in Figure 1 are used, are now depicted as horizontal bar (circle) for C1 (0) and color coded in green (red) for E1 (0). The larger impact of EffLoc on the ValPars compared to ClimCor is also visible in these figures, since the "colors" deviate more than the "symbols".

The major driver for the differences in the ValPars for the individual location is the influence on the effective O_3 temperature (TempO3). Whereas both systems, OMI and Pandora, are sensitive to TempO3, it is taken into account for the OMI retrieval but not for Pandora. The Pandora standard TotO3 retrieval assumes a constant TempO3 of 225 K. This value is a compromise in latitude and season. Thus largest deviations are expected in winter and summer for high and low latitudes (this is clearly visible from the time series shown in section 4.2). This temperature error is a constant relative error in the slant columns meaning a not constant error in the vertical columns (= TotO3). This leads to a seasonal bias and change in the slope for TotO3 comparison. Hence we see the strongest effect in mid latitude summer (winter) with a common underestimation (overestimation) for Pandora and slopes > (<) 1.

This effect has two major implications for TotO3 validation. First if a data set at a ValSite spans at least a year, that is it includes all seasons, an enhanced RMS can be observed. But since the different seasons counteract, small MEDD and a SLP close to 1 is observed. Examples beside others are Busan (South Kora), GSFC (MD, USA) or Seoul (South Korea), all shown in section 4.1. Second if a data set at a ValSite only covers a shorter time period, e.g. only one season, it depends on the season in which "direction" the comparison is biased or tilted (in terms of MEDD and SLP). Examples for this seasonal effect are beside others Lauder (New Zealand), Baengnyeongdo (South Korea) and Golden (TX, USA) for summer differences and Hanford (CA, USA), Parlier (CA, USA) and Madera (CA, USA) for winter differences (again shown in section 4.1).

ValSites like Doi Ang Khang in Thailand, Galveston, TX or RockyFlasts, CO both in the USA benefit in particular from utilizing EffLoc. The improvement is even stronger, when GeoFilt is applied to the data.

2.1.4 Stability

How do we know that the Pandora data are stable over time? Most of the Pandora instruments are calibration once ore twice, since the network calibration strategy proposed for Pandonia has not been implemented yet. Therefore we can not be sure about the stability of the Pandora instruments. Changes in the instrument calibration can be a smooth function of time (e.g. the aging of the filter) or a sudden change (e.g. caused by transportation). The latter can possibly be detected by analyzing the time series with respect to break points (for break point analysis methods see e.g. *Cryer and Chan* [6]). Methods for an automated detection for such events exist, but we have not implemented any of them yet. In some situations they can be even detected by eye, like in IZO. Therefore in this report we use the deseasonalized difference in the time series of OMI minus Pandora as a stability criteria (see section 4.2.1). Obviously a "trend" in the difference can be attributed to either the satellite or the ground instrument. This means that this section of the report is not satellite validation in a strict sense.

A rather surprising observation is the almost missing seasonality in TotO3 for Seoul, South Korea. We do not have an explanation for that yet.

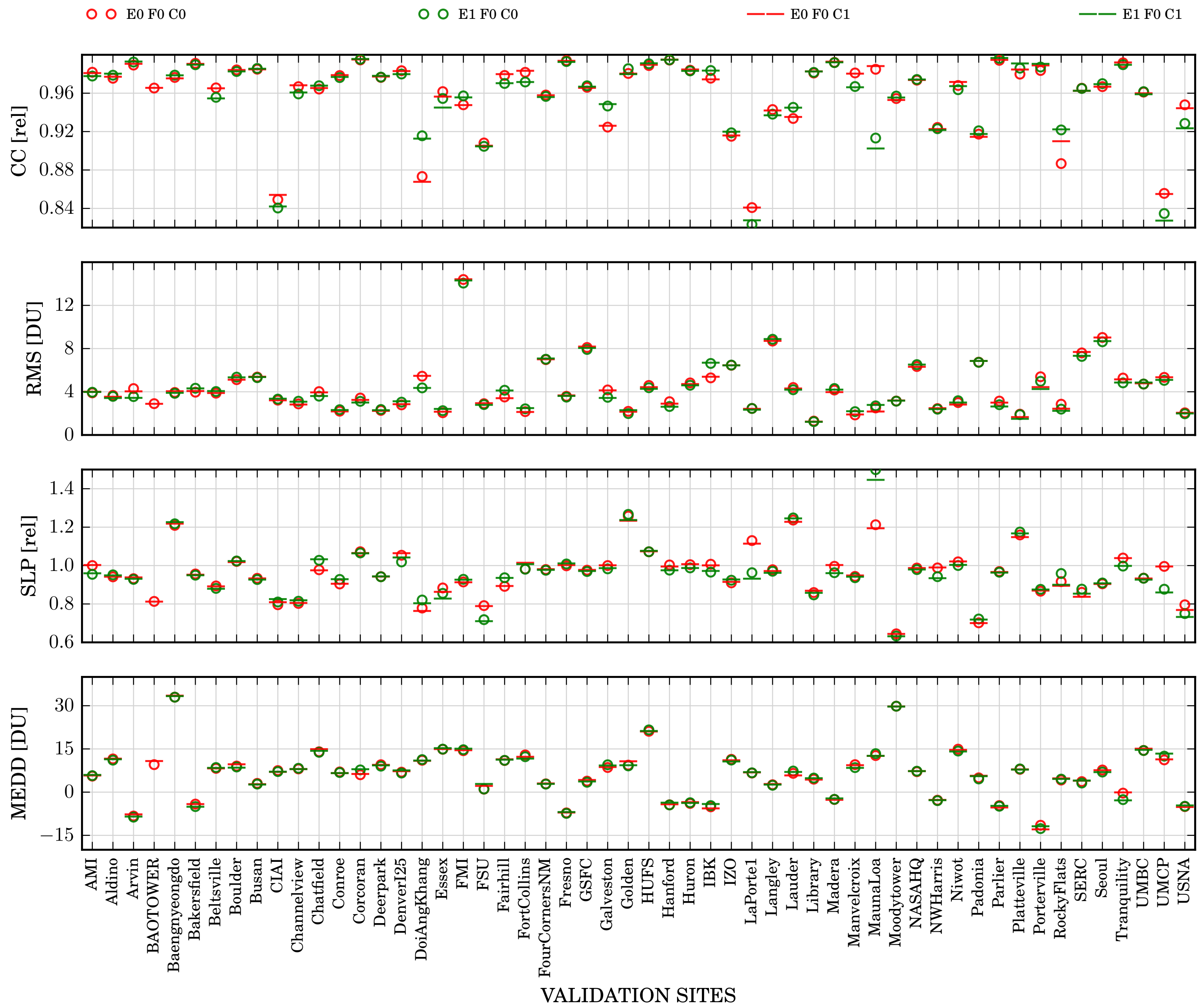

Figure 2: Specific network validation results for TotO3 without GeoFilt applied. The validation parameters listed in Table 1 are shown for different validation scenarios for all validation sites. Applied (not applied) EffLoc is indicated by green (red) colors and applied (not applied) ClimCor is indicated by bars (circles).

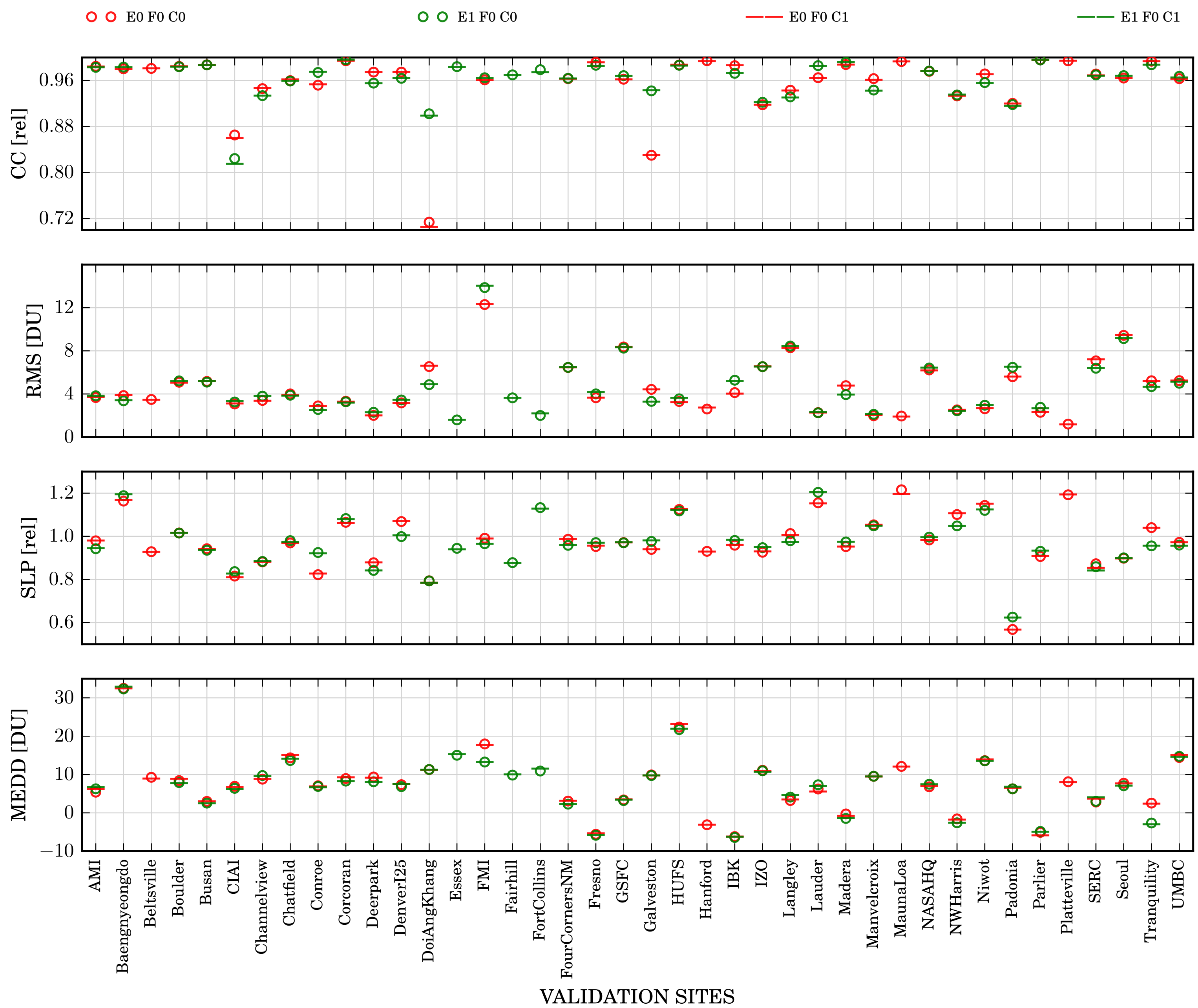

Figure 3: Specific network validation results for TotO3 with applied GeoFilt. Explanation like in Figure 2.

2.2 NO_2 Validation

2.2.1 NO_2 data version comparison

In version 1 of this report we have exploited the OMINO2 v2.1 data set. In this report, the new data set OMINO2 v3.0 (released in September 2016), forms the baseline for the NO_2 satellite validation. As a preliminary point, we want to compare both data versions by contrasting the validation parameters listed in Table 1. Figure 4 shows the parameters for the network as ensemble, Figure 5 for the individual ValSites.

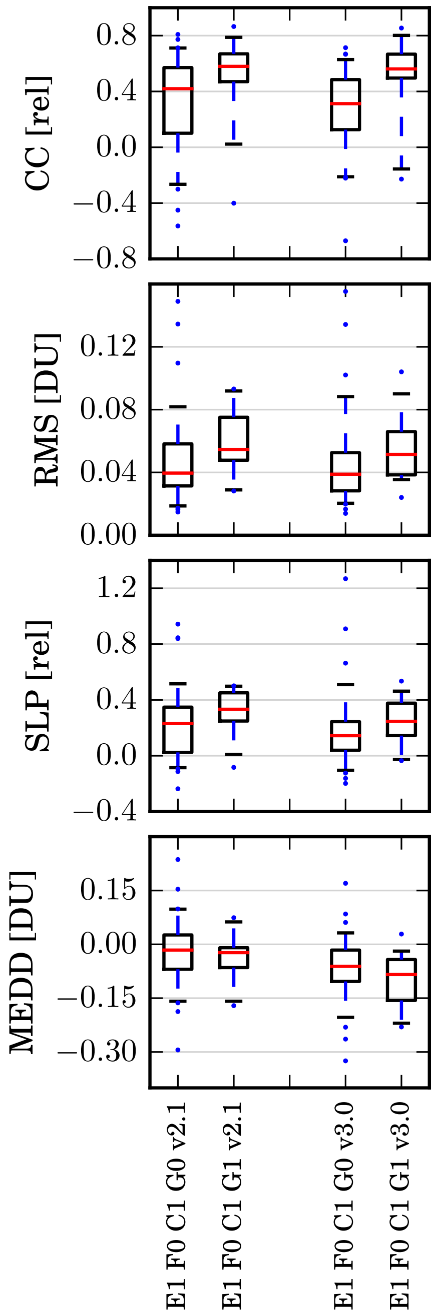

Figure 4: Network validation results for TotNO2 when comparing to OMINO2 v2.1 (the two box-plots on the left) and OMINO2 v3.0 (the two box-plots on the right). The validation parameters for two validation scenarios are shown: EffLoc and ClimCor is for all applied for all scenarios, and GeoFilt is (not) applied for the right (left) plot of each pair. The box plot description is as given in Figure 1.

All validation parameters except the RMS perform distinguishable worse with the OMINO2 v3.0 data set compared to the OMINO2 v2.1 version, in particular MEDD and SLP. The deterioration is more pronounced when no GeoFilt is applied, except for MEDD, where it is the other way around. As far as we know, it is the first time that OMINO2 v3.0 is part of an validation study against direct sun ground data.

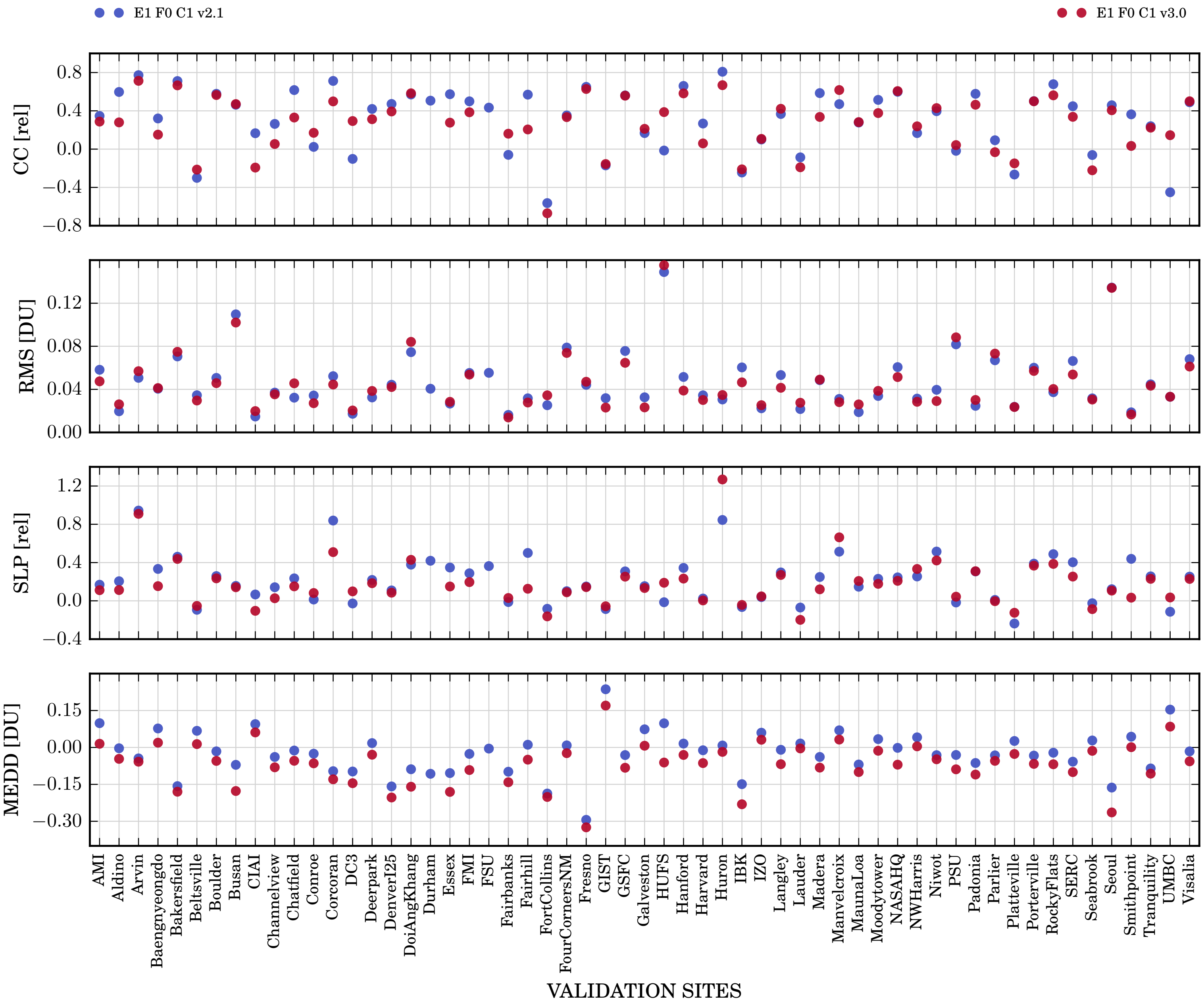

Figure 5: Specific network validation results validation results for TotNO2 (without GeoFilt) from the comparison to OMINO2 v2.1 (in blue) and OMINO2 v.3.0 (in red). The same scenario is shown as in Figure 4 (with GeoFilt applied).

2.2.2 Data Filtering Thresholds

The sensitivity study for TotNO2 validation suggests to omit OMI data showing cloud fractions > 0.1 and $TotNO_2$ uncertainties > 0.1 DU. Pandora data, averaged $\pm$ 15 min. around the OMI overpass time, turned out to be the best choice for TotNO2 validation. Further, applied GeoFilt strongly improves the validation quality but also strongly reduces the number of available ValSites from 58 to 14 locations. This again emphasizes the necessity of long, continuous time series of ground based validation data.

2.2.3 Network Validation

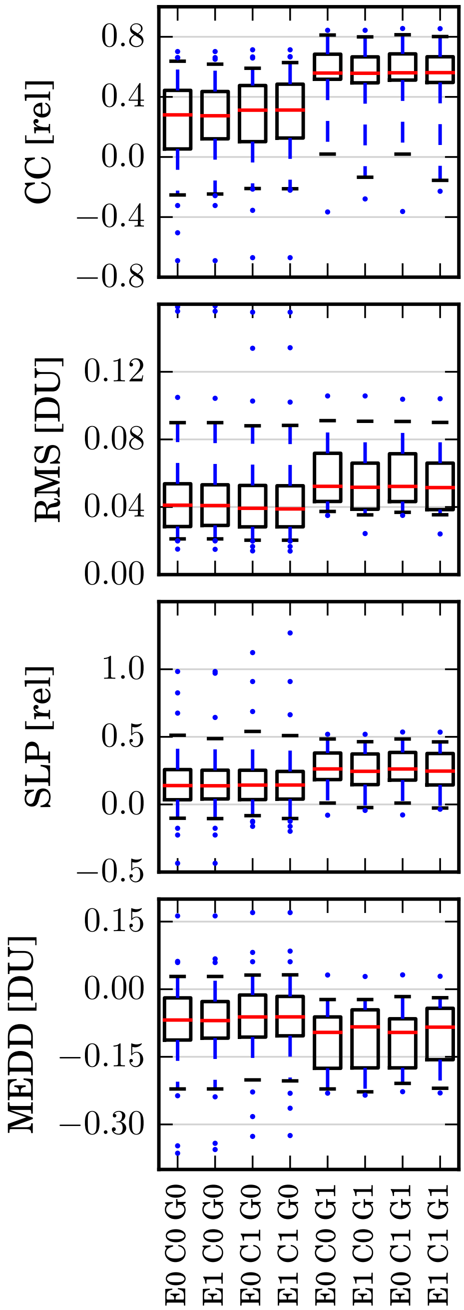

Figure 6: Network validation results for TotNO2. Explanation like in Figure 1.

The TotNO2 validation assessment condensed in Figure 6 comprises again the entire data base as an ensemble. Explanations the figures are like in section 2.1.2. We can highlight three observations. First, applying GeoFilt significantly improves all ValPars except RMS. The data population is much denser and the median values are clearly improved. The reason that RMS is getting worse could be that the majority of the ValSites are short time series, mainly showing smaller RMS. Applying GeoFilt excludes shorter time series, which makes the RMS larger on average. The second observation is that ClimCor clearly improves all ValPars when GeoFilt is not applied, but has a diminishing effect when GeoFilt is applied. This makes sense since both applying ClimCor and GeoFilt reduce the influence on varying positions of the overpass pixels. The third observation confirms the assumption that EffLoc has a minor impact on TotNO2 validation due to the low effective height of NO_2 in the atmosphere.

To quantify the final validation result for TotNO2, we utilize the scenario yielding the best overall validation quality (compare Figure 6). This is scenario E1 C1 G1, meaning applied EffLoc, ClimCor and GeoFilt. The 25, 50 and 75 percentile values for the ValPars are given in Table 4.

ValPar	Value: 25 perc | 50 perc | 75 perc
CC	0.50 | 0.56 | 0.67
RMS [DU]	0.04 | 0.05 | 0.07
SLP	0.15 | 0.25 | 0.38
MEDD [DU]	-0.16 | -0.08 | -0.04

Table 4: ValPars for validation scenario E1 C0 G1. Shown are the 25, 50 and 75 percentiles.

The CC is as expected clearly below the CC for TotO3, but thanks to ClimCor and/or GeoFilt still quite good with roughly 0.6. Expressed in an absolute number, the median RMS is near 0.05 DU.

We state that outliers are often associated with restricted NO_2 plumes penetrated by the direct-sun beam, but underestimated due to the size of an OMI footprint pixel. This would force the slope of a linear fit (SLP) to be clearly below unity, as is indeed seen here with a value of about 0.3. The vast majority of the outliers could be identified by taking into account the approximated diurnal range of TotNO_2 (DNO_2R) (see scatter plots in section 4.1)). It is estimated by the difference of the highest to the lowest value measured by the Pandora in the time range $\pm$ 4 hours of the OMI overpass time. A further consequence is a negative MEDD. In version 1 of this report MEDD was rather small with -0.02. The new satellite data version exploited here moves MEDD further to -0.08 (50 perc). Similar for SLP, which used to be 0.33 (50 perc) for the former satellite data set.

2.2.4 Station Validation

The results for each ValSite separately are shown in Figure 7 (8) for data with no (with) GeoFilt applied. All explanations to the figures are like in section 2.1.3.

Basically we can partition the ValSites without GeoFilt into 3 groups: Group 1 comprises about 10 % of the ValSites and show extraordinary good CC ($\approx$ 0.8) with SLPs up to 1.0. This very good agreement for OMI and Pandora may be also a consequence of the comparably low DNO_2R. These locations are e.g. Arvin, Bakersfield and Huron, all located in CA, USA (and all are short time data collected during a campaign).

Group 2 comprises the major part of the ValSites and can be further split up into densely and sparsely populated ValSites. The main characteristic is a low SLP of $\approx$ 0.2. In both cases, an enhanced DNO_2R is expected to be the major driver. In the case of the sparsely populated ValSites this manifests however still in a relatively high CC. Examples are e.g. Fresno, CA and Denver, CO in the USA. The densely populated ValSites clearly show the low SLP driven by enhanced DNO_2R. Examples are Four corners, NM in the USA, Seoul and Busan in South Korea or FMI in Finland.

Group 3 comprises questionable ValSites showing unexpected results. This group splits further up into ValSites with probably insufficient Pandora TotNO_2 calibration and ValSites with still missing explanation. Both subgroups show negative SLP and/or positive values for MEDD. This would mean that Pandora data underestimate the OMI data. Those cases would e.g. occur when a Pandora would be next to a large city. The error due to this cases should, however, be mitigated by the ClimCor. An obvious calibration issue is given for e.g. IZO Tenerife, Spain, with Pandora values near zero (which are not to expect due to the rather constant stratospheric NO_2 background). IZO shows almost only stratospheric NO_2. An offset in the NO_2 calibration has a larger impact for low values. A representative of the second subgroup is e.g. UMBC, MA in the USA or GIST in South Korea.

In terms of ClimCor, the majority of the ValSites benefit from its application. ClimCor could significantly improve the validation quality of Smithpoint, Padonia, Niwot and in particular Seoul (highly polluted area).

2.2.5 Stability

The same stability considerations as mentioned in section 2.1.4 for TotO3 also apply for the TotNO2 validation (see section 4.2.2).

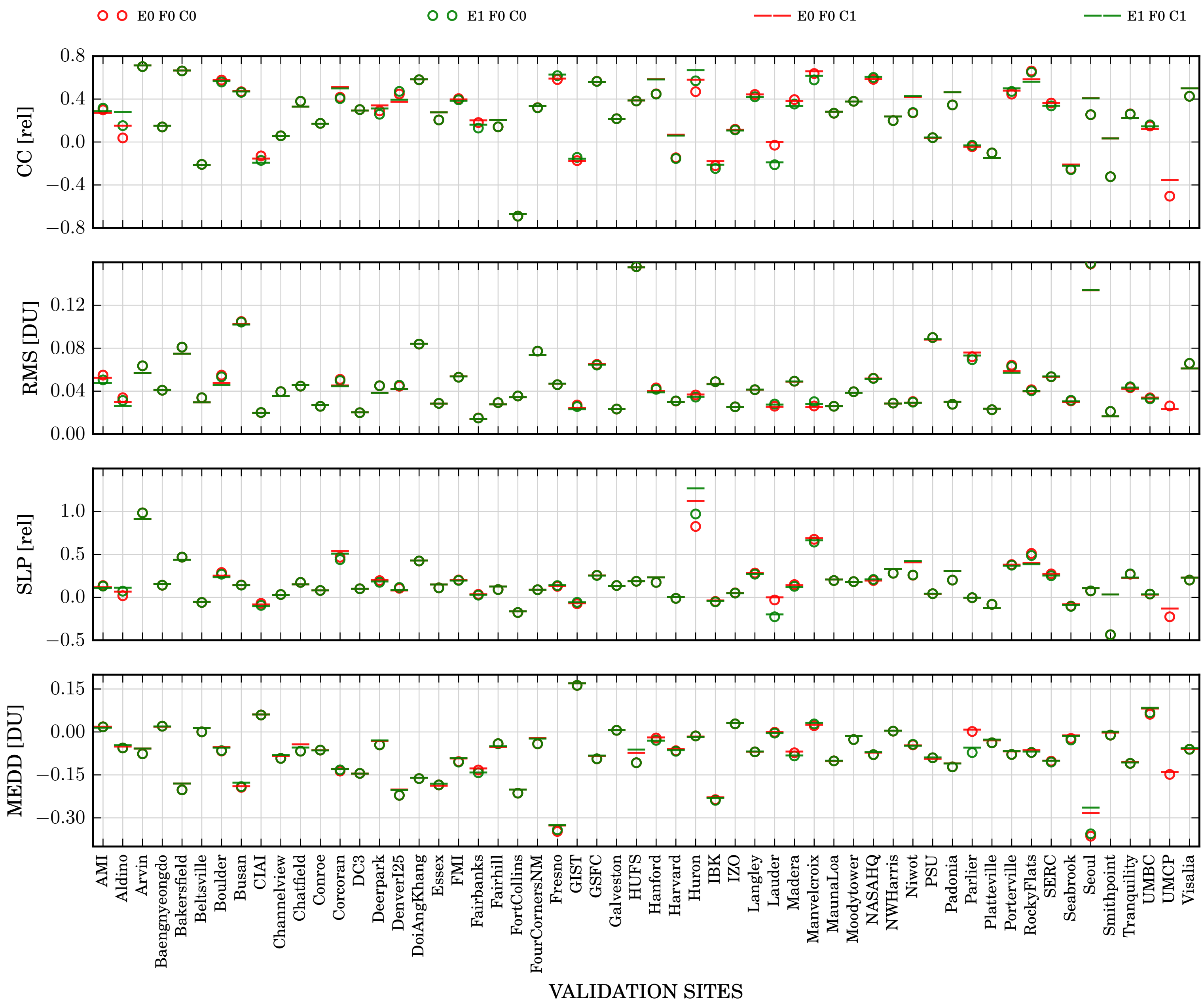

Figure 7: Specific network validation results validation results for TotNO2 without GeoFilt applied. Explanation like in Figure 2.

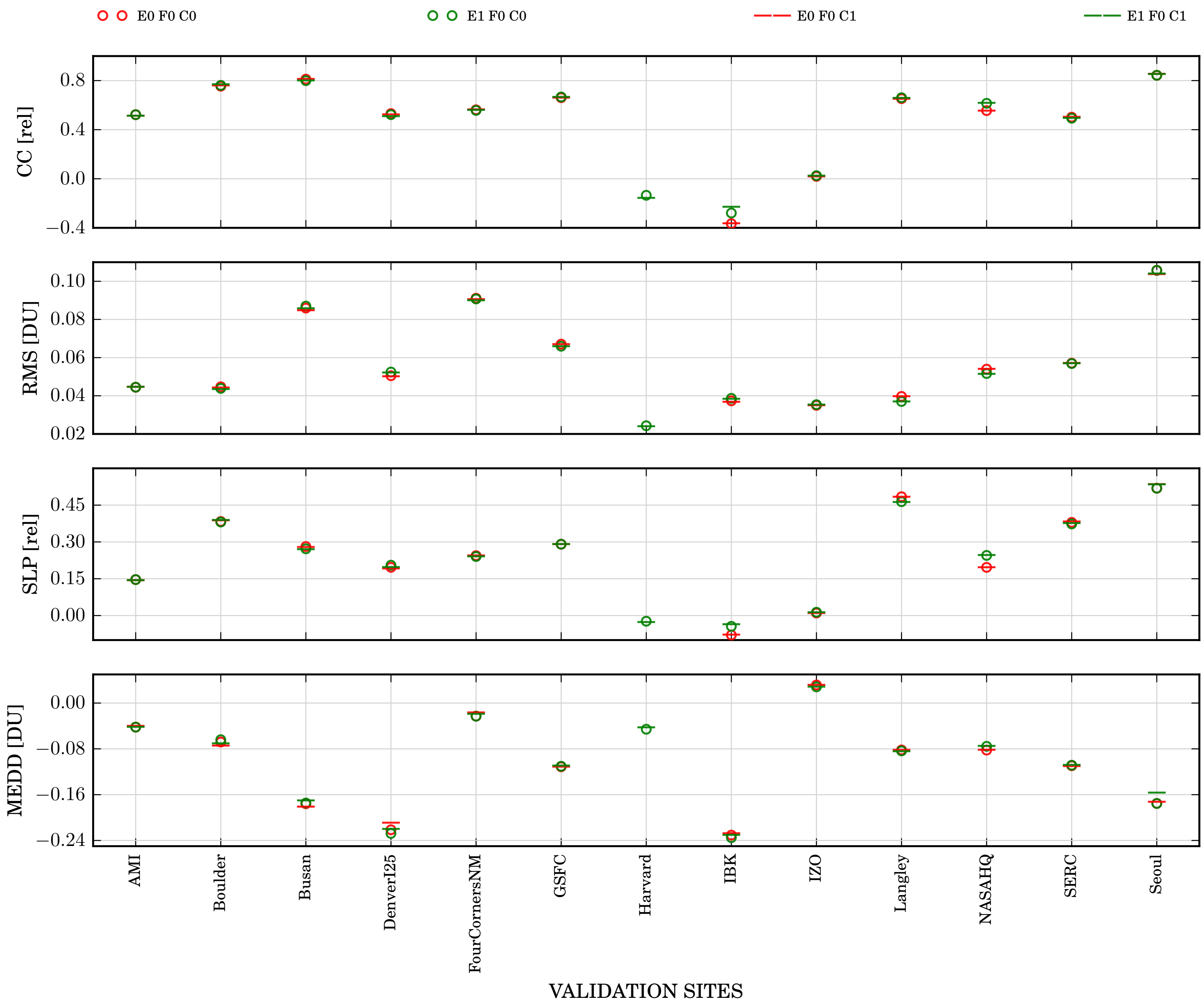

Figure 8: Specific network validation results validation results for TotNO2 with GeoFilt applied. Explanation like in Figure 2.

2.3 Conclusions

Based on this study we come to the following conclusions:

- O_3 validation:
  - The concept of utilizing the effective rather than the physical location of a validation site turned out to be a useful tool to enhance the representativeness of TotO3 from the satellite and Pandora.
  - The overall uncertainty in the validation is driven by two topics: first, seasonality in the TotO3 differences due to changing effective O_3 temperature. Seasonal subsets show different slopes and median differences, which makes it difficult to interpret short validation time periods but also enhances the "data scattering" for longer validation time periods. Second, neglecting the instruments spectral response and spectral stray light seem to introduce a negative bias, underestimating TotO3 compared to OMI. This effect is different in magnitude for each Pandora but tends to go into the same direction.
  - To reduce systematic differences in the satellite validation we plan in a next step to
    - Include the retrieval of the effective O_3 temperature in the spectral fitting algorithm operationally (see *Cede* [3] for algorithm details).
    - Include the correction of the instruments spectral response into the L1 processing.
    - Include the spectral stray light correction in the L1 processing.
  - The overall drift of the Pandora TotO3 of about 1 DU per year is small and is well captured by the planned operational network inter-calibration suggested in *Cede et al.* [5] to be performed at least once in two years.
- NO_2 validation:
  - The new OMI dataset version 3.0 performs worse than the version 2.1 in terms of statistical analysis. Speaking of the network as an ensemble, particular changes can be found for the median offset (from -0.02 to -0.08) and the slope (from 0.33 to 0.25) between the satellite and the ground-based dataset.
  - The majority of the comparison outliers were found to be associated to enhanced diurnal TotNO2 variations around the overpass time.
  - To apply to each OMI pixel a climatological correction turned out to be very useful to enhance the representativeness of TotNO2 from satellite and Pandora. It can be used as a "quasi" geolocation filtering of the OMI pixels in the case of shorter time series.
  - The systematic difference between OMI and Pandora is very small.
  - The main driver of the differences of ground and satellite data is the very different viewing geometry in combination with the strong spatial variation of NO2. Since OMI already gives much better comparison results as previous satellites, which have much larger pixel size (e.g. SCIAMACHY, GOME) we expect the comparisons will further improve when Pandora data are compared to retrieval of the upcoming Sentinel 5P mission.
- Long, continues time series are of great value for TotO3 and TotNO2 satellite validation. Strict data filter criteria can be applied to the data, still offering good statistics. By this also seasonal dependencies as well as long term stability checks can be investigated. However, even long ground based time series have only limited use for satellite validation, if no periodic calibration of the ground-based instruments is performed. Such satellite validation strategy is one major goal of the Pandonia network.

3 Materials and Methods

3.1 Input Data and Validation Sites

The OMI overpass data are provided by the Aura Validation Data Center (AVDC) hosted by the National Aeronautics and Space Administration (NASA) and has been extracted by Michael M. Yan for each ValSite in Figure 9. The O_3 data product used for the validation is OMTO3 v8.5, Collection 3, and OMNO2 v3.0, Collection 3, for NO_2.

The extracted OMI data sets contain all overpass pixels where the center of the pixel does not exceed a radius of 100 km around each ValSite. The additional OMI pixels, although not directly overlapping the ValSite, are used to process the climatological footprint correction maps, which will be explained in the following section.

Both OMI datasets are validated against the entire direct-sun Pandora dataset, which has recently been extended and refined from version 001 [10] to version 002 [12]. The maximum time periods covered for each dataset are given in Table 5. Whereas OMI data are continues, Pandora data include a lot of campaign data and hence also include rather short time periods for some ValSites.

Data set	Version Number	Maximum time period	Data format
OMI O_3	EOS Aura OMI OMTO3 v8.5, Collection 3	2009-01-01 to 2015-09-30	GEOMS H5
OMI NO_2	EOS Aura OMI OMNO2 v3.0, Collection 3	2009-01-01 to 2015-09-30	GEOMS H5
Pandora	v002	2009-01-01 to 2015-09-30	GEOMS H5

Table 5: Details on OMI and Pandora data sets.

Figure 9 shows a global map depicting all possible ValSites. ValSites are represented by an empty circle when the site has to be omitted due to lack of data after filtering. ValSites indicated by a filled circle are accepted ValSites.

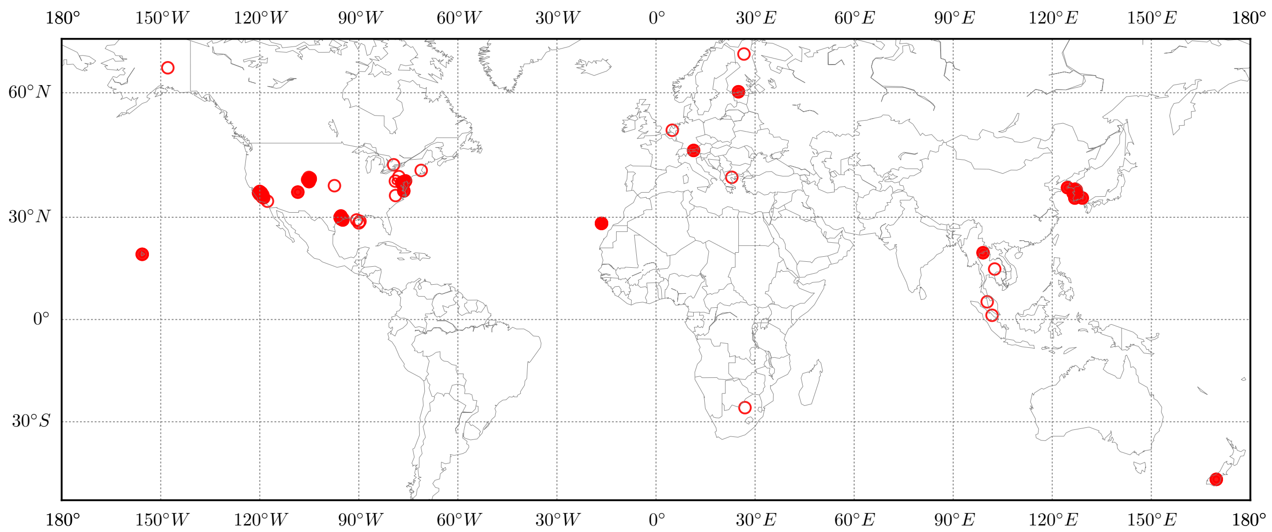

Figure 9: Validation locations. Explanation in the text.

3.2 Validation Support

Satellite retrievals and ground-based direct sun data sample different air masses due to their different observation geometry. This difference in the footprint poses a central difficulty in satellite validation. In this section we present three methods which may help to reduce the error introduced by this spatial sampling difference.

3.2.1 Effective Validation Location

The SZA changes with the ValSite and the overpass time of OMI. In the morning hours for example, the direct-sun data from Pandora are measured at moderate to high SZA. We assume the effective absorption layer height of O_3 to be at 21.0 km and for NO_2 to be at 1.0 km (for O_3 compare e.g. *Bernhard et al.* [4]). Thus the effective validation location is not the physical ground location (geolocation) itself. Instead, the effective location on the Northern Hemisphere is shifted towards the South-East direction. This displacement can be taken into account in the validation by using the effective validation location instead of the geolocation. Of course, the unknown exact position of the effective gas height is an error source, but should be small for O_3. The effect is also suggested to be small for NO_2 validation due to its low effective height.

3.2.2 Climatological Footprint Correction

If a ValSite is located within an area of significant trace gas gradients, the measured TotGAS by OMI is different for each overpass. This is clear, since the position of the footprint pixel relative to the Pandora location varies for each overpass. For illustration lets assume a NO_2 hot spot North of the ValSite (compare Figure 10). If e.g. a large footprint pixel covers the ValSite only with its corner (e.g. the large OMI pixel in Figure 10), the data would be biased since also less polluted areas fall within the pixel. We take this into account by compiling a large number of overpass data, covering a radius of 100 km around the Pandora location, to a high resolution climatological footprint map. The overpass data are averaged on a grid with resolution of e.g. 0.05°. The ClimCor is finally carried out by subtracting the mean value of a footprint pixel in the high resolution map from the value in the high resolution map where the Pandora is located. As seen from Figure 10, the effect can be significant for TotNO2. The dominance of boundary layer NO_2 for polluted sites forces strong spatial gradients in TotNO2. In contrast, TotO3 is dominated by stratospheric amounts facilitating smooth gradients in spatially averaged TotO3 (compare Figure 11).

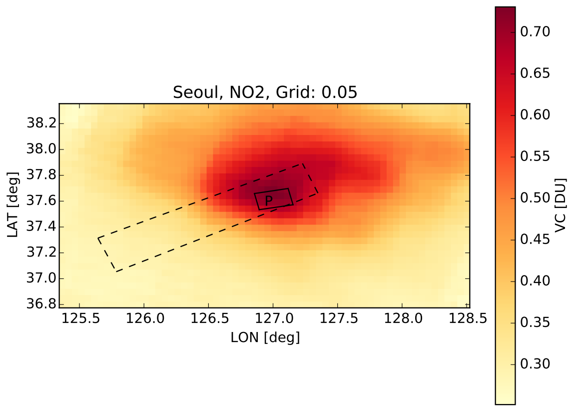

Figure 10: Climatological footprint correction map for TotNO2 retrievals compiled from one year of OMI overpass data. Data are averaged on a 0.05 deg latitude and longitude grid. Explanation like in Figure 11, except that for TotNO2 the variation across a OMI pixel can be quite significant.

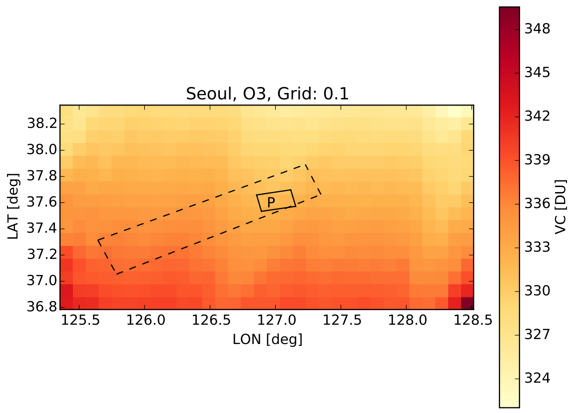

Figure 11: Climatological footprint correction map for TotO3 retrievals compiled from one year of OMI overpass data. Data are averaged on a 0.1 deg latitude and longitude grid. The Pandora position is marked with a "P". Two example OMI pixels are shown: in dashed lines a central pixel (small area, cross tack position around 30) and in continuous lines an edge pixel (large area, cross tack position around 1 or 60.). The TotO3 variation is rather small across the OMI pixel.

In version 1 of this report we calculated high resolution climatological footprint maps for each year from 2009 to 2015 to be able to take into account possible variations in the location of anthropogenic sources. The value used for the footprint correction is utilized on a yearly basis which means that a weighted average between the considered high resolution maps is calculated. For example, if the footprint has been measured at March 1st 2014, we take 25 % of the 2014 map and 75 % of the 2013 map, for July 1st we take 100 % of the 2014 map, for October 1st 2014 we take 25 % of the 2014 map and 75 % of 2015 map, and so on.

Since the variations of NO_2 and especially O_3 may also be seasonal, we tried to include this by going from yearly maps to seasonal maps. For these cases, the ClimCor was on shorter time scales, e.g. if the high resolution maps were calculated for one month, we just corrected for one month. That means, a measurement from March 1st gets corrected by 50 % from the March map and by 50 % from the February map. In Figure 12 the seasonal variations are shown for four pixels.

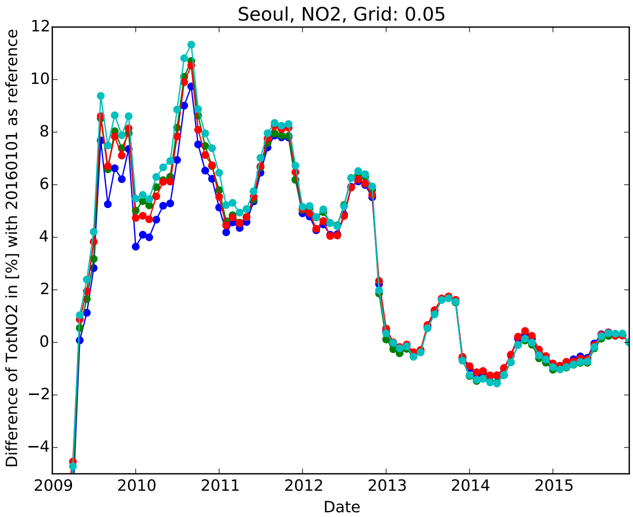

Figure 12: The monthly variations in Seoul of the high resolution files for TotNO2 for the four closest pixels to the Pandora from 2009 till 2016. A seasonal cycle is visible and also a trend between 2009 to 2016.

Because the calculation of the high resolution maps is computationally very expensive, larger grid sizes would be beneficial. It turned out, that for NO_2 we can go up to 0.1° and up to 0.3° for O_3. This can be understood considering the stronger horizontal gradients of NO_2.

The main idea of the climatological correction is to correct for ground locations with short time series. Long time series can be rigorously filtered by also applying GeoFilt, which rejects the big overpass pixels (low and high cross track positions CTP [9]). For short time series, as they are gathered e.g. during campaigns, strict filtering can only be done at the expense of statistical robustness. So, the most difficult task is, to correct for the biggest pixels which are larger than 3000 km^2 compared to the smallest pixels which are just slightly above 300km ^{2} [9]. That we are on the right track is shown in Figure 13 which shows a higher ClimCor for bigger pixels. It is obvious that the correction is dependent on the pixel size for Seoul, because the NO_2 hot spot is at the Pandora location and the bigger the pixel, the lower the average TotNO2 amount and the difference between the TotNO2 at the Pandora location and the whole pixel is bigger. But not for all locations the correction is so significant for large pixels. An example would be Langley where the pattern of the ClimCor as a function of the CTPs is not as distinct (see Figure 14).

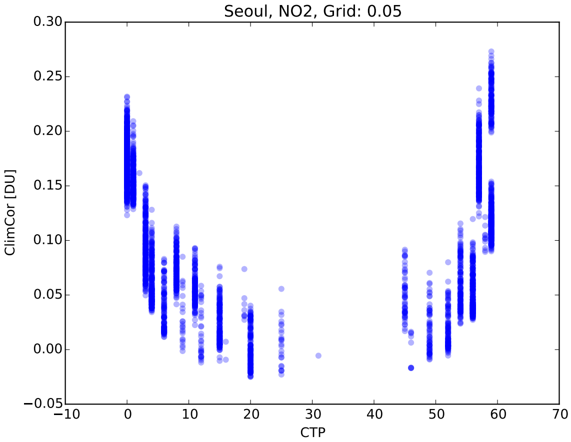

Figure 13: Climatological footprint correction against the cross track position CTP in Seoul. The bigger the pixel, the higher the magnitude of the climatological correction.

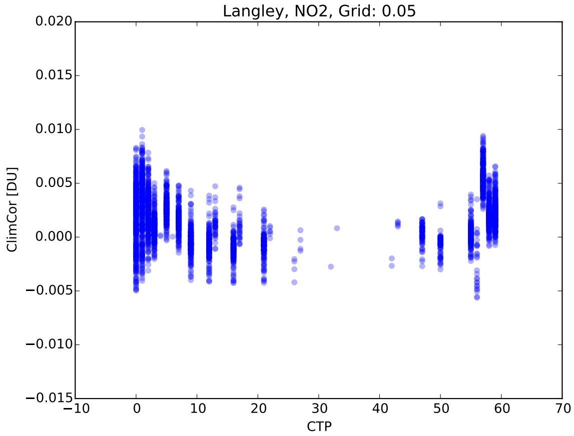

Figure 14: The same is shown as in figure 13 but for Langley. The pattern of the climatological correction as pronounced as for Seoul.

ClimCor appears to perform better for ValSites with comparably high TotNO2 values, since the magnitude of the correction more easily surpasses the overall discrepancies between both data sets. Hence, the beneficial effect of the ClimCor for ValSites with lower TotNO2 is not that pronounced.

3.2.3 Effective Footprint Location

We believe that another correction on the data might be useful, which we call the "effective footprint correction". However since the current version of the OMI overpass files does not include the VZAs associated with the CTPs, we do not apply effective footprint correction to the data yet. Nevertheless we describe the concept of it in this section.

Whereas for the direct sun ground instrument we just have one light path, the measurement by a satellite combines two different light paths: the one from the sun to the ground and the one from the ground to the measuring device. Hence the absorbing layer is penetrated twice. As explained in more detail in *Vandenbussche et al.* [14], the measured information is diluted horizontally towards the sun for direct nadir measurements and additionally towards the satellite for off-nadir measurements. Like for the Pandora, the SZA changes with the overpass time of the satellite and so we expect different impacts depending on the season and the location. Further, absorbers with a higher effective layer height like O_3 will be diluted stronger due to geometrical reasons.

The dilution effect towards the sun depends mainly on the SZA and towards the satellite on the VZA. Parametrizations are given by *Vandenbussche et al.* [14] for O_3 and NO_2 as follows.

$$\begin{aligned}
\mathrm{dilSun(O3)} &= 4.10^{-3}\cdot \mathrm{SZA} + 2.10^{-14}\cdot \exp(0.35\cdot \mathrm{SZA}) + 16.10^{-3}\cdot \exp(6.10^{-4}\cdot \mathrm{SZA}^2)\\
\mathrm{dilSun(NO2)} &= 43.10^{-4}\cdot \mathrm{SZA} + 312.10^{-10}\cdot \exp(0.2\cdot \mathrm{SZA}) + 33.10^{-3}\cdot \exp(5.10^{-4}\cdot \mathrm{SZA}^2)\\
\mathrm{dilSat(O3)} &= 0.0051\cdot \mathrm{VZA}\\
\mathrm{dilSat(NO2)} &= 0.0056\cdot \mathrm{VZA}
\end{aligned}$$

3.3 Validation Data Filtering

To ensure reliable data participating in the validation study proper data filtering has to be applied. For estimating the influence of a filter parameter threshold we carried out a simple sensitivity study. Pandora data filter parameters are not further tested, since we only accept data passing the strictest quality flag DQ0. This flagging procedure is explained in detail in *Tiefengraber and Müller* [12] and the values are summarized in Table 6. For Pandora, we only tested for the effect of averaging the Pandora data around the overpass time (PanAVG). PanAVG is regarded as $\pm$ PanAVG/2 around the OMI overpass time.

For OMI data we selected two groups of filter parameters. From the first group (GeoFilts) we tested for the longitudinal (latitudinal) distance of the footprint center to the Pandora location (dLON (dLAT)) and the footprint size (SatFPT). An other approach would be to use only one filter, the spatial distance of the ground location to the pixel center, instead of both dLAT and dLON. We decided to use the latter, since the OMI pixel size does not change significantly with dLAT, but does so with dLON. In this way we have also considered the effect of the CTP of the OMI pixel. Beside that, as a quality filter, we tested for the cloud fraction (SatCF) assumed in the OMI pixel and in the case of TotNO2, also for the OMI retrieval uncertainty (SatUncNO2).

The sensitivity of the selection of the filter parameter thresholds is validated against the ValPars listed in Table 1. Since we are interested in the relative change of the test parameters when altering the filter parameter thresholds, we express the test parameters as relative changes with respect to an initial guess (dCC, dRMS, dSLP, dMEDD). The initial guesses are given in the third columns in Table 7 and Table 8. The values are estimated from the know average OMI footprint geometry and experience from former studies.

The sensitivity test is carried out by varying only one of the filter parameter thresholds at the same time and leave the others at the initial guesses. We applied the sensitivity tests on four locations with long time series (even strong filter thresholds keep good statistics), but with different characteristics. Langley (Fairfax, Virginia, USA) as a location considered to be rural and with the longest Pandora time series available, Los Alamos (Four Corners, USA) as a second rural site but with high trace gas variability (nearby power plant), GSFC (Greenbelt, Maryland, USA) as an urban location and as the Pandora “headquarter” with the densest time series of Pandoras and finally Seoul (South Korea) due to its very high air pollution.

Parameter	**Abbreviation**	**Threshold**
TotO3		
Uncertainty	PanUQ	1 DU
normalized rms of spectral fitting residual	PanWRMS	2.0×10^{-2}
wavelength shift	PanWVL	2.0×10^{-1} nm
direct sun air mass factor	PanAMF	5
enhanced data scatter	PanSCAT	1.0×10^{-2}
TotNO2		
Uncertainty	PanUQ	1.0×10^{-2} DU
normalized rms of spectral fitting residual	PanWRMS	5.0×10^{-3}
wavelength shift	PanWVL	1.0×10^{-1} nm
direct sun air mass factor	PanAMF	7
enhanced data scatter	PanSCAT	4.0×10^{-4}

Table 6: Filter criteria applied for the Pandora quality flag DQ0.

3.3.1 Validation Data Filtering: TotO3

Figure 15 shows the filter parameters sensitivities for TotO3 validation. The different ValSites are depicted in different colors and the mean over all ValSites is shown in black. The rows in the plot refer to the filter parameters and the columns to the ValPars. Each subplot is visualized in a way to show 4 quarters (divided by the vertical and horizontal bar in gray) to give an immediate information about the improvement or deterioration of a test parameter by varying a selected filter parameter threshold. Improvement means, that positive values for e.g. dCC mean higher CC and positive values for dMEDD mean lower MEDD, since it is preferable. Hence the upper (lower) left quarter means improvement (deterioration) by reducing the filter parameter threshold and the upper (lower) right quarter means improvement (deterioration) by enhancing the threshold. Please not the different scales for each subplot.

The geolocation filter parameters (dLAT, dLON, SatFPT) are especially dependent on the surroundings of the location. Hence different sensitivities can be seen for remote and urban ValSites. Having in mind the pixel shape of OMI the stronger sensitivity of dLAT than dLON is plausible. We select a dLAT threshold values of 0.08 deg, since below remote and urban locations are affected very differently. The selection of dLON and SatFPT thresholds have no clear tendency on the ValPars. We shift the initial guess for dLON of 0.3 deg to 0.2 deg and for SatFPT form 0.3 to 0.35 deg^2. The geolocation filters can only be applied to ValSites with long time series, since it strongly reduces the available number of footprints. Rather intuitively is the improvement of the ValPars with smaller SatCF thresholds. Again ValSites react differently. Urban ValSites benefit in particular when adjusting the initial value of 0.3 to 0.1. We decided to increase the PanAVG from 90 min to 120 min because dCC increases for remote sites and does not decrease for urban sites. The overall effect is rather small though.

The final selection of the filter parameter thresholds applied for this validation study are summarized in Table 7 in the fourth column. The asterisks highlight filter parameters which can only be applied to ValSites with long time series.

Sensitivity parameter	**Abbreviation**	**Initial threshold**	**Best threshold**
OMI geolocation filter (GeoFilt)			
lat. footprint center distance to Pandora *	dLAT	0.1 °	0.1 °
lon. footprint center distance to Pandora *	dLON	0.3 °	0.2 °
footprint area *	SatFPT	0.3 °x°	0.35 °x°
OMI quality filter			
cloud fraction	SatCF	0.3	0.1
Pandora data averaging time			
data averaging time	PanAVG	90 min	120 min

Table 7: Optimized filter parameter thresholds applied for TotO3 validation. The best guess thresholds are the conclusion from the sensitivity test.

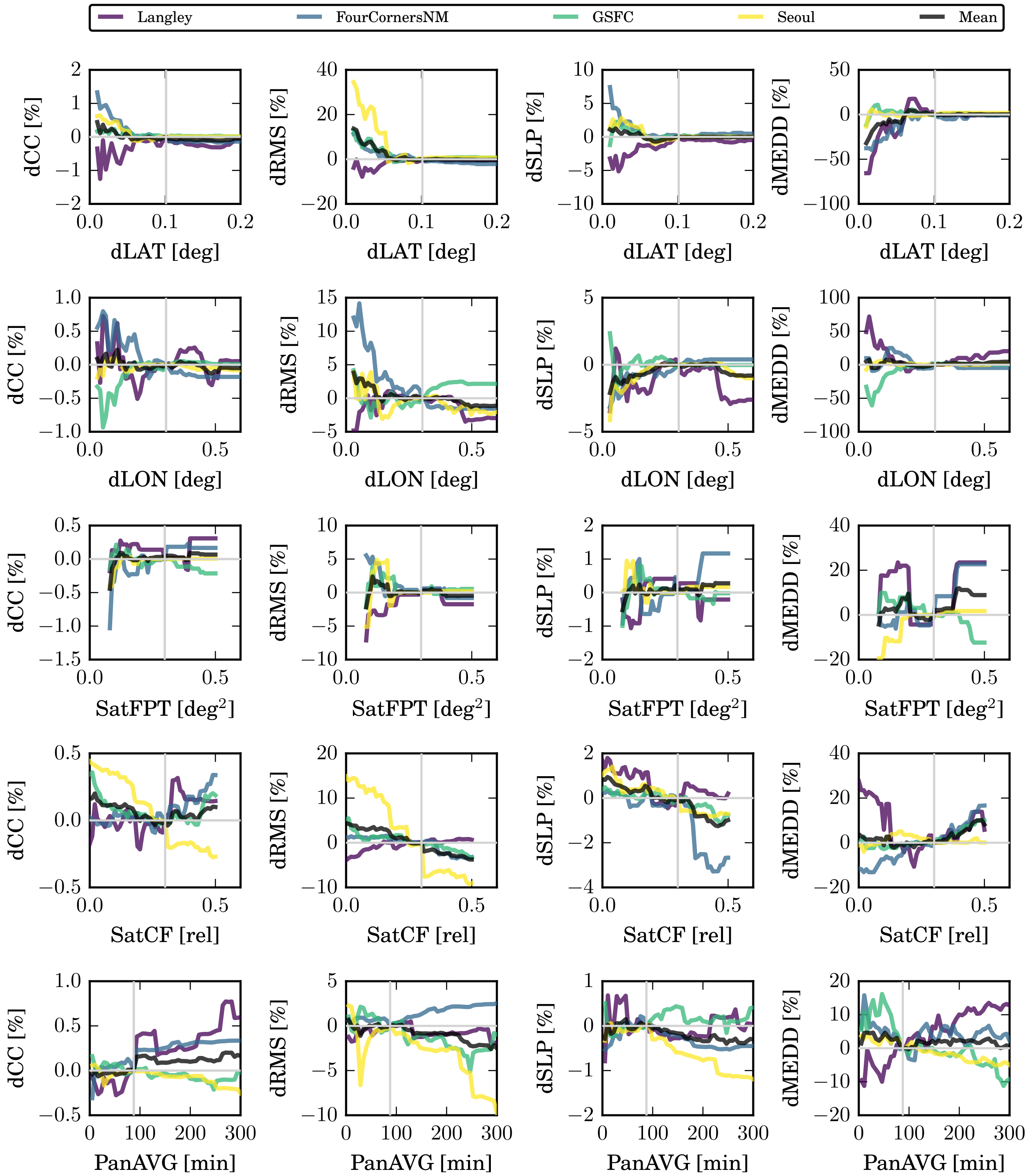

Figure 15: Filter parameter threshold sensitivity test for TotO3 validation assessed at for four validation locations (and its mean): GSFC, Langley, Four Corners and Seoul. The columns show the four validation parameters (from Table 1) and exhibit the differential change to a reference value. The rows show the tested filter parameters (dLat, dLon, SatFPT, SatCF and PanAVG). Each subplot is partitioned into four quadrants. E.g. the upper right (left) quadrant suggest improvement in a validation parameter when increasing (decreasing) the threshold of the filter parameter. The lower quadrants the respective deterioration of the validation parameter.

3.3.2 Validation Data Filtering: TotNO2

Figure 16 shows the filter parameters sensitivities for TotNO2 validation. The Figure has to be read in the same way as explained in section 3.3.1.

For TotNO2 validation the geolocation filter parameters (dLAT, dLON, SatFPT) have a even stronger affect on ValPars due to its high spatial inhomogeneity. For dLat the initial choice of 0.1° seems to be already appropriate. When being more stringent in dLON (from 0.3° to 0.14°) and SatFPT (from 0.3 to 0.13 °x°), all ValPars can be improved. This could be expected. Reducing the threshold for CC from 0.3 to 0.1 is again beneficial, except for dRMS. SatUncNO2 is not further reduced since it would strongly limit the available data points. We decided further to increase PanAVG only from 20 min to 30 min although even higher PanAVG would give slightly better ValPars. We want to avoid to blur the NO_2 information to much.

The final selection of the filter parameter thresholds applied for this validation study are summarized in Table 8 in the fourth column. The asterisks highlight filter parameters which can only be applied to ValSites with long time series.

Sensitivity parameter	**Abbreviation**	**Initial threshold**	**Best threshold**
OMI geolocation filter			
lat. footprint center distance to Pandora *	dLAT	0.1 °	0.08 °
lon. footprint center distance to Pandora *	dLON	0.3 °	0.14 °
footprint area *	SatFPT	0.3 °x°	0.13 °x°
OMI quality filter			
cloud fraction	SatCF	0.3	0.1
$TotNO_2$ uncertainty	SatUncNO2	0.1 DU	0.1 DU
Pandora data averaging time			
data averaging time	PanAVG	20min	30 min

Table 8: Optimized filter parameter thresholds applied for the $TotNO_2$ validation. The best guess thresholds are the conclusions from the sensitivity test.

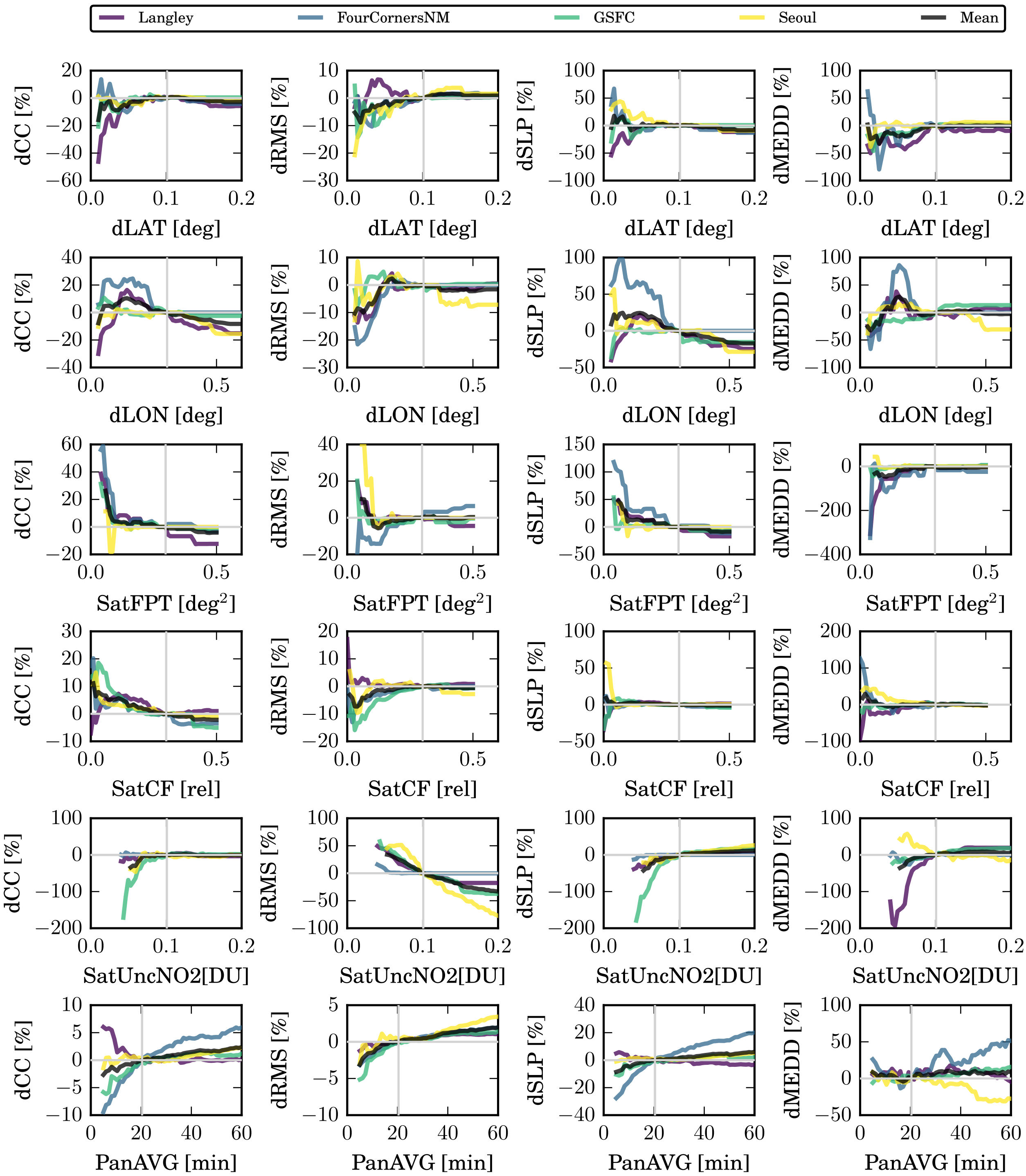

Figure 16: Filter parameter threshold sensitivity test for TotNO2 validation assessed at four validation locations. Explanation like in Figure 15.

3.4 Validation Procedure

- OMI data preparation

  1. ClimCor maps are produced and EffLocs are calculated.

  2. A thinned out OMI dataset is compiled only containing pixels overlapping the geo -and/or effective Pandora location. This data set is given in the same format as the Pandora data and contains also information about ClimCor and EffLoc.

$\rightarrow$ SV0 data.

3. Data quality filtering according to Table 7/8 and possibly ClimCor is applied to the SV0 data.
$\rightarrow$ SV1 data.

- Pandora data preparation

4. Temporally overlapping Pandoras are identified and combined for each footprint in SV1. By this noise and potential systematic errors of one Pandora can be reduced.
$\rightarrow$ PV0 data.
5. Data quality filtering according to Table 6 and possibly EffLoc correction is applied to PV0.
$\rightarrow$ PV1 data.

- Validation procedure

6. PV1 data points are averaged around SV1 footprint measurement times. The averaging time is PanAVG from Table 7/8.
$\rightarrow$ PV2 data.
7. SV1 is validated against PV2 for the desired scenario (introduced in section 2). If less than 10 data points are available the ValSite is not considered. Scatter plots are generated and statistics are calculated. For time series covering more than 1 year of data, trend analyses are carried out too.

4 Individual Validation Results

4.1 Scatter Plots

In the following pages we present scatter plots and statistics for each ValSite. TotO3 validation is based on scenario E1 C0 G0 and E1 C0 G1 (marked with an asterisk) and given in section 4.1.1. The scatter plots are color coded to highlight data points which are collected in different seasons: purple for winter, blue for spring, green for summer and yellow for autumn.

TotNO2 validation is based on scenario E1 C1 G0 and E1 C1 G1 (marked with an asterisk) and given in section 4.1.2. The color code of the plots emphasizes the diurnal NO_2 range within $\pm$ 4 hours of the OMI overpass time.
The statistics are described in Table 9.

Short Description	Long Description
longitude, latitude	ground geolocation of the Pandora unit (not its effective location)
num data points	number of data points passing the filter criteria
max Pan. (Pans.)	maximum number of Pandora units involved (Pandora ID(s) operating at this location)
CC	correlation coefficient between OMI and Pandora
RMS	root mean square error to a linear fit in Pandora minus OMI
SLP	slope term in the linear fit including OMI uncertainty (Pandora uncertainty is omitted due to the large number of points)
mean	arithmetic mean of the difference OMI minus Pandora
MEDD	median value for OMI minus Pandora difference
25-75 perc. range	25 to 75 percentile range for OMI minus Pandora difference
10-90 perc. range	10 to 90 percentile range for OMI minus Pandora difference
min-max range	minimum value to maximum value range for OMI minus Pandora difference
OMI CF	percentage of OMI data passing the OMI CF filter
Pandora DQ0	percentage of Pandora data passing the DQ0 filter

Table 9: Description on the additional information and statistics given for each ValSite.

4.1.1 Scatter Plots: TotO3

AMI

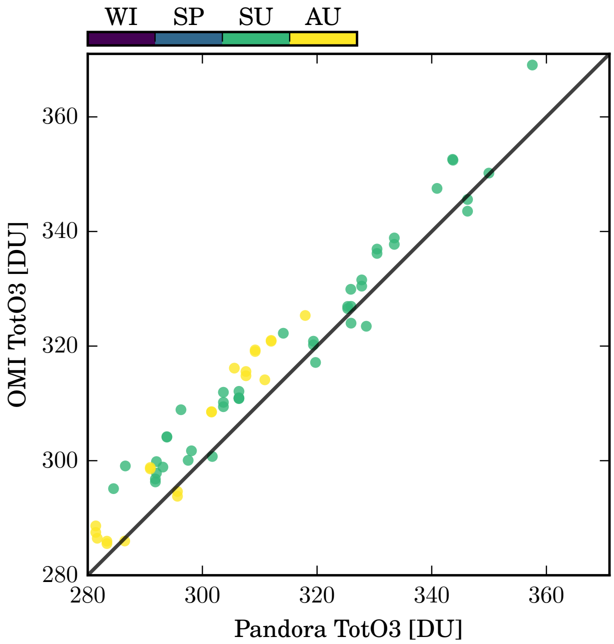

longitude, latitude	126.33, 36.538
num data points	64
max Pan. (Pans.)	1 (21)
CC	0.98
RMS	3.96 DU
SLP	0.95 ± 0.03
mean	5.05 DU
MEDD	5.72 DU
25-75 perc. range	2.45 DU to 7.91 DU
10-90 perc. range	-0.89 DU to 10.25 DU
min-max range	-5.13 DU to 12.63 DU
OMI CF	40.19 %
Pandora DQ0	26.62 %

AMI*

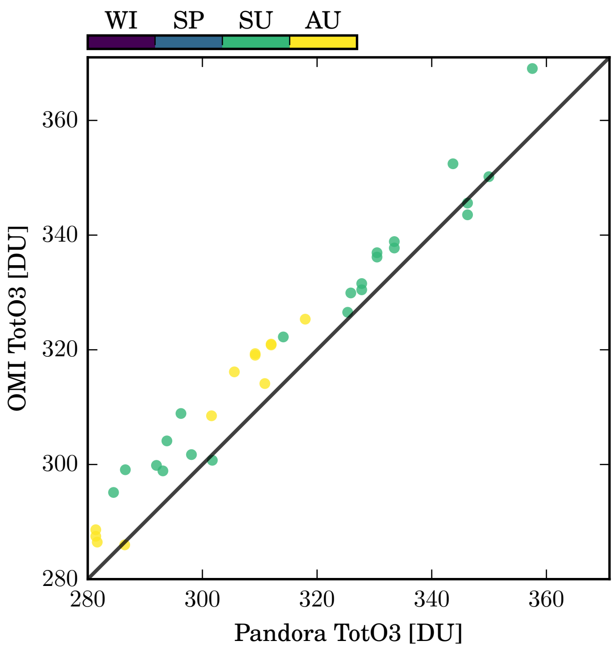

longitude, latitude	126.33, 36.538
num data points	34
max Pan. (Pans.)	1 (21)
CC	0.98
RMS	3.83 DU
SLP	0.94 ± 0.03
mean	6.02 DU
MEDD	6.28 DU
25-75 perc. range	3.66 DU to 8.96 DU
10-90 perc. range	-0.26 DU to 10.61 DU
min-max range	-2.70 DU to 12.63 DU
OMI CF	40.19 %
Pandora DQ0	26.62 %

Aldino

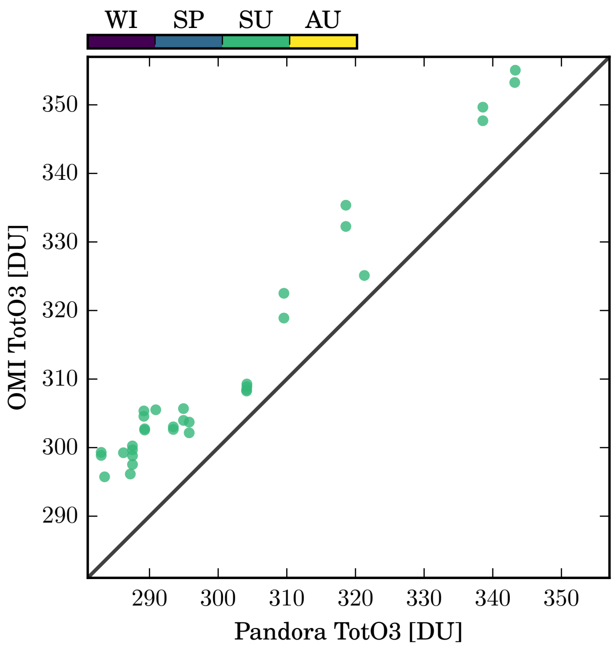

longitude, latitude	-76.203889, 39.563333
num data points	33
max Pan. (Pans.)	1 (23)
CC	0.98
RMS	3.58 DU
SLP	0.95 ± 0.04
mean	10.76 DU
MEDD	11.10 DU
25-75 perc. range	9.02 DU to 13.27 DU
10-90 perc. range	4.79 DU to 15.80 DU
min-max range	3.82 DU to 16.76 DU
OMI CF	50.75 %
Pandora DQ0	61.08 %

Arvin

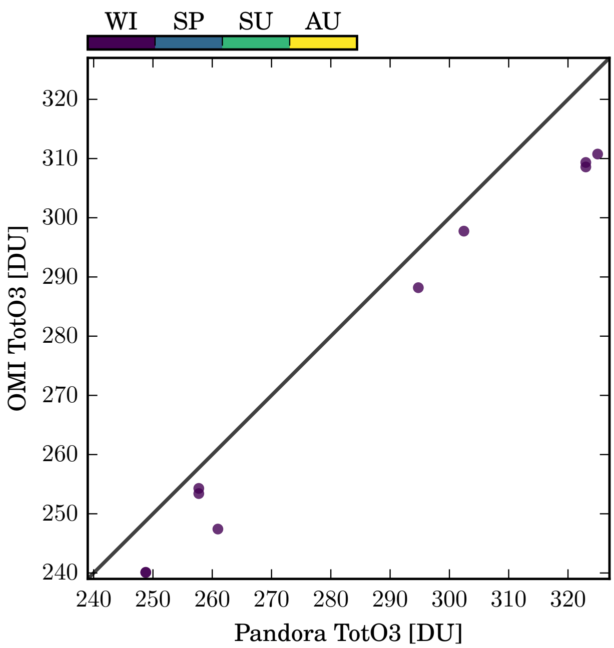

longitude, latitude	-118.7887, 35.291
num data points	10
max Pan. (Pans.)	1 (35)
CC	0.99
RMS	3.56 DU
SLP	0.93 ± 0.04
mean	-9.23 DU
MEDD	-8.69 DU
25-75 perc. range	-13.63 DU to -5.17 DU
10-90 perc. range	-14.26 DU to -4.23 DU
min-max range	-14.43 DU to -3.44 DU
OMI CF	55.65 %
Pandora DQ0	27.57 %

Baengnyeongdo

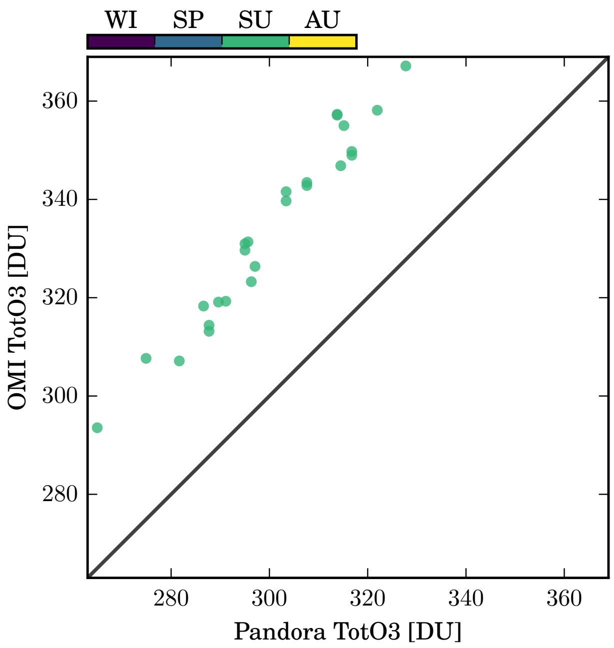

longitude, latitude	124.631, 37.965
num data points	25
max Pan. (Pans.)	1 (35)
CC	0.98
RMS	3.86 DU
SLP	1.22 ± 0.05
mean	33.45 DU
MEDD	32.97 DU
25-75 perc. range	29.30 DU to 36.19 DU
10-90 perc. range	26.79 DU to 39.67 DU
min-max range	25.45 DU to 43.52 DU
OMI CF	44.26 %
Pandora DQ0	19.24 %

Baengnyeongdo*

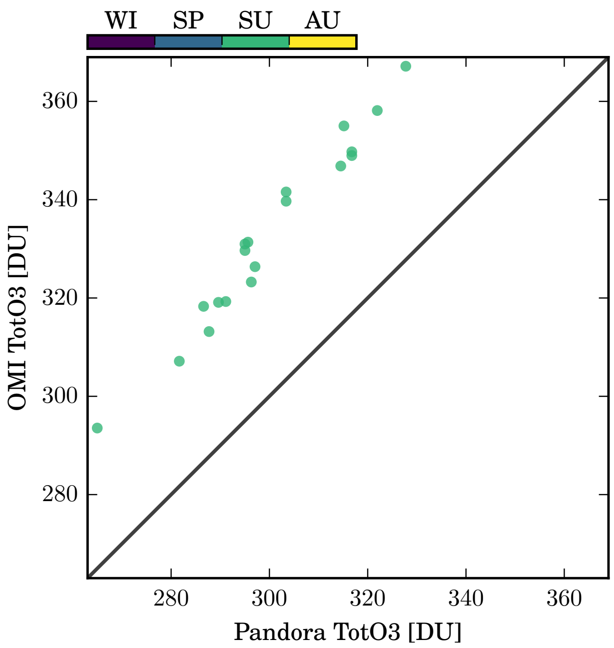

longitude, latitude	124.631, 37.965
num data points	19
max Pan. (Pans.)	1 (35)
CC	0.98
RMS	3.37 DU
SLP	1.19 ± 0.05
mean	32.57 DU
MEDD	32.33 DU
25-75 perc. range	28.94 DU to 36.07 DU
10-90 perc. range	26.64 DU to 38.41 DU
min-max range	25.45 DU to 39.85 DU
OMI CF	44.26 %
Pandora DQ0	19.24 %

Bakersfield

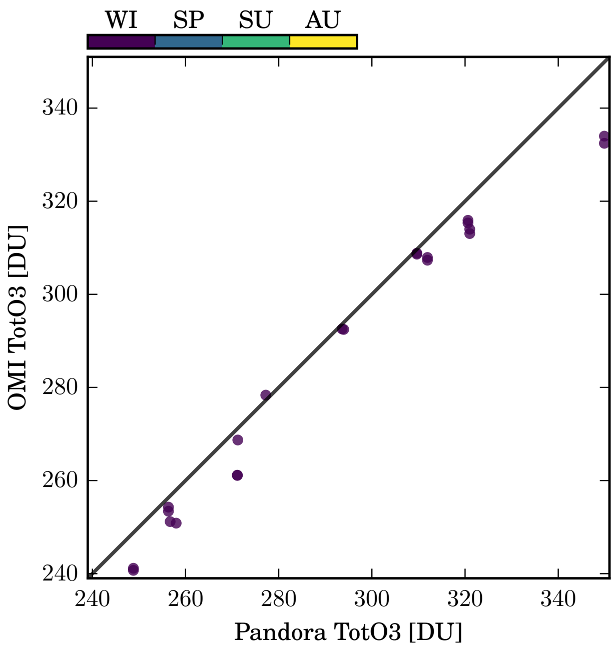

longitude, latitude	-118.9976, 35.3246
num data points	22
max Pan. (Pans.)	2 (33, 36)
CC	0.99
RMS	4.33 DU
SLP	0.95 ± 0.03
mean	-5.73 DU
MEDD	-5.01 DU
25-75 perc. range	-7.87 DU to -2.15 DU
10-90 perc. range	-10.00 DU to -1.03 DU
min-max range	-17.46 DU to 1.13 DU
OMI CF	48.89 %
Pandora DQ0	49.04 %

Beltsville

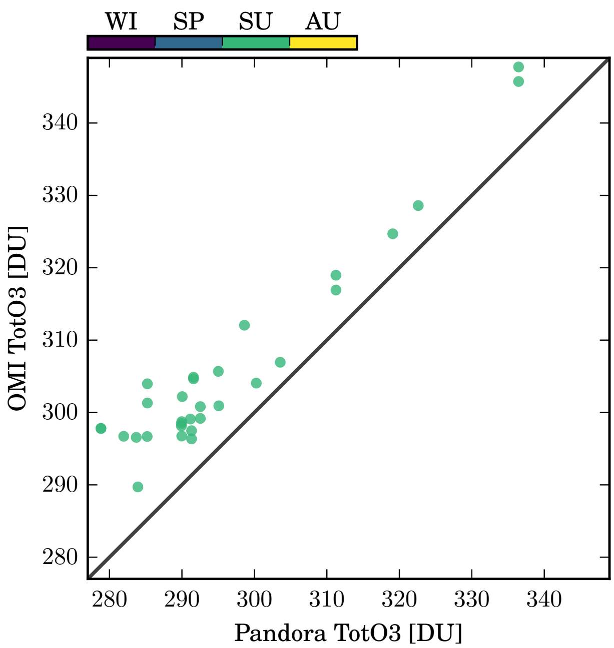

longitude, latitude	-76.878333, 39.055277
num data points	31
max Pan. (Pans.)	1 (20)
CC	0.96
RMS	4.02 DU
SLP	0.88 ± 0.05
mean	9.84 DU
MEDD	8.55 DU
25-75 perc. range	6.07 DU to 12.96 DU
10-90 perc. range	5.60 DU to 16.08 DU
min-max range	3.38 DU to 18.99 DU
OMI CF	54.84 %
Pandora DQ0	70.56 %

Boulder

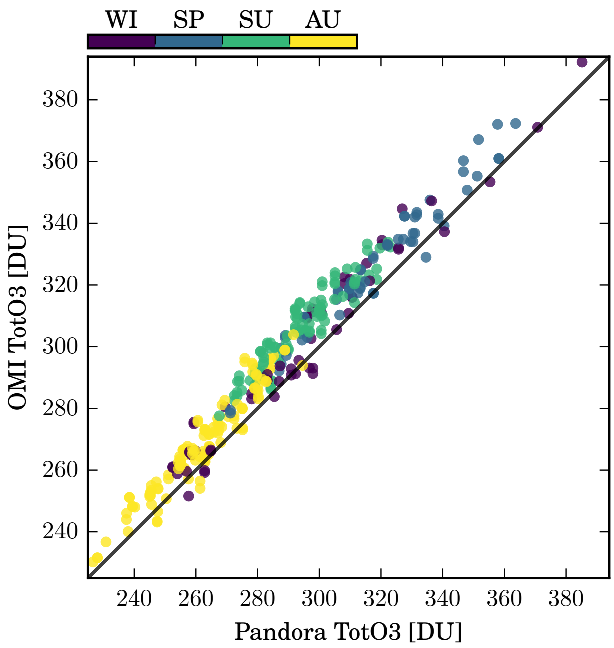

longitude, latitude	-105.26067, 39.99093
num data points	346
max Pan. (Pans.)	1 (34)
CC	0.98
RMS	5.36 DU
SLP	1.02 ± 0.01
mean	8.49 DU
MEDD	8.74 DU
25-75 perc. range	5.37 DU to 11.91 DU
10-90 perc. range	1.49 DU to 15.38 DU
min-max range	-7.29 DU to 20.60 DU
OMI CF	34.41 %
Pandora DQ0	48.08 %

Boulder*

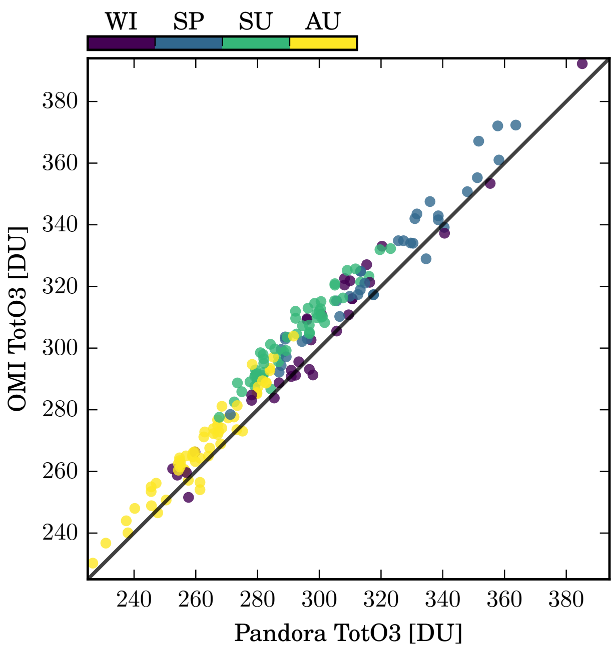

longitude, latitude	-105.26067, 39.99093
num data points	181
max Pan. (Pans.)	1 (34)
CC	0.98
RMS	5.21 DU
SLP	1.02 ± 0.01
mean	7.58 DU
MEDD	7.90 DU
25-75 perc. range	4.84 DU to 11.58 DU
10-90 perc. range	0.25 DU to 14.14 DU
min-max range	-7.29 DU to 19.67 DU
OMI CF	34.41 %
Pandora DQ0	48.08 %

Busan

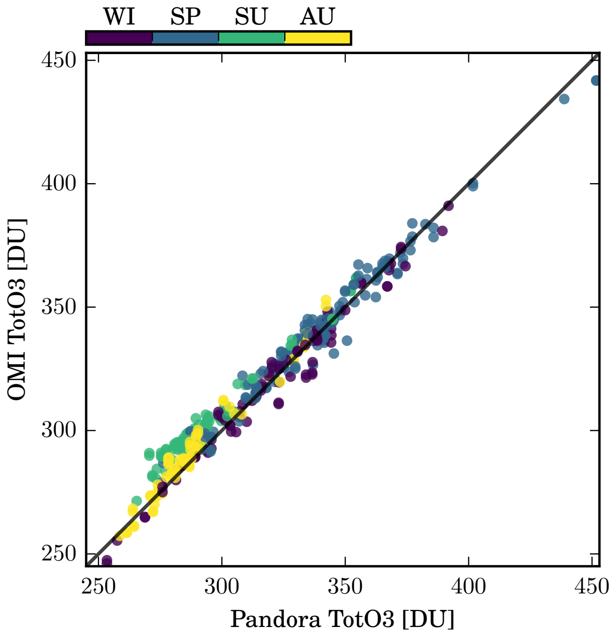

longitude, latitude	129.0825, 35.2353
num data points	394
max Pan. (Pans.)	2 (20, 36)
CC	0.99
RMS	5.31 DU
SLP	0.93 ± 0.01
mean	2.95 DU
MEDD	2.80 DU
25-75 perc. range	-0.29 DU to 6.97 DU
10-90 perc. range	-3.85 DU to 10.78 DU
min-max range	-14.29 DU to 20.25 DU
OMI CF	44.15 %
Pandora DQ0	44.18 %

Busan*

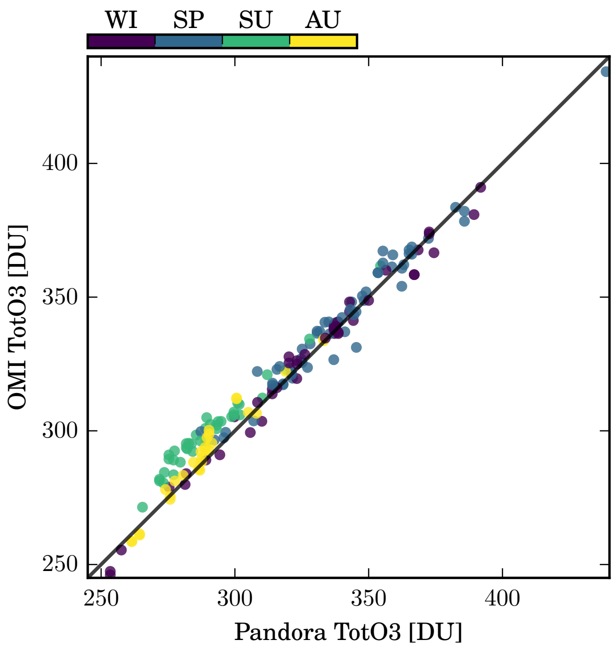

longitude, latitude	129.0825, 35.2353
num data points	173
max Pan. (Pans.)	2 (20, 36)
CC	0.99
RMS	5.10 DU
SLP	0.94 ± 0.01
mean	3.02 DU
MEDD	2.55 DU
25-75 perc. range	-0.45 DU to 6.78 DU
10-90 perc. range	-3.35 DU to 11.03 DU
min-max range	-14.19 DU to 15.64 DU
OMI CF	44.15 %
Pandora DQ0	44.18 %

CIAI

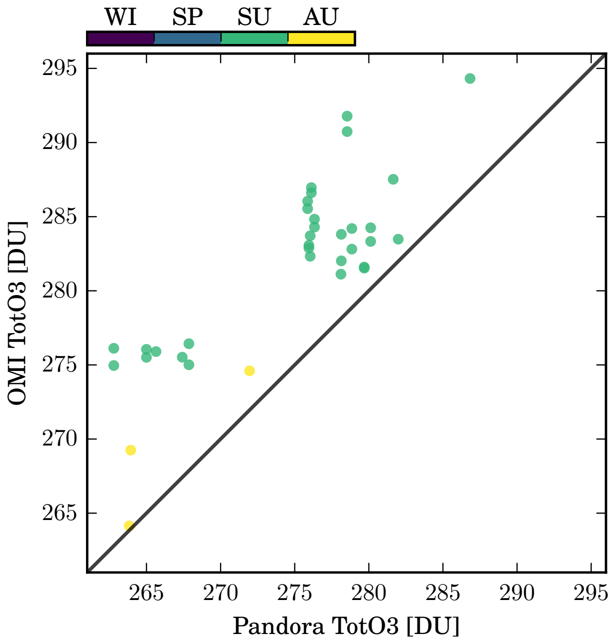

longitude, latitude	-16.4994, 28.309
num data points	35
max Pan. (Pans.)	1 (101)
CC	0.84
RMS	3.32 DU
SLP	0.81 ± 0.09
mean	7.09 DU
MEDD	7.15 DU
25-75 perc. range	4.04 DU to 10.21 DU
10-90 perc. range	2.20 DU to 11.72 DU
min-max range	0.30 DU to 13.32 DU
OMI CF	54.90 %
Pandora DQ0	71.26 %

CIAI*

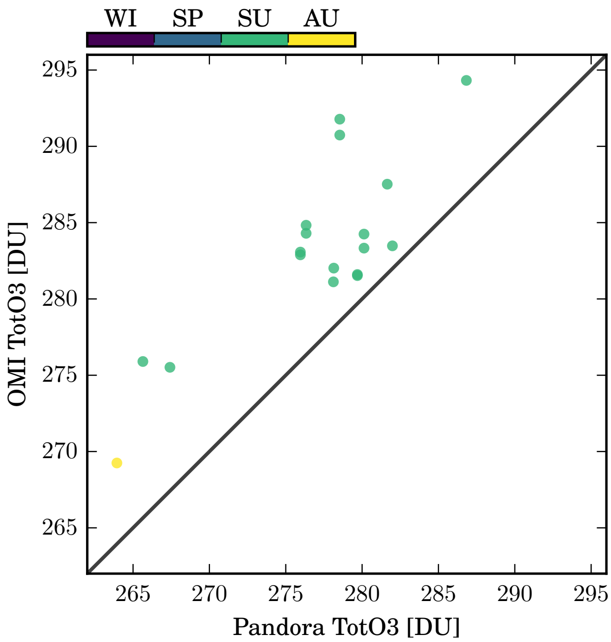

longitude, latitude	-16.4994, 28.309
num data points	18
max Pan. (Pans.)	1 (101)
CC	0.82
RMS	3.26 DU
SLP	0.84 ± 0.14
mean	6.25 DU
MEDD	6.40 DU
25-75 perc. range	3.37 DU to 8.07 DU
10-90 perc. range	1.89 DU to 10.84 DU
min-max range	1.49 DU to 13.24 DU
OMI CF	54.90 %
Pandora DQ0	71.26 %

Cabauw

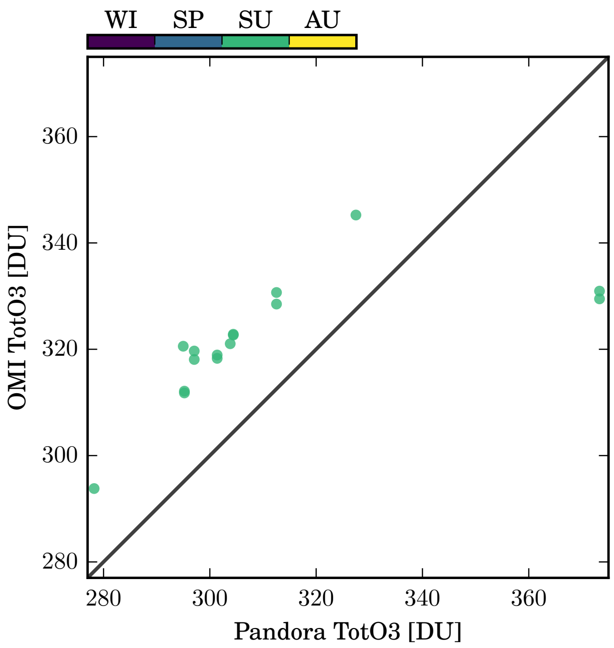

longitude, latitude	4.92625, 51.9704
num data points	16
max Pan. (Pans.)	2 (3, 9)
CC	0.64
RMS	8.19 DU
SLP	0.27 ± 0.09
mean	10.76 DU
MEDD	17.37 DU
25-75 perc. range	16.42 DU to 18.29 DU
10-90 perc. range	-13.40 DU to 21.81 DU
min-max range	-43.83 DU to 25.57 DU
OMI CF	27.50 %
Pandora DQ0	14.11 %

Channelview

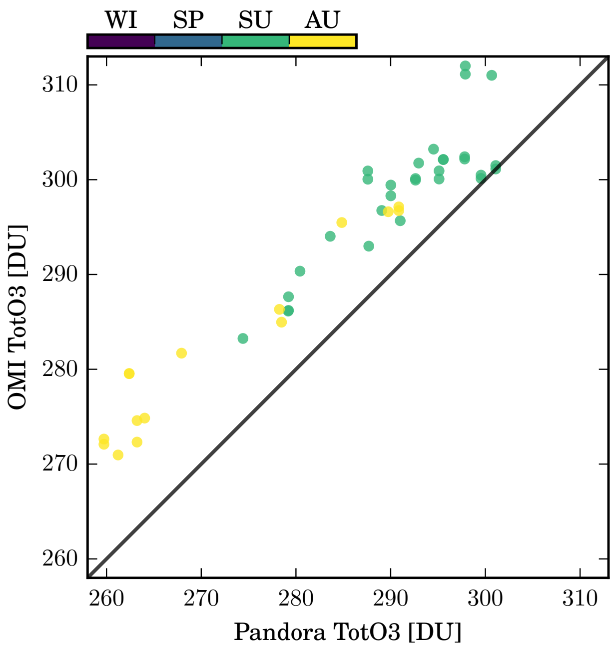

longitude, latitude	-95.1255, 29.8025
num data points	45
max Pan. (Pans.)	1 (26)
CC	0.96
RMS	3.12 DU
SLP	0.81 ± 0.04
mean	8.36 DU
MEDD	8.28 DU
25-75 perc. range	6.27 DU to 10.64 DU
10-90 perc. range	4.46 DU to 13.30 DU
min-max range	0.04 DU to 17.16 DU
OMI CF	52.27 %
Pandora DQ0	53.12 %

Channelview*

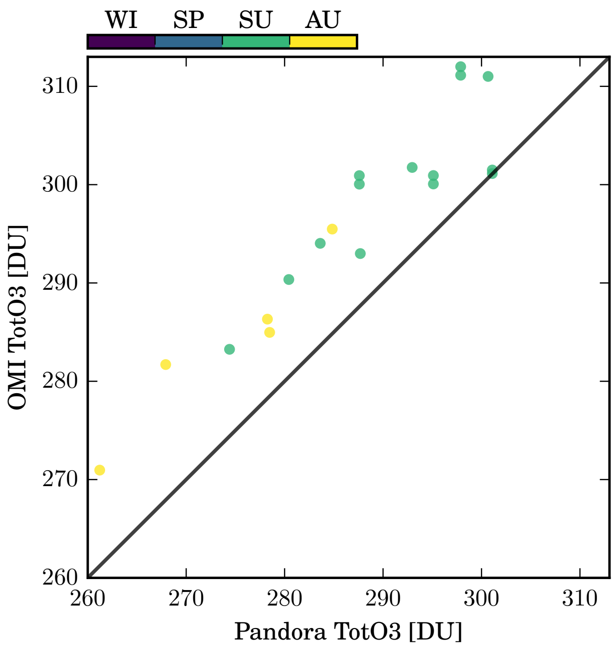

longitude, latitude	-95.1255, 29.8025
num data points	19
max Pan. (Pans.)	1 (26)
CC	0.93
RMS	3.80 DU
SLP	0.88 ± 0.08
mean	8.77 DU
MEDD	9.74 DU
25-75 perc. range	6.16 DU to 11.55 DU
10-90 perc. range	4.05 DU to 13.42 DU
min-max range	0.04 DU to 14.12 DU
OMI CF	52.27 %
Pandora DQ0	53.12 %

Chatfield

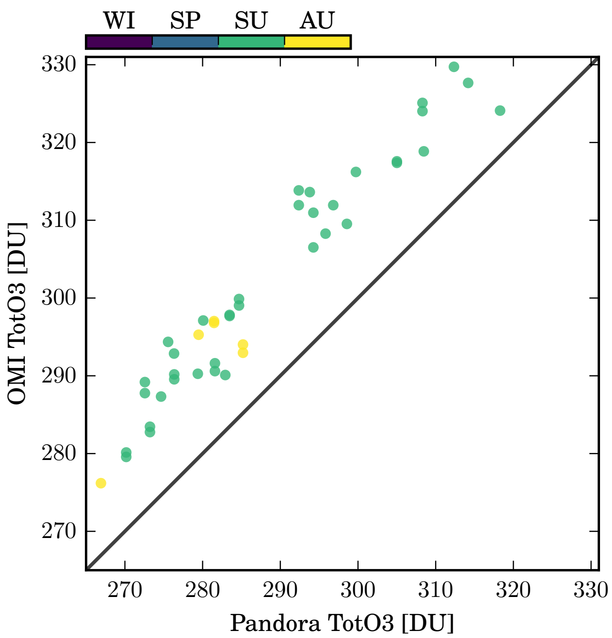

longitude, latitude	-105.07, 39.53
num data points	43
max Pan. (Pans.)	1 (26)
CC	0.97
RMS	3.59 DU
SLP	1.03 ± 0.04
mean	13.49 DU
MEDD	13.83 DU
25-75 perc. range	10.31 DU to 16.14 DU
10-90 perc. range	9.07 DU to 17.31 DU
min-max range	5.81 DU to 21.46 DU
OMI CF	34.56 %
Pandora DQ0	49.65 %

Chatfield*

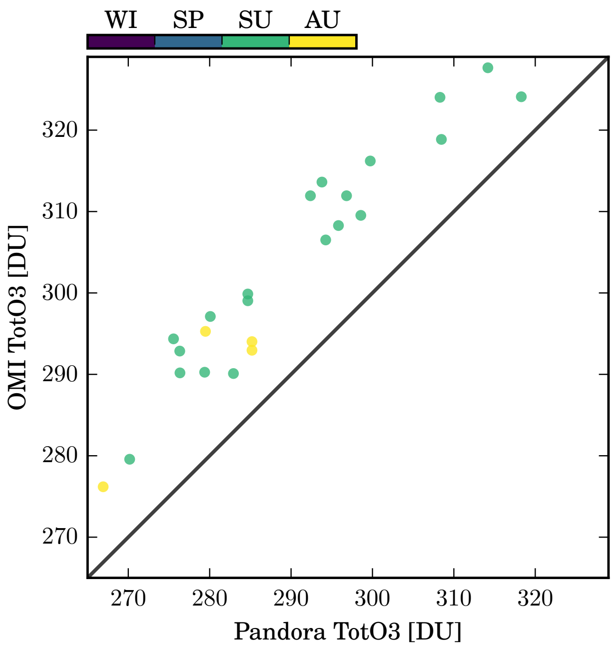

longitude, latitude	-105.07, 39.53
num data points	24
max Pan. (Pans.)	1 (26)
CC	0.96
RMS	3.89 DU
SLP	0.98 ± 0.06
mean	13.21 DU
MEDD	13.66 DU
25-75 perc. range	10.14 DU to 15.97 DU
10-90 perc. range	8.08 DU to 18.27 DU
min-max range	5.81 DU to 19.83 DU
OMI CF	34.56 %
Pandora DQ0	49.65 %

Conroe

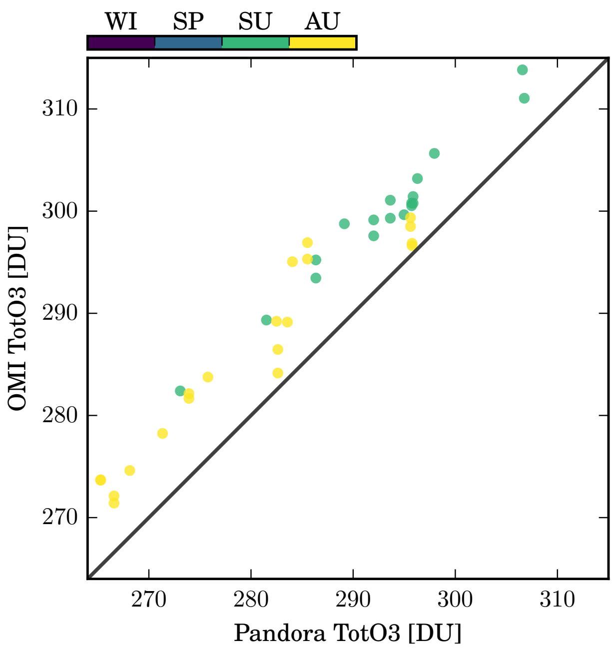

longitude, latitude	-95.425, 30.350
num data points	38
max Pan. (Pans.)	1 (31)
CC	0.98
RMS	2.34 DU
SLP	0.93 ± 0.03
mean	6.38 DU
MEDD	6.81 DU
25-75 perc. range	4.85 DU to 7.94 DU
10-90 perc. range	3.49 DU to 9.41 DU
min-max range	0.85 DU to 11.39 DU
OMI CF	47.87 %
Pandora DQ0	50.16 %

Conroe*

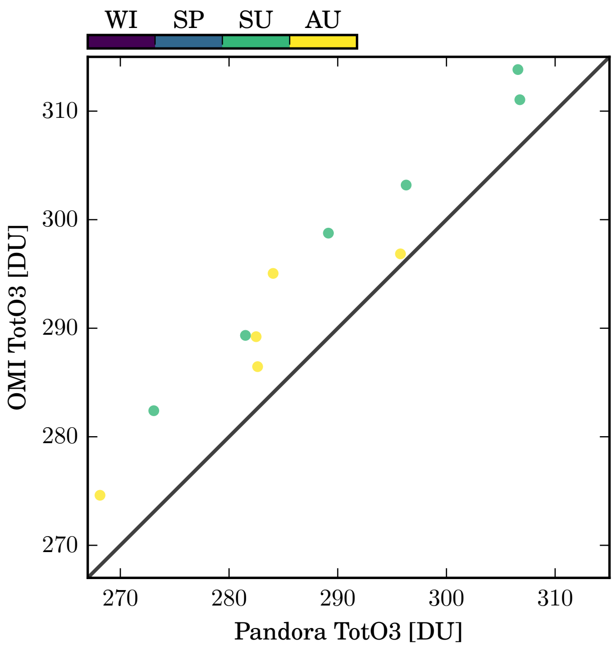

longitude, latitude	-95.425, 30.350
num data points	11
max Pan. (Pans.)	1 (31)
CC	0.97
RMS	2.56 DU
SLP	0.92 ± 0.07
mean	6.76 DU
MEDD	6.90 DU
25-75 perc. range	5.39 DU to 8.58 DU
10-90 perc. range	3.83 DU to 9.62 DU
min-max range	1.08 DU to 10.99 DU
OMI CF	47.87 %
Pandora DQ0	50.16 %

Corcoran

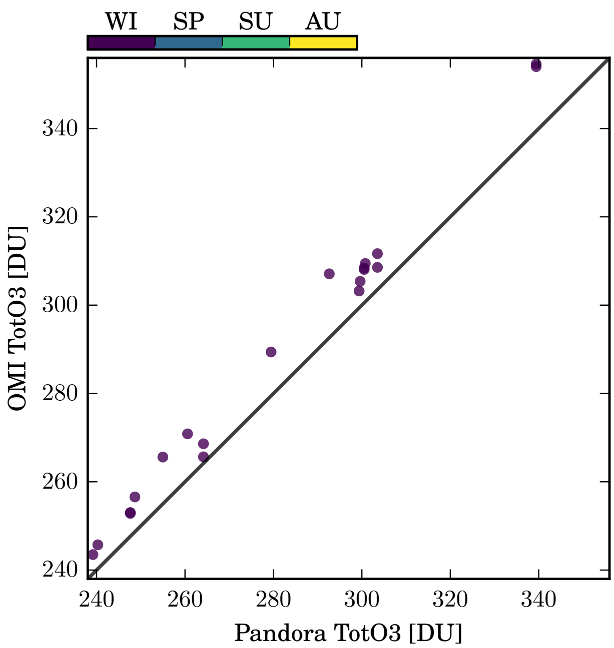

longitude, latitude	-119.5656, 36.1022
num data points	20
max Pan. (Pans.)	1 (34)
CC	1.00
RMS	3.12 DU
SLP	1.07 ± 0.02
mean	7.81 DU
MEDD	7.73 DU
25-75 perc. range	5.17 DU to 10.01 DU
10-90 perc. range	4.29 DU to 14.47 DU
min-max range	1.47 DU to 15.17 DU
OMI CF	58.54 %
Pandora DQ0	57.48 %

Corcoran*

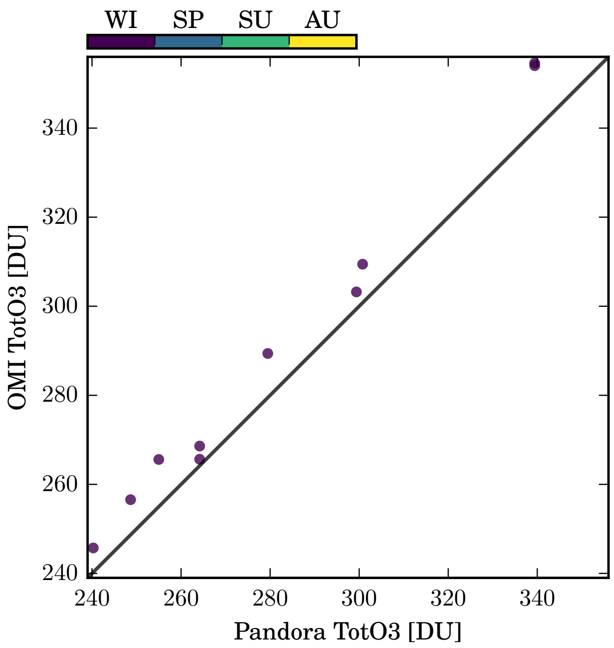

longitude, latitude	-119.5656, 36.1022
num data points	10
max Pan. (Pans.)	1 (34)
CC	1.00
RMS	3.27 DU
SLP	1.08 ± 0.03
mean	8.20 DU
MEDD	8.28 DU
25-75 perc. range	4.68 DU to 10.43 DU
10-90 perc. range	3.61 DU to 14.65 DU
min-max range	1.47 DU to 15.17 DU
OMI CF	58.54 %
Pandora DQ0	57.48 %

DC3

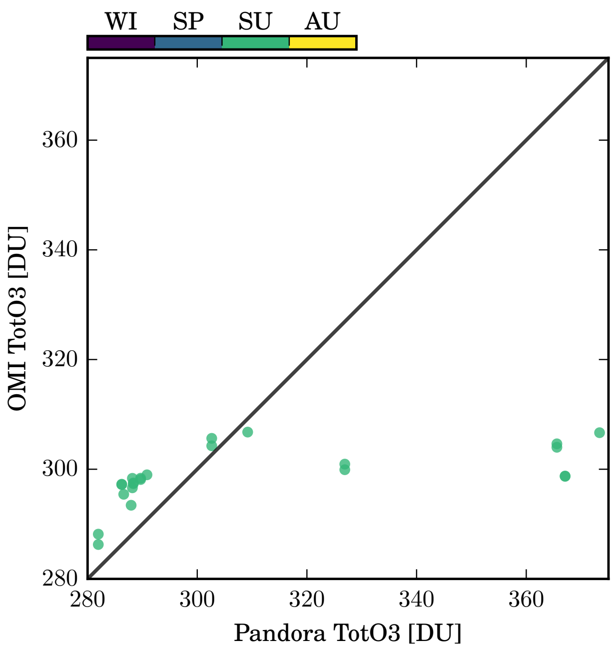

longitude, latitude	-97.3855, 38.4746
num data points	23
max Pan. (Pans.)	1 (17)
CC	0.56
RMS	4.21 DU
SLP	0.09 ± 0.03
mean	-11.64 DU
MEDD	5.49 DU
25-75 perc. range	-26.49 DU to 8.76 DU
10-90 perc. range	-65.68 DU to 9.97 DU
min-max range	-68.39 DU to 11.03 DU
OMI CF	81.90 %
Pandora DQ0	47.06 %

Deerpark

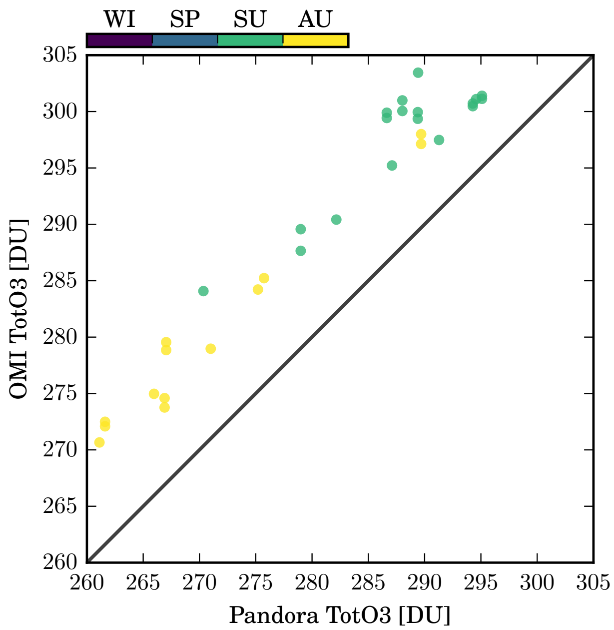

longitude, latitude	-95.1283, 29.6700
num data points	31
max Pan. (Pans.)	1 (32)
CC	0.98
RMS	2.36 DU
SLP	0.94 ± 0.04
mean	9.47 DU
MEDD	9.03 DU
25-75 perc. range	7.56 DU to 11.34 DU
10-90 perc. range	6.30 DU to 12.97 DU
min-max range	6.03 DU to 14.03 DU
OMI CF	40.00 %
Pandora DQ0	44.32 %

Deerpark*

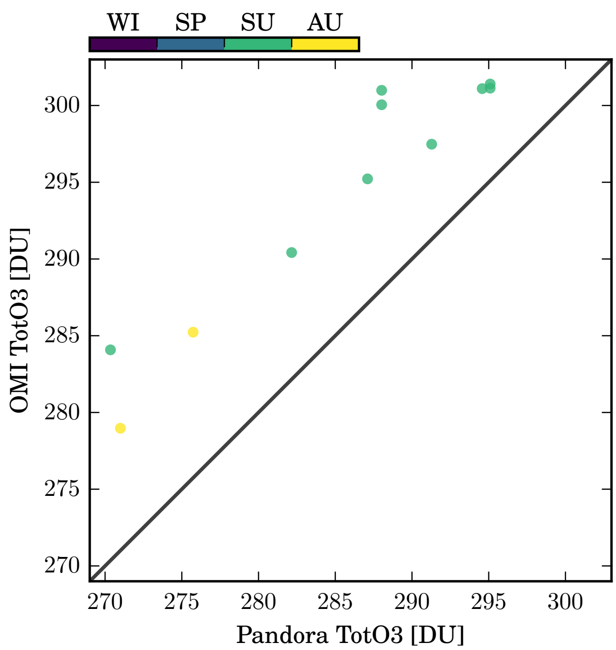

longitude, latitude	-95.1283, 29.6700
num data points	11
max Pan. (Pans.)	1 (32)
CC	0.96
RMS	2.30 DU
SLP	0.84 ± 0.09
mean	8.88 DU
MEDD	8.12 DU
25-75 perc. range	6.42 DU to 10.76 DU
10-90 perc. range	6.20 DU to 12.97 DU
min-max range	6.03 DU to 13.73 DU
OMI CF	40.00 %
Pandora DQ0	44.32 %

DenverI25

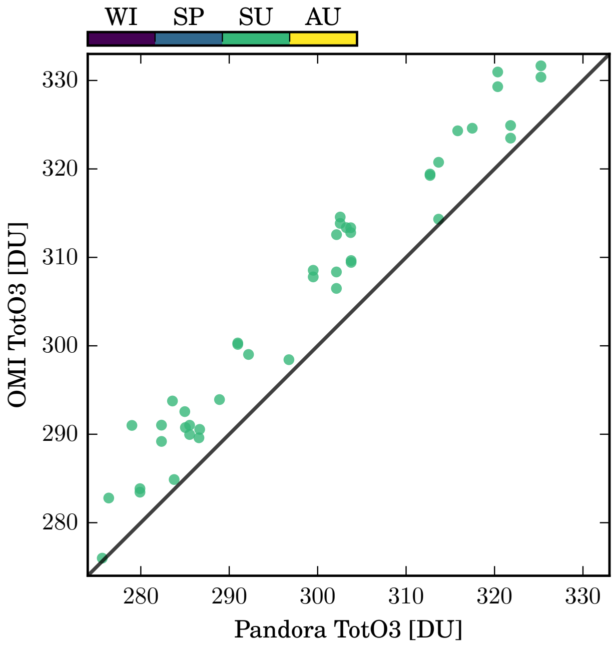

longitude, latitude	-105.015, 39.732
num data points	44
max Pan. (Pans.)	1 (27)
CC	0.98
RMS	3.04 DU
SLP	1.02 ± 0.03
mean	6.58 DU
MEDD	6.63 DU
25-75 perc. range	4.43 DU to 9.05 DU
10-90 perc. range	2.08 DU to 10.36 DU
min-max range	0.35 DU to 12.01 DU
OMI CF	40.48 %
Pandora DQ0	43.27 %

DenverI25*

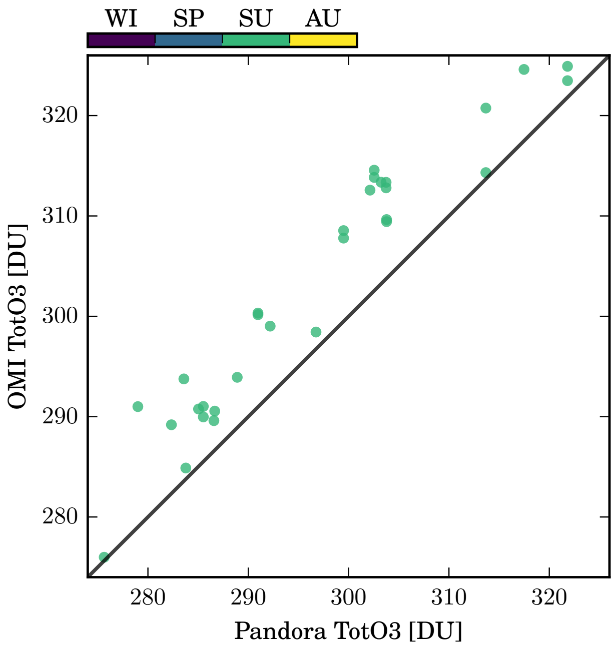

longitude, latitude	-105.015, 39.732
num data points	30
max Pan. (Pans.)	1 (27)
CC	0.96
RMS	3.44 DU
SLP	1.00 ± 0.05
mean	6.54 DU
MEDD	6.84 DU
25-75 perc. range	4.03 DU to 9.31 DU
10-90 perc. range	1.61 DU to 10.52 DU
min-max range	0.35 DU to 12.01 DU
OMI CF	40.48 %
Pandora DQ0	43.27 %

DoiAngKhang

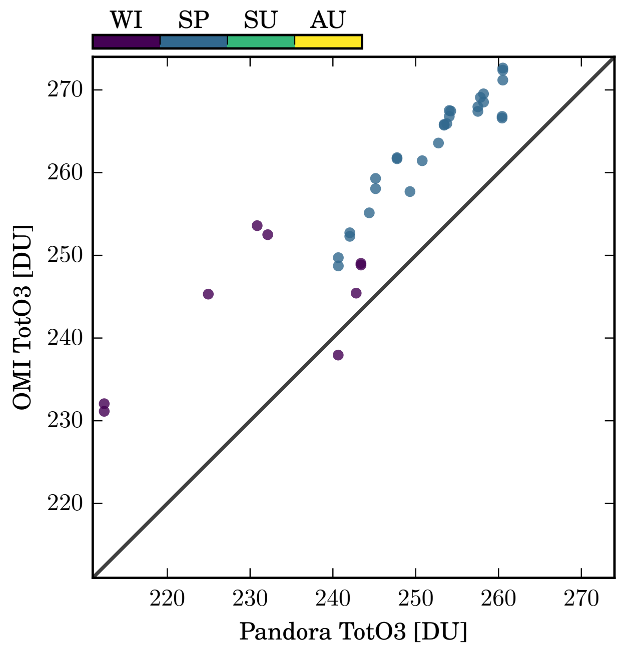

longitude, latitude	99.04526, 19.9332
num data points	37
max Pan. (Pans.)	2 (16, 42)
CC	0.92
RMS	4.36 DU
SLP	0.82 ± 0.06
mean	11.45 DU
MEDD	11.30 DU
25-75 perc. range	9.91 DU to 13.22 DU
10-90 perc. range	5.96 DU to 19.12 DU
min-max range	-2.70 DU to 22.74 DU
OMI CF	36.46 %
Pandora DQ0	47.22 %

DoiAngKhang*

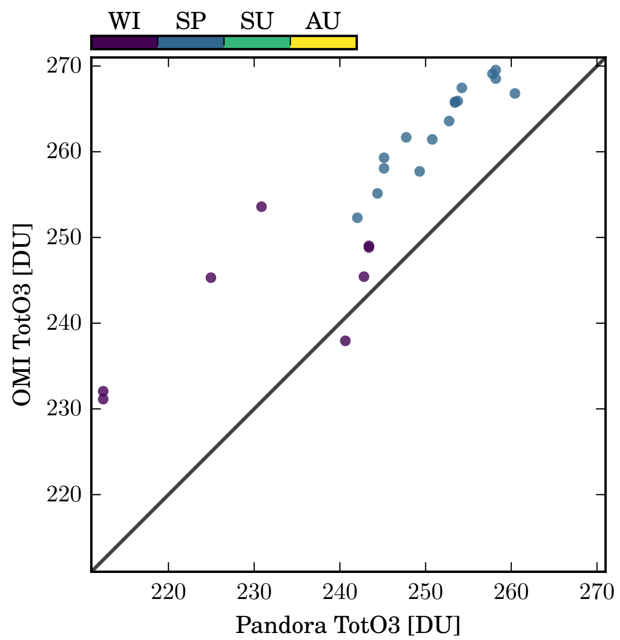

longitude, latitude	99.04526, 19.9332
num data points	24
max Pan. (Pans.)	2 (16, 42)
CC	0.90
RMS	4.86 DU
SLP	0.79 ± 0.08
mean	11.41 DU
MEDD	11.32 DU
25-75 perc. range	9.80 DU to 13.40 DU
10-90 perc. range	5.50 DU to 19.40 DU
min-max range	-2.70 DU to 22.74 DU
OMI CF	36.46 %
Pandora DQ0	47.22 %

Essex

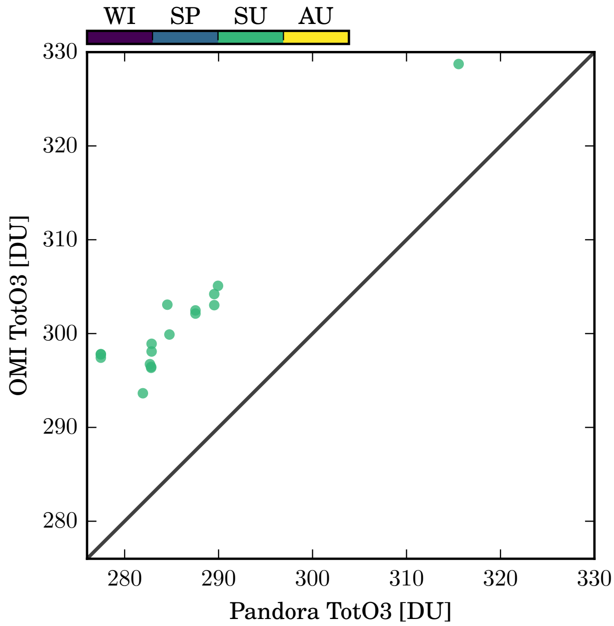

longitude, latitude	-76.474444, 39.310833
num data points	17
max Pan. (Pans.)	1 (19)
CC	0.95
RMS	2.25 DU
SLP	0.86 ± 0.07
mean	15.56 DU
MEDD	14.93 DU
25-75 perc. range	13.64 DU to 16.04 DU
10-90 perc. range	13.37 DU to 20.10 DU
min-max range	11.70 DU to 20.34 DU
OMI CF	48.39 %
Pandora DQ0	54.50 %

Essex*

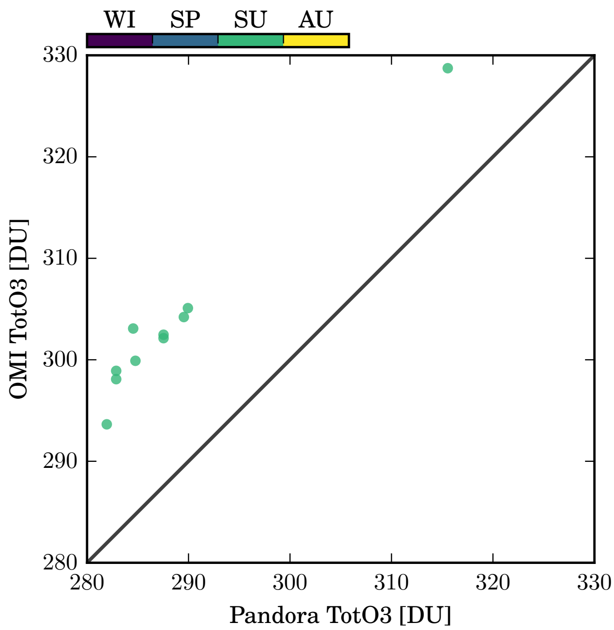

longitude, latitude	-76.474444, 39.310833
num data points	10
max Pan. (Pans.)	1 (19)
CC	0.98
RMS	1.59 DU
SLP	0.94 ± 0.06
mean	14.92 DU
MEDD	15.03 DU
25-75 perc. range	14.61 DU to 15.20 DU
10-90 perc. range	13.04 DU to 16.29 DU
min-max range	11.70 DU to 18.53 DU
OMI CF	48.39 %
Pandora DQ0	54.50 %

FMI

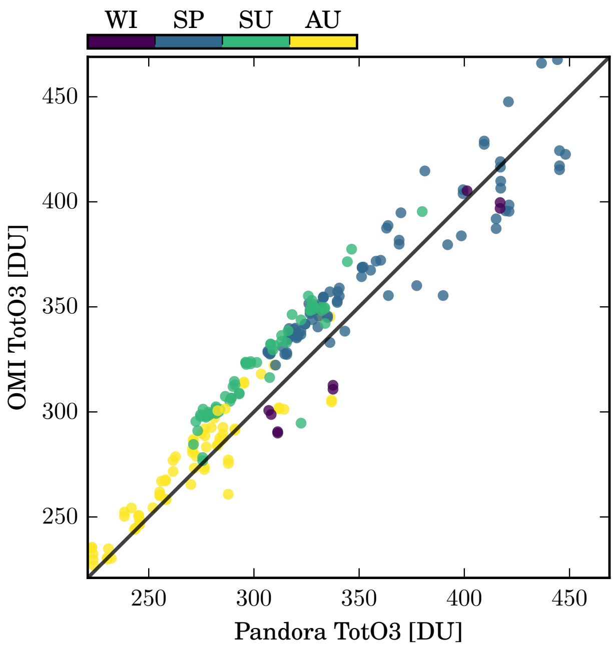

longitude, latitude	24.9612, 60.2037
num data points	235
max Pan. (Pans.)	1 (21)
CC	0.96
RMS	14.06 DU
SLP	0.93 ± 0.02
mean	9.80 DU
MEDD	14.73 DU
25-75 perc. range	2.53 DU to 20.04 DU
10-90 perc. range	-12.43 DU to 23.34 DU
min-max range	-34.53 DU to 33.46 DU
OMI CF	43.86 %
Pandora DQ0	30.23 %

FMI*

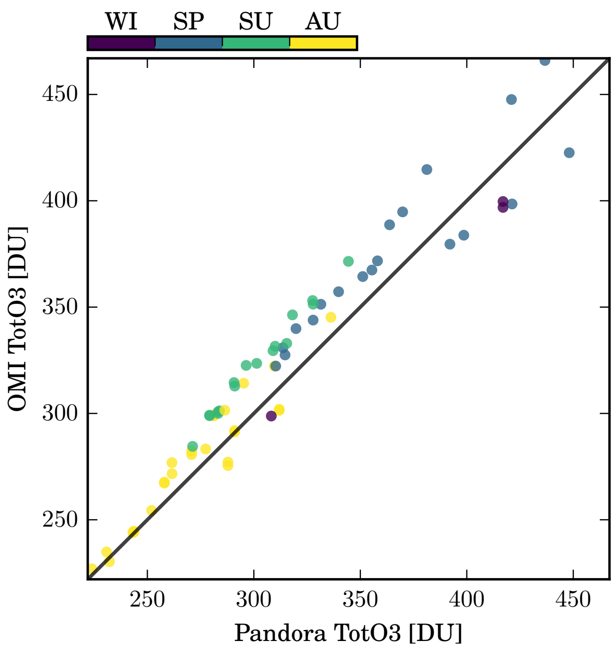

longitude, latitude	24.9612, 60.2037
num data points	65
max Pan. (Pans.)	1 (21)
CC	0.96
RMS	13.86 DU
SLP	0.97 ± 0.03
mean	10.23 DU
MEDD	13.27 DU
25-75 perc. range	0.98 DU to 19.94 DU
10-90 perc. range	-11.68 DU to 25.29 DU
min-max range	-25.50 DU to 33.46 DU
OMI CF	43.86 %
Pandora DQ0	30.23 %

FSU

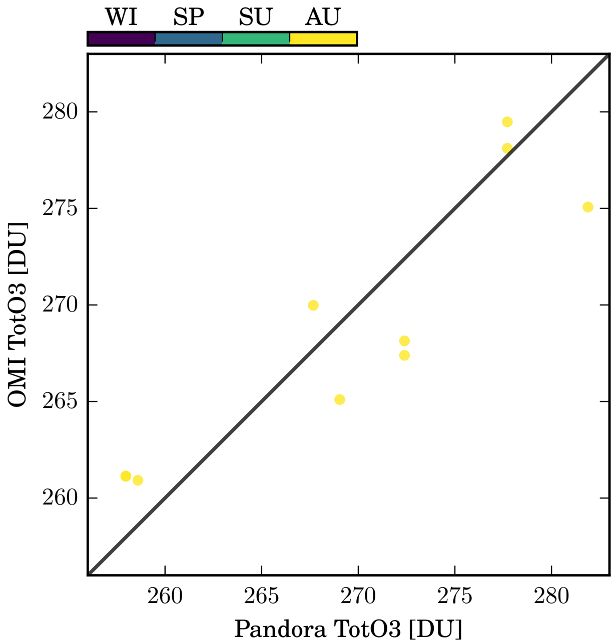

longitude, latitude	-78.9329, 39.6511
num data points	10
max Pan. (Pans.)	3 (2, 3, 9)
CC	0.90
RMS	2.82 DU
SLP	0.72 ± 0.12
mean	-0.69 DU
MEDD	1.08 DU
25-75 perc. range	-4.17 DU to 2.32 DU
10-90 perc. range	-5.18 DU to 3.16 DU
min-max range	-6.82 DU to 3.17 DU
OMI CF	81.82 %
Pandora DQ0	26.10 %

Fairhill

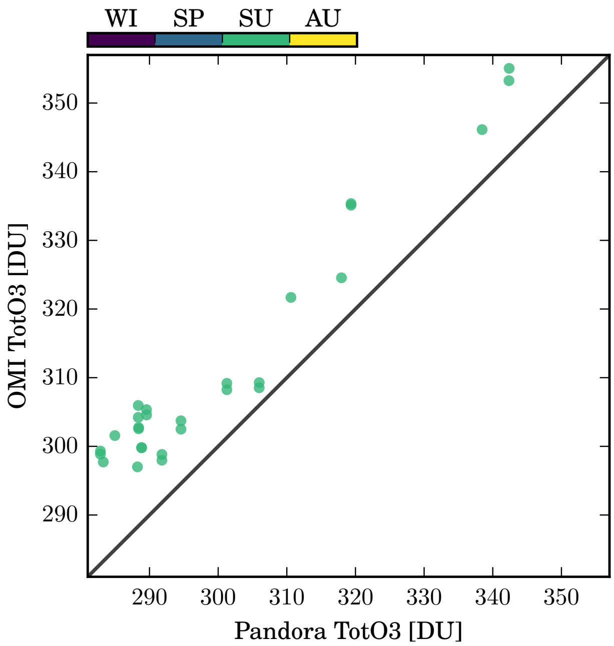

longitude, latitude	-75.868, 39.701111
num data points	28
max Pan. (Pans.)	1 (16)
CC	0.97
RMS	4.14 DU
SLP	0.94 ± 0.05
mean	11.38 DU
MEDD	11.04 DU
25-75 perc. range	7.86 DU to 15.77 DU
10-90 perc. range	6.47 DU to 16.15 DU
min-max range	2.55 DU to 17.59 DU
OMI CF	39.44 %
Pandora DQ0	53.69 %

Fairhill*

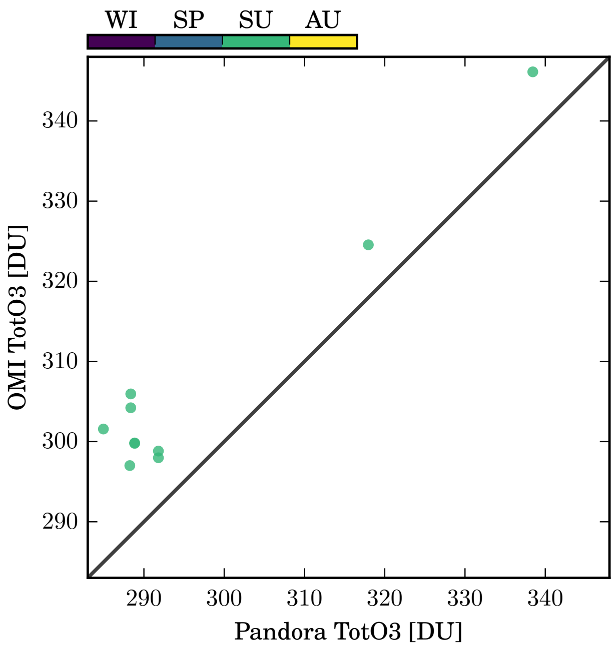

longitude, latitude	-75.868, 39.701111
num data points	10
max Pan. (Pans.)	1 (16)
CC	0.97
RMS	3.64 DU
SLP	0.88 ± 0.08
mean	10.82 DU
MEDD	9.85 DU
25-75 perc. range	7.18 DU to 14.64 DU
10-90 perc. range	6.55 DU to 16.72 DU
min-max range	6.18 DU to 17.59 DU
OMI CF	39.44 %
Pandora DQ0	53.69 %

FourCornersNM

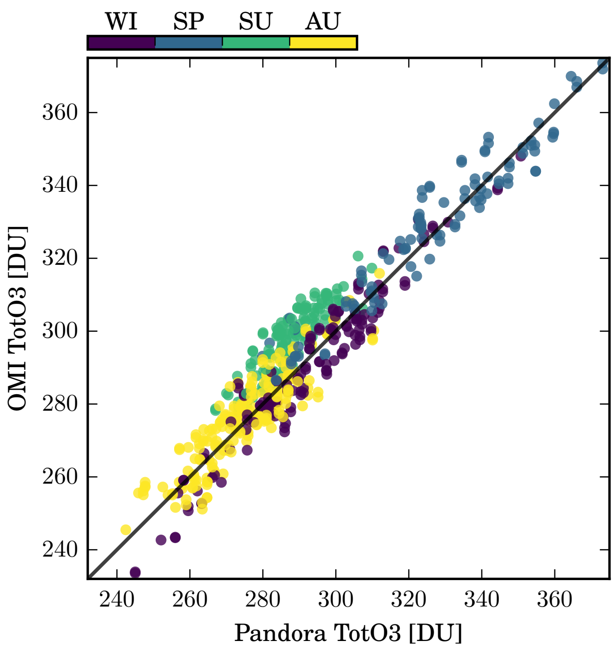

longitude, latitude	-108.480, 36.797
num data points	597
max Pan. (Pans.)	1 (23)
CC	0.96
RMS	7.01 DU
SLP	0.98 ± 0.01
mean	2.58 DU
MEDD	2.79 DU
25-75 perc. range	-2.68 DU to 7.64 DU
10-90 perc. range	-6.41 DU to 11.92 DU
min-max range	-13.61 DU to 19.52 DU
OMI CF	60.10 %
Pandora DQ0	50.47 %

FourCornersNM*

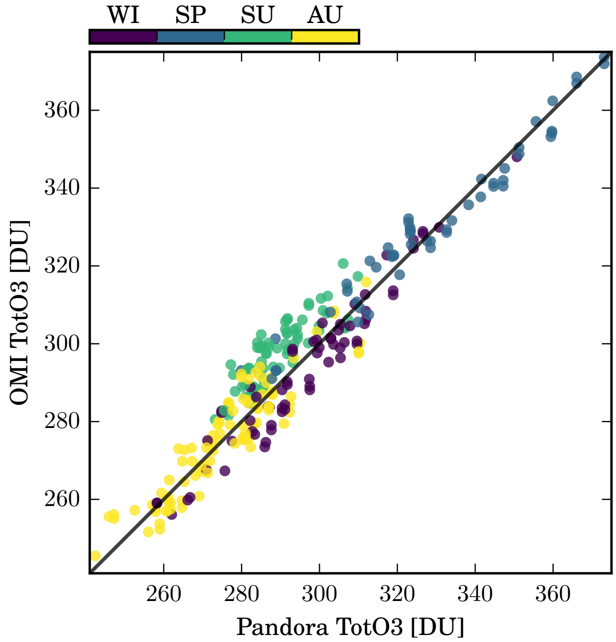

longitude, latitude	-108.480, 36.797
num data points	290
max Pan. (Pans.)	1 (23)
CC	0.96
RMS	6.47 DU
SLP	0.96 ± 0.02
mean	1.85 DU
MEDD	2.28 DU
25-75 perc. range	-3.38 DU to 6.50 DU
10-90 perc. range	-6.40 DU to 10.97 DU
min-max range	-12.52 DU to 17.39 DU
OMI CF	60.10 %
Pandora DQ0	50.47 %

Fresno

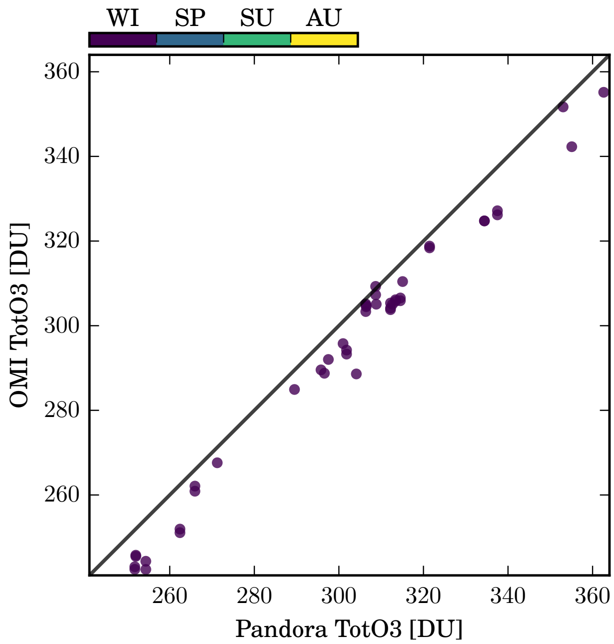

longitude, latitude	-119.7731, 36.7854
num data points	44
max Pan. (Pans.)	2 (30, 31)
CC	0.99
RMS	3.50 DU
SLP	1.01 ± 0.02
mean	-6.72 DU
MEDD	-7.37 DU
25-75 perc. range	-8.85 DU to -3.83 DU
10-90 perc. range	-11.06 DU to -1.76 DU
min-max range	-15.53 DU to 0.60 DU
OMI CF	45.10 %
Pandora DQ0	36.52 %

Fresno*

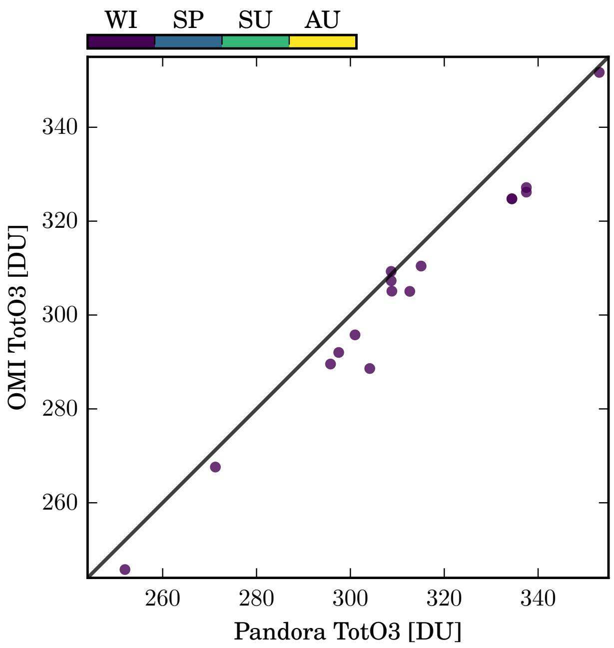

longitude, latitude	-119.7731, 36.7854
num data points	16
max Pan. (Pans.)	2 (30, 31)
CC	0.99
RMS	4.01 DU
SLP	0.97 ± 0.04
mean	-6.34 DU
MEDD	-5.84 DU
25-75 perc. range	-9.65 DU to -3.72 DU
10-90 perc. range	-10.82 DU to -1.37 DU
min-max range	-15.53 DU to 0.60 DU
OMI CF	45.10 %
Pandora DQ0	36.52 %

GIST

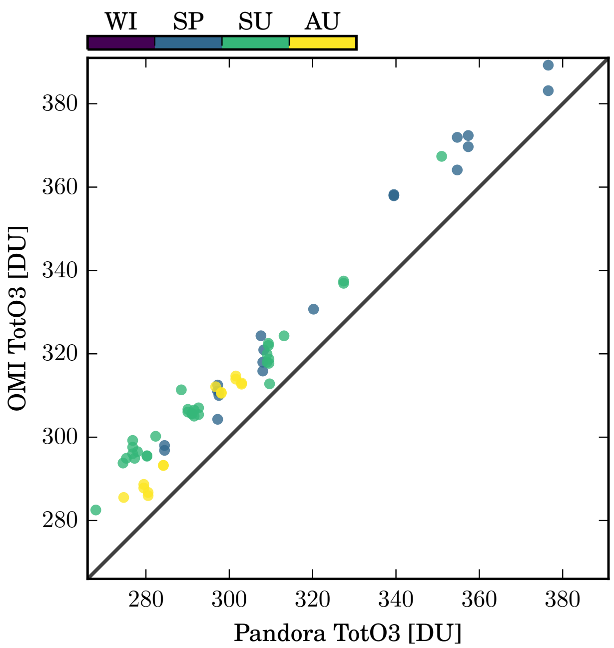

longitude, latitude	126.843, 35.226
num data points	66
max Pan. (Pans.)	1 (26)
CC	0.99
RMS	4.12 DU
SLP	0.98 ± 0.02
mean	13.22 DU
MEDD	12.95 DU
25-75 perc. range	9.97 DU to 15.81 DU
10-90 perc. range	8.27 DU to 18.64 DU
min-max range	3.13 DU to 22.87 DU
OMI CF	38.68 %
Pandora DQ0	32.58 %

GIST*

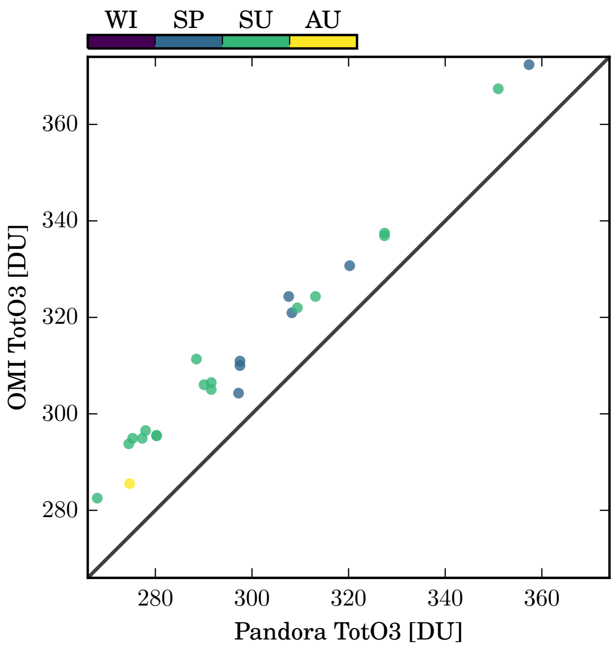

longitude, latitude	126.843, 35.226
num data points	24
max Pan. (Pans.)	1 (26)
CC	0.99
RMS	3.38 DU
SLP	0.95 ± 0.03
mean	14.41 DU
MEDD	14.73 DU
25-75 perc. range	12.17 DU to 16.49 DU
10-90 perc. range	10.16 DU to 19.07 DU
min-max range	7.08 DU to 22.87 DU
OMI CF	38.68 %
Pandora DQ0	32.58 %

GSFC

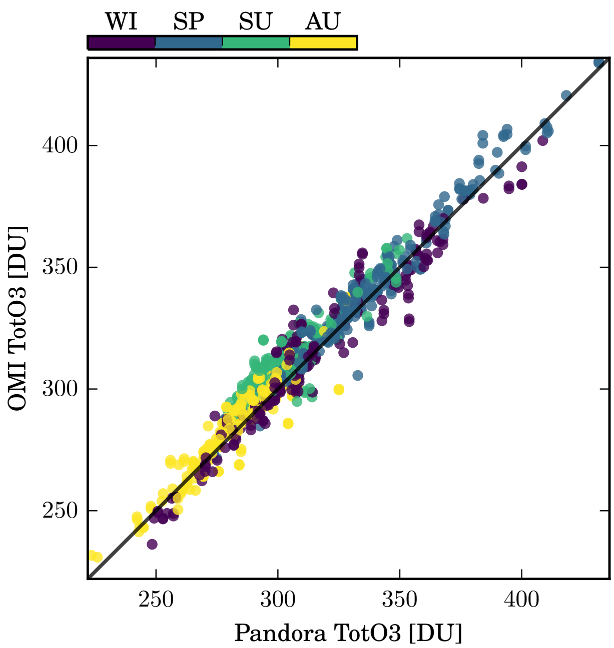

longitude, latitude	-76.8396, 38.9926
num data points	867
max Pan. (Pans.)	11 (18, 19, 21, 25, 26, 28, 2, 3, 43, 7, 9), not all considered!
CC	0.97
RMS	7.25 DU
SLP	0.97 ± 0.01
mean	3.31 DU
MEDD	3.18 DU
25-75 perc. range	-1.00 DU to 8.23 DU
10-90 perc. range	-5.45 DU to 12.12 DU
min-max range	-27.21 DU to 26.18 DU
OMI CF	41.42 %
Pandora DQ0	26.89 %

GSFC*

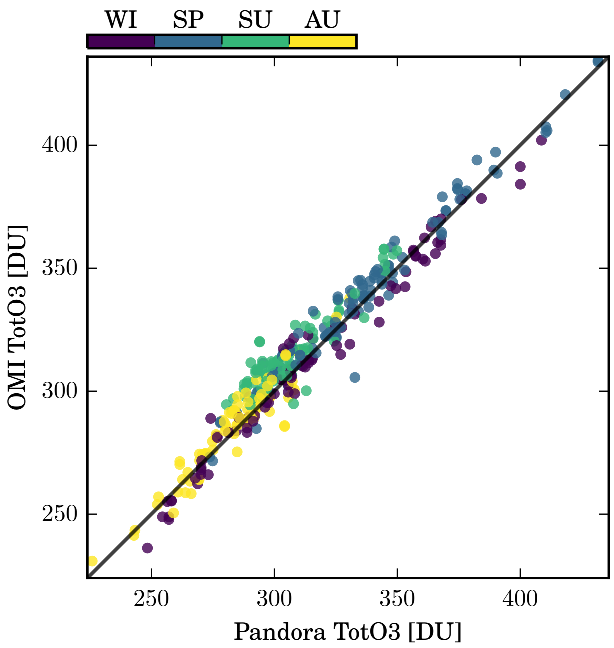

longitude, latitude	-76.8396, 38.9926
num data points	378
max Pan. (Pans.)	11 (18, 19, 21, 25, 26, 28, 2, 3, 43, 7, 9), not all considered!
CC	0.98
RMS	7.00 DU
SLP	0.97 ± 0.01
mean	3.16 DU
MEDD	3.13 DU
25-75 perc. range	-1.29 DU to 7.93 DU
10-90 perc. range	-5.77 DU to 11.72 DU
min-max range	-27.21 DU to 26.18 DU
OMI CF	41.42 %
Pandora DQ0	26.89 %

Galveston

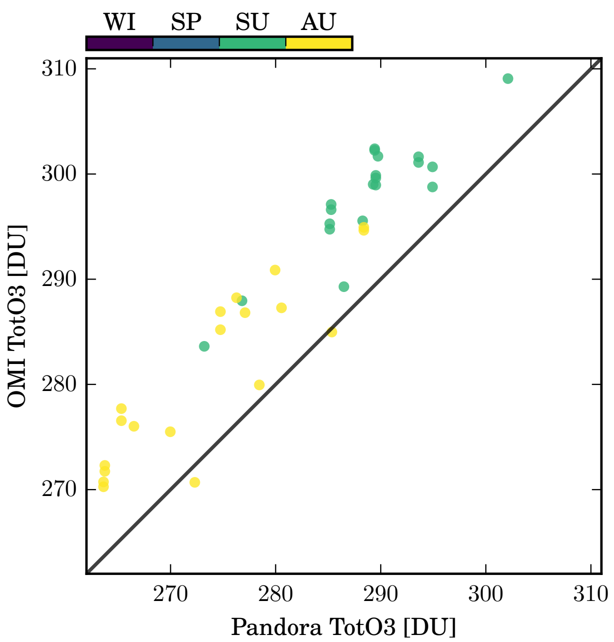

longitude, latitude	-94.8612, 29.2544
num data points	39
max Pan. (Pans.)	1 (34)
CC	0.95
RMS	3.49 DU
SLP	0.98 ± 0.06
mean	8.39 DU
MEDD	9.51 DU
25-75 perc. range	6.69 DU to 11.04 DU
10-90 perc. range	3.63 DU to 12.00 DU
min-max range	-1.62 DU to 12.98 DU
OMI CF	51.28 %
Pandora DQ0	55.86 %

Galveston*

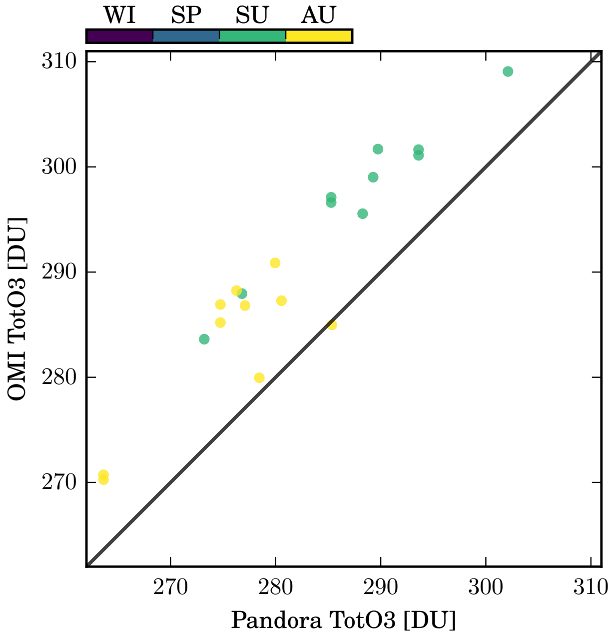

longitude, latitude	-94.8612, 29.2544
num data points	20
max Pan. (Pans.)	1 (34)
CC	0.94
RMS	3.31 DU
SLP	0.98 ± 0.08
mean	8.65 DU
MEDD	9.74 DU
25-75 perc. range	7.07 DU to 11.20 DU
10-90 perc. range	6.13 DU to 11.96 DU
min-max range	-0.37 DU to 12.17 DU
OMI CF	51.28 %
Pandora DQ0	55.86 %

Golden

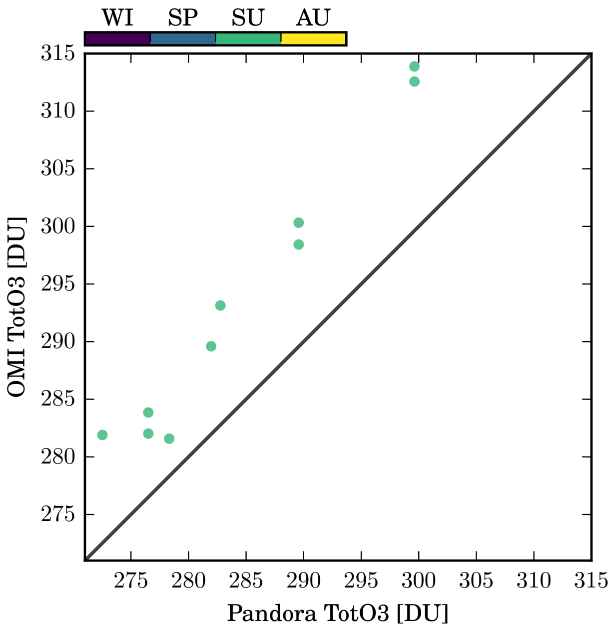

longitude, latitude	-105.1779, 39.7437
num data points	10
max Pan. (Pans.)	1 (38)
CC	0.99
RMS	1.98 DU
SLP	1.27 ± 0.08
mean	9.03 DU
MEDD	9.12 DU
25-75 perc. range	7.41 DU to 10.66 DU
10-90 perc. range	5.28 DU to 13.08 DU
min-max range	3.26 DU to 14.26 DU
OMI CF	21.57 %
Pandora DQ0	40.63 %

HUFS

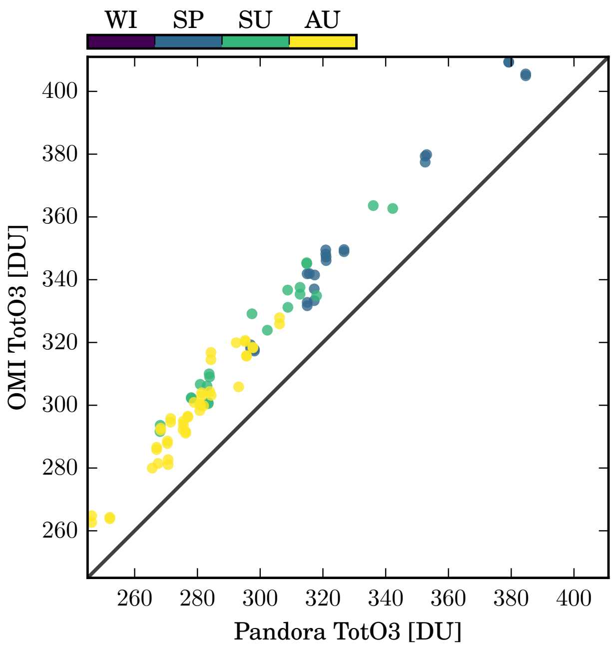

longitude, latitude	127.265, 37.338
num data points	89
max Pan. (Pans.)	1 (18)
CC	0.99
RMS	4.38 DU
SLP	1.07 ± 0.02
mean	21.68 DU
MEDD	21.62 DU
25-75 perc. range	18.47 DU to 25.08 DU
10-90 perc. range	15.96 DU to 27.65 DU
min-max range	10.41 DU to 32.49 DU
OMI CF	38.55 %
Pandora DQ0	30.33 %

HUFS*

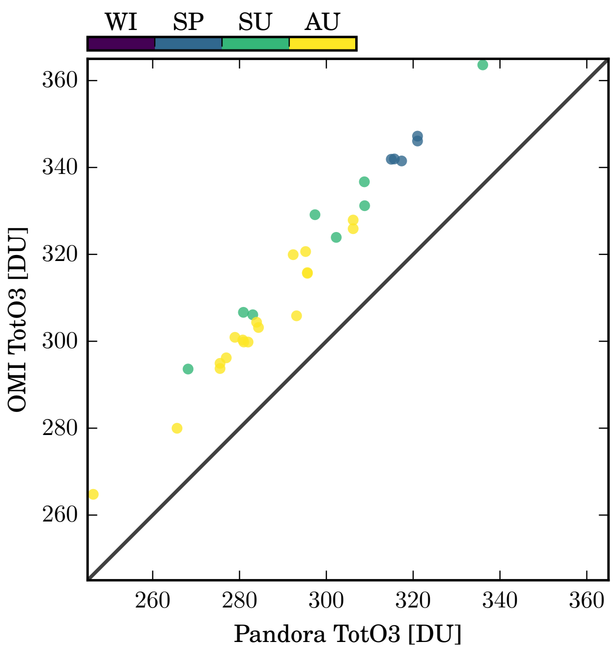

longitude, latitude	127.265, 37.338
num data points	31
max Pan. (Pans.)	1 (18)
CC	0.99
RMS	3.55 DU
SLP	1.12 ± 0.03
mean	22.22 DU
MEDD	21.72 DU
25-75 perc. range	19.33 DU to 25.61 DU
10-90 perc. range	18.22 DU to 27.57 DU
min-max range	12.72 DU to 31.74 DU
OMI CF	38.55 %
Pandora DQ0	30.33 %

Hanford

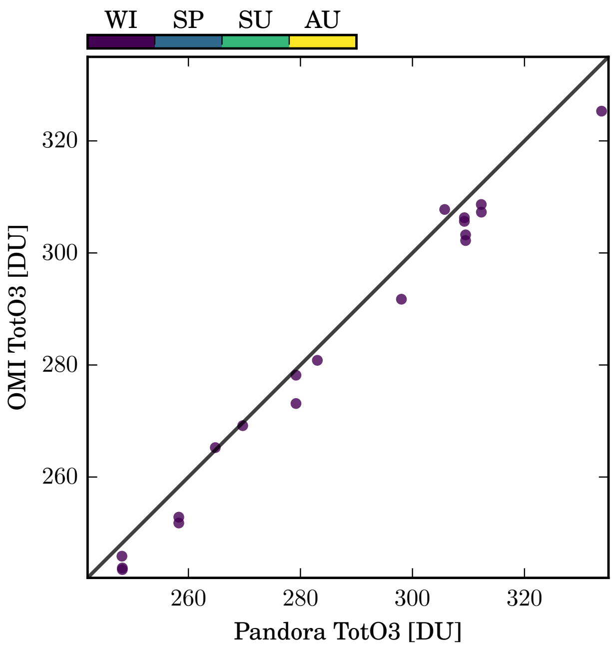

longitude, latitude	-119.6433, 36.3193
num data points	19
max Pan. (Pans.)	2 (18, 32)
CC	0.99
RMS	2.64 DU
SLP	0.98 ± 0.02
mean	-3.91 DU
MEDD	-4.44 DU
25-75 perc. range	-6.17 DU to -2.23 DU
10-90 perc. range	-6.65 DU to -0.33 DU
min-max range	-8.45 DU to 2.01 DU
OMI CF	46.88 %
Pandora DQ0	51.57 %

Huron

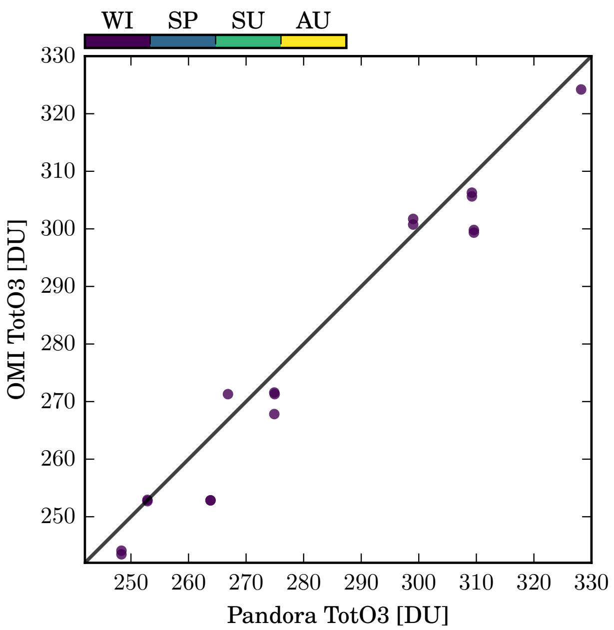

longitude, latitude	-120.105, 36.206
num data points	17
max Pan. (Pans.)	1 (2)
CC	0.98
RMS	4.60 DU
SLP	0.99 ± 0.05
mean	-3.93 DU
MEDD	-3.67 DU
25-75 perc. range	-7.07 DU to -0.15 DU
10-90 perc. range	-10.53 DU to 2.12 DU
min-max range	-10.98 DU to 4.44 DU
OMI CF	66.67 %
Pandora DQ0	62.34 %

IBK

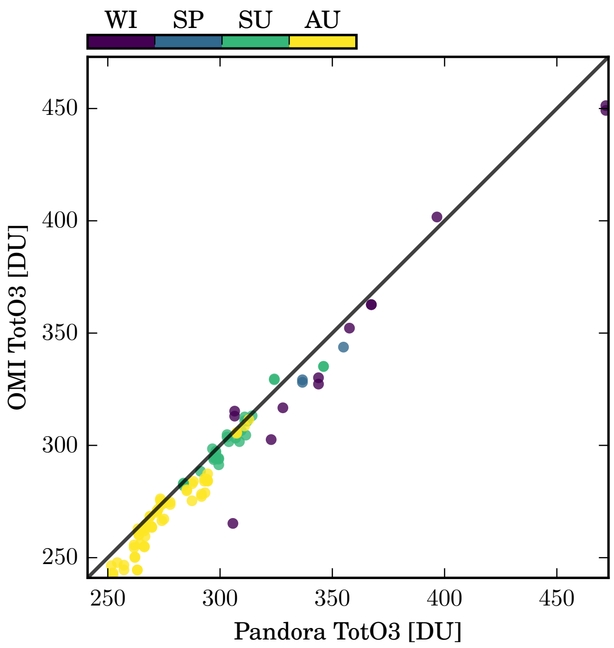

longitude, latitude	11.3852, 47.2643
num data points	106
max Pan. (Pans.)	2 (106, 110)
CC	0.98
RMS	6.62 DU
SLP	0.97 ± 0.02
mean	-5.80 DU
MEDD	-4.67 DU
25-75 perc. range	-9.11 DU to -1.40 DU
10-90 perc. range	-13.04 DU to 0.31 DU
min-max range	-40.46 DU to 8.75 DU
OMI CF	20.35 %
Pandora DQ0	38.58 %

IBK*

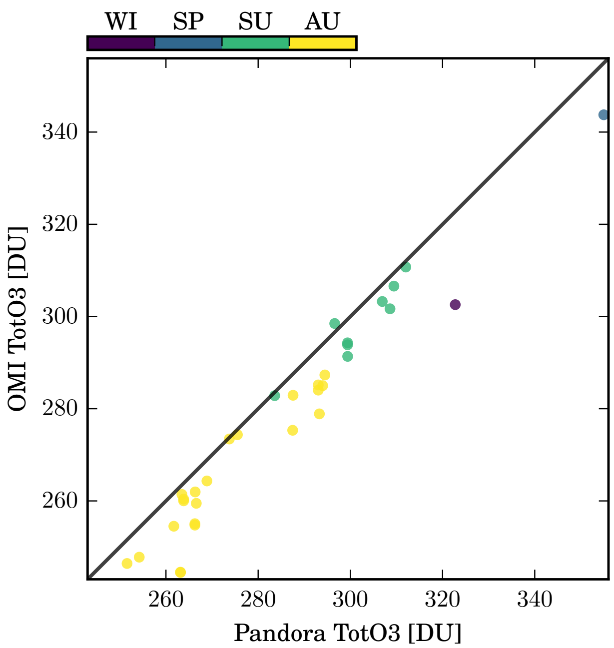

longitude, latitude	11.3852, 47.2643
num data points	33
max Pan. (Pans.)	2 (106, 110)
CC	0.97
RMS	5.28 DU
SLP	0.98 ± 0.04
mean	-7.08 DU
MEDD	-6.41 DU
25-75 perc. range	-9.01 DU to -3.68 DU
10-90 perc. range	-13.96 DU to -1.17 DU
min-max range	-20.19 DU to 1.87 DU
OMI CF	20.35 %
Pandora DQ0	38.58 %

IZO

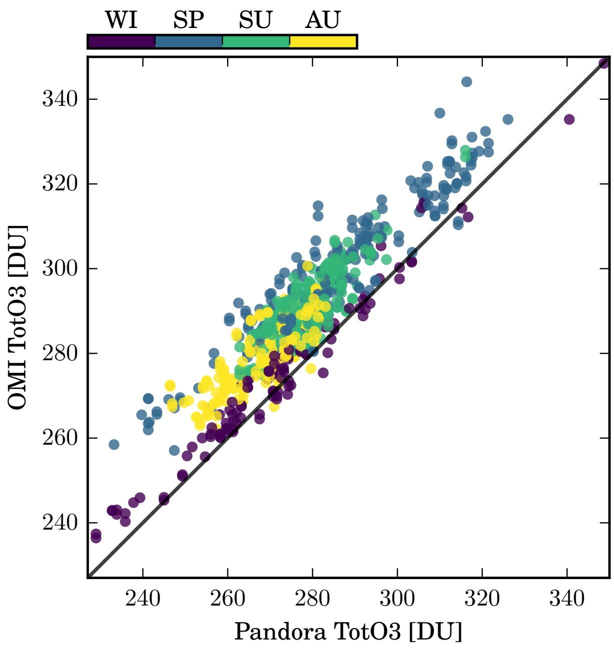

longitude, latitude	-16.4994, 28.309
num data points	744
max Pan. (Pans.)	1 (101)
CC	0.92
RMS	6.47 DU
SLP	0.92 ± 0.01
mean	11.26 DU
MEDD	11.14 DU
25-75 perc. range	6.57 DU to 15.73 DU
10-90 perc. range	2.63 DU to 19.69 DU
min-max range	-7.13 DU to 33.52 DU
OMI CF	54.11 %
Pandora DQ0	69.59 %

IZO*

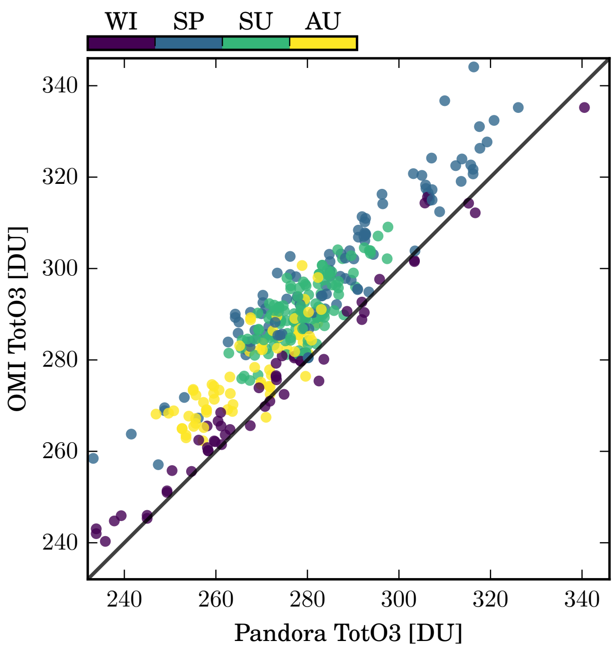

longitude, latitude	-16.4994, 28.309
num data points	348
max Pan. (Pans.)	1 (101)
CC	0.92
RMS	6.53 DU
SLP	0.95 ± 0.02
mean	10.77 DU
MEDD	10.98 DU
25-75 perc. range	6.13 DU to 15.68 DU
10-90 perc. range	1.89 DU to 18.61 DU
min-max range	-7.13 DU to 27.77 DU
OMI CF	54.11 %
Pandora DQ0	69.59 %

LaPorte1

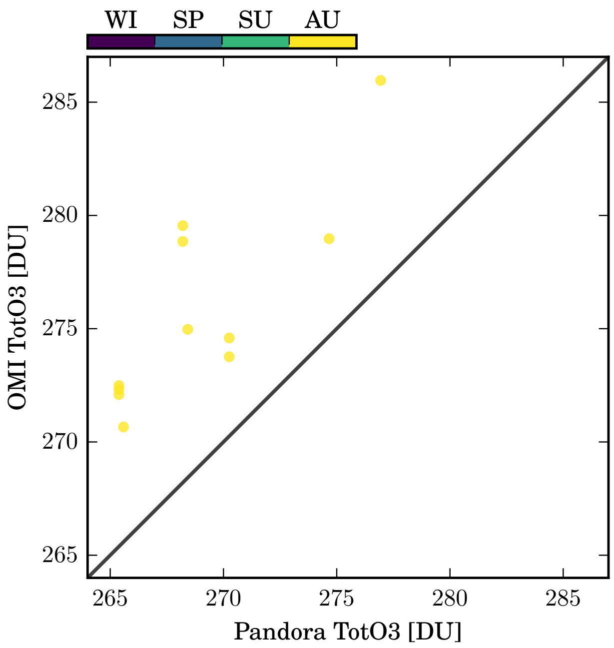

longitude, latitude	-95.0647, 29.672
num data points	11
max Pan. (Pans.)	1 (38)
CC	0.82
RMS	2.46 DU
SLP	0.96 ± 0.22
mean	6.87 DU
MEDD	6.71 DU
25-75 perc. range	4.71 DU to 8.06 DU
10-90 perc. range	4.31 DU to 10.65 DU
min-max range	3.51 DU to 11.35 DU
OMI CF	32.35 %
Pandora DQ0	49.54 %

Langley

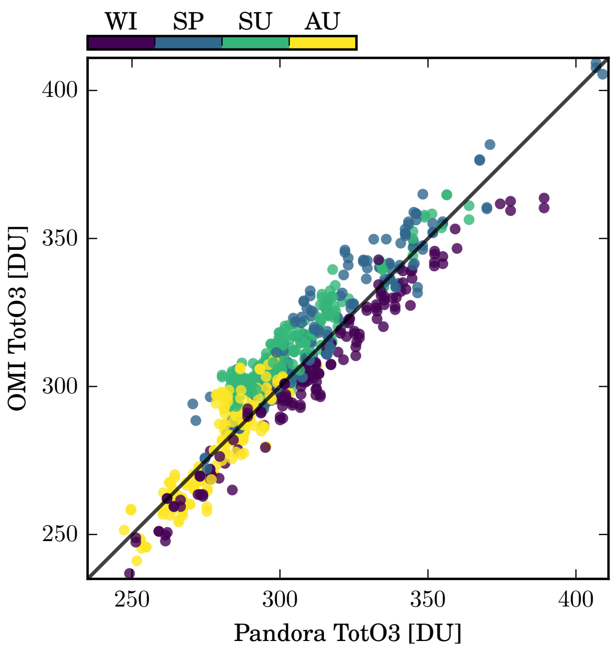

longitude, latitude	-76.3868, 37.1036
num data points	754
max Pan. (Pans.)	3 (37, 39, 6)
CC	0.94
RMS	8.86 DU
SLP	0.97 ± 0.01
mean	2.88 DU
MEDD	2.39 DU
25-75 perc. range	-3.68 DU to 9.75 DU
10-90 perc. range	-8.54 DU to 14.21 DU
min-max range	-28.92 DU to 24.15 DU
OMI CF	51.10 %
Pandora DQ0	23.56 %

Langley*

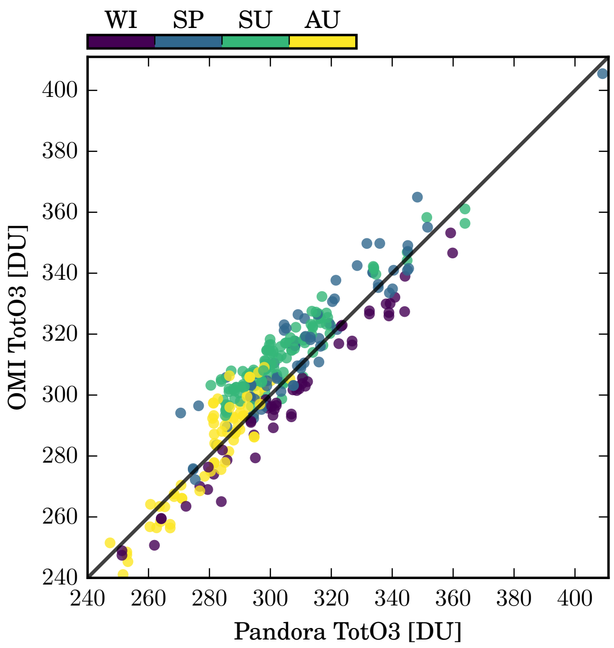

longitude, latitude	-76.3868, 37.1036
num data points	307
max Pan. (Pans.)	3 (37, 39, 6)
CC	0.93
RMS	8.44 DU
SLP	0.98 ± 0.02
mean	3.76 DU
MEDD	4.11 DU
25-75 perc. range	-2.96 DU to 10.27 DU
10-90 perc. range	-7.41 DU to 13.97 DU
min-max range	-18.87 DU to 23.55 DU
OMI CF	51.10 %
Pandora DQ0	23.56 %

Lauder

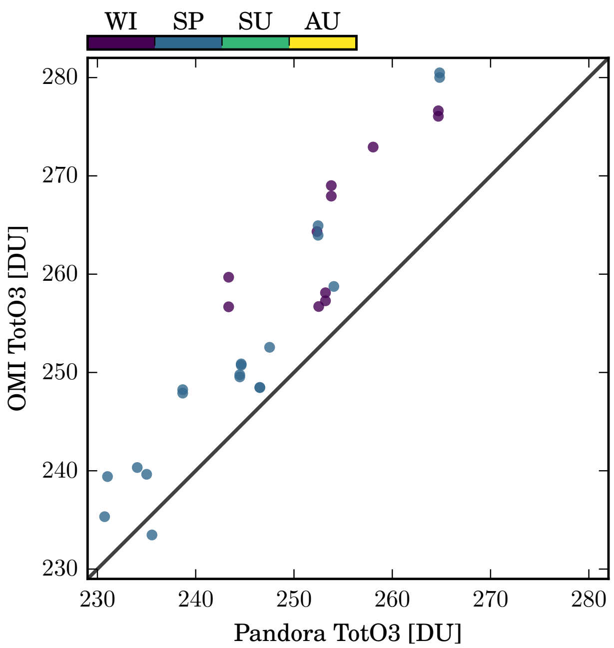

longitude, latitude	169.684, -45.038
num data points	30
max Pan. (Pans.)	1 (37)
CC	0.95
RMS	4.19 DU
SLP	1.25 ± 0.08
mean	8.47 DU
MEDD	7.33 DU
25-75 perc. range	4.75 DU to 12.36 DU
10-90 perc. range	3.87 DU to 15.19 DU
min-max range	-2.08 DU to 16.34 DU
OMI CF	66.67 %
Pandora DQ0	47.49 %

Lauder*

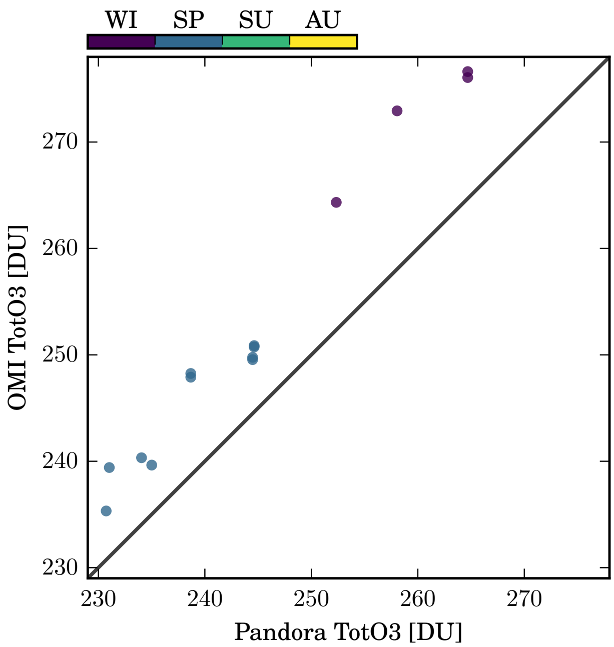

longitude, latitude	169.684, -45.038
num data points	14
max Pan. (Pans.)	1 (37)
CC	0.99
RMS	2.26 DU
SLP	1.20 ± 0.06
mean	8.25 DU
MEDD	7.33 DU
25-75 perc. range	5.49 DU to 10.92 DU
10-90 perc. range	4.76 DU to 11.97 DU
min-max range	4.60 DU to 14.88 DU
OMI CF	66.67 %
Pandora DQ0	47.49 %

Library

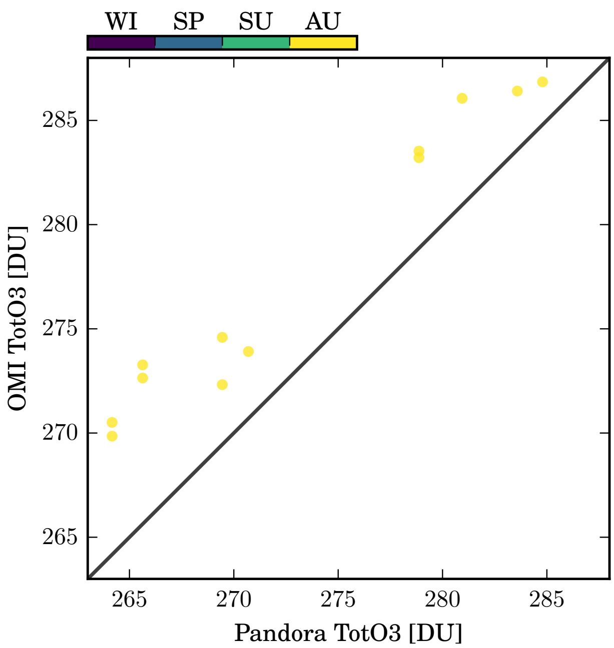

longitude, latitude	-95.657, 29.8334
num data points	12
max Pan. (Pans.)	1 (18)
CC	0.98
RMS	1.24 DU
SLP	0.85 ± 0.05
mean	4.74 DU
MEDD	4.89 DU
25-75 perc. range	3.13 DU to 5.85 DU
10-90 perc. range	2.83 DU to 6.94 DU
min-max range	2.06 DU to 7.64 DU
OMI CF	39.02 %
Pandora DQ0	28.49 %

Madera

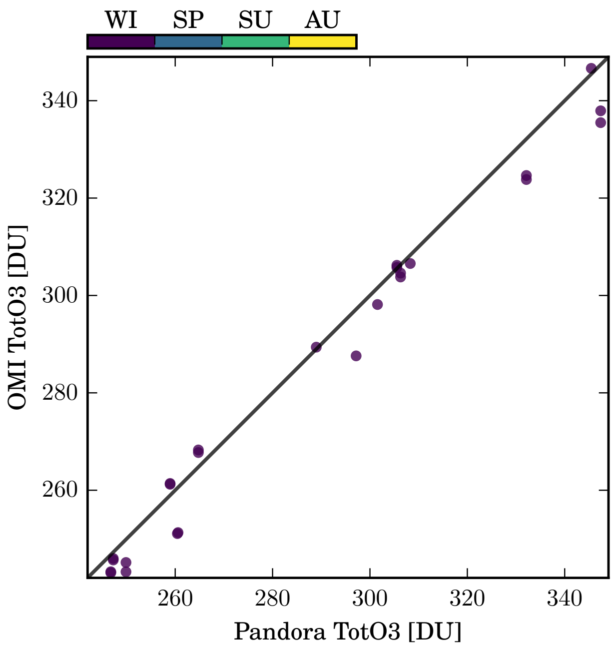

longitude, latitude	-120.0342, 36.9533
num data points	25
max Pan. (Pans.)	1 (29)
CC	0.99
RMS	4.30 DU
SLP	0.96 ± 0.03
mean	-3.30 DU
MEDD	-2.50 DU
25-75 perc. range	-7.49 DU to 0.41 DU
10-90 perc. range	-9.43 DU to 2.37 DU
min-max range	-11.90 DU to 3.51 DU
OMI CF	48.31 %
Pandora DQ0	40.77 %

Madera*

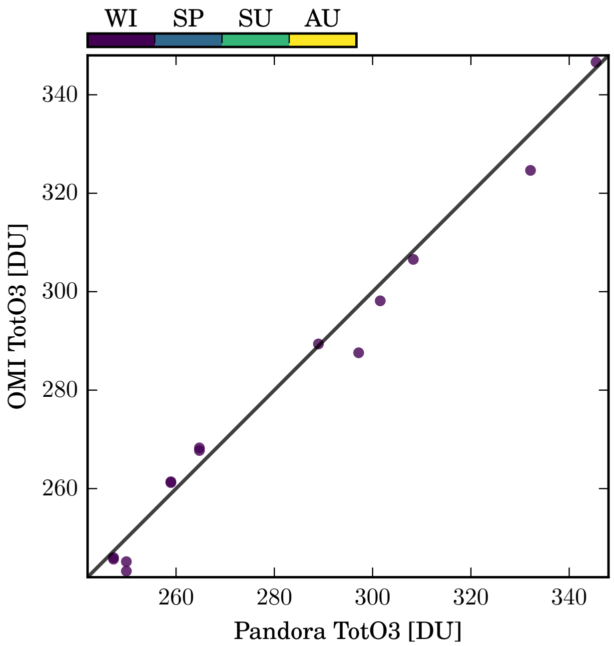

longitude, latitude	-120.0342, 36.9533
num data points	14
max Pan. (Pans.)	1 (29)
CC	0.99
RMS	3.94 DU
SLP	0.97 ± 0.04
mean	-1.69 DU
MEDD	-1.45 DU
25-75 perc. range	-4.40 DU to 2.00 DU
10-90 perc. range	-7.24 DU to 2.82 DU
min-max range	-9.57 DU to 3.51 DU
OMI CF	48.31 %
Pandora DQ0	40.77 %

Manvelcroix

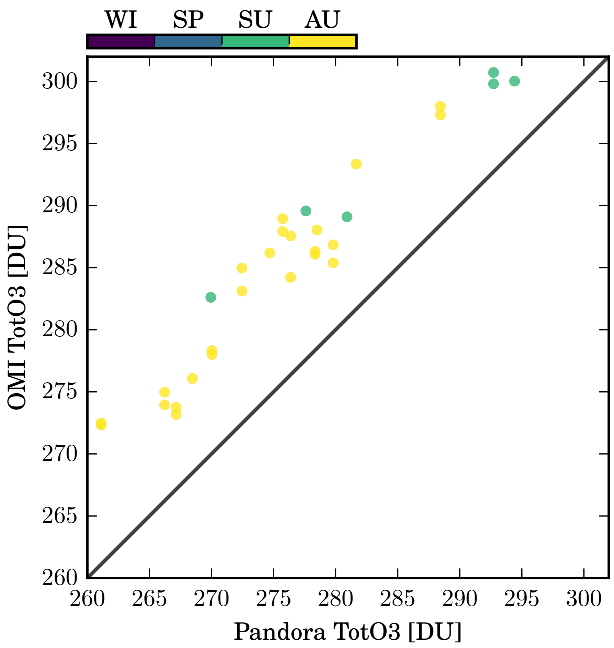

longitude, latitude	-95.392, 29.520
num data points	30
max Pan. (Pans.)	1 (33)
CC	0.97
RMS	2.16 DU
SLP	0.94 ± 0.05
mean	9.21 DU
MEDD	8.52 DU
25-75 perc. range	7.73 DU to 11.34 DU
10-90 perc. range	6.56 DU to 12.22 DU
min-max range	5.59 DU to 13.22 DU
OMI CF	48.45 %
Pandora DQ0	41.67 %

Manvelcroix*

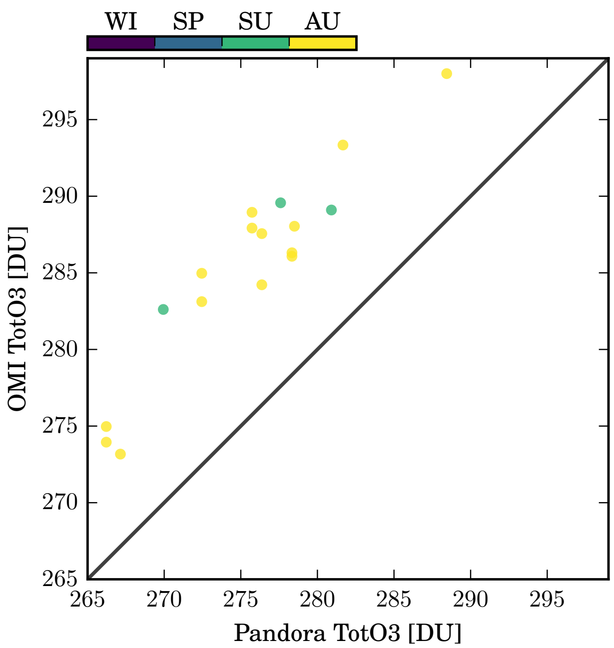

longitude, latitude	-95.392, 29.520
num data points	17
max Pan. (Pans.)	1 (33)
CC	0.94
RMS	2.11 DU
SLP	1.05 ± 0.10
mean	9.97 DU
MEDD	9.56 DU
25-75 perc. range	7.97 DU to 11.97 DU
10-90 perc. range	7.74 DU to 12.58 DU
min-max range	6.03 DU to 13.22 DU
OMI CF	48.45 %
Pandora DQ0	41.67 %

MaunaLoa

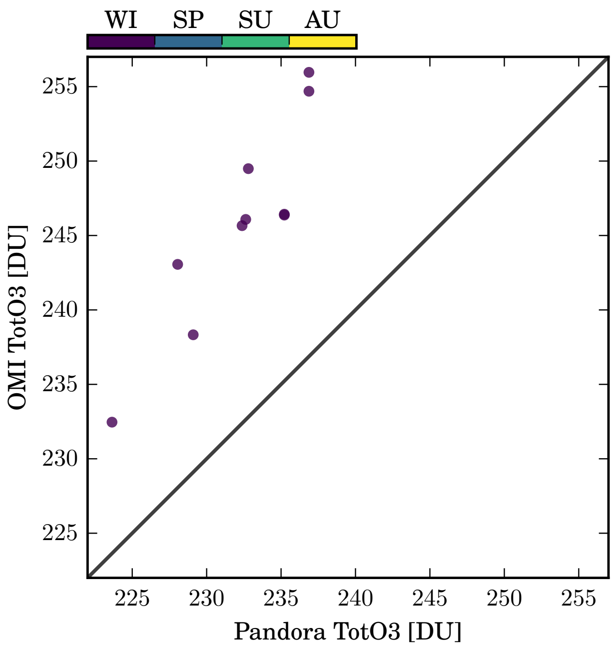

longitude, latitude	-155.6027, 19.4795
num data points	10
max Pan. (Pans.)	1 (31)
CC	0.91
RMS	2.70 DU
SLP	1.50 ± 0.24
mean	13.57 DU
MEDD	13.37 DU
25-75 perc. range	11.17 DU to 16.27 DU
10-90 perc. range	9.19 DU to 17.94 DU
min-max range	8.82 DU to 19.09 DU
OMI CF	18.29 %
Pandora DQ0	58.29 %

Moodytower

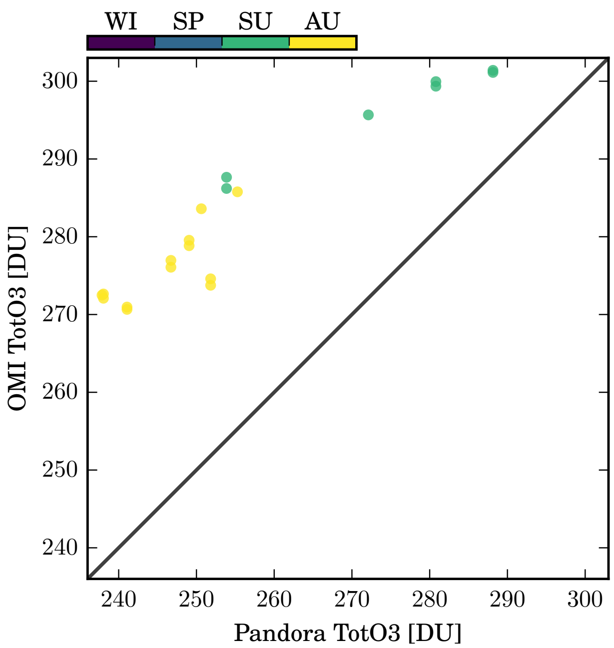

longitude, latitude	-95.3413, 29.7175
num data points	20
max Pan. (Pans.)	1 (35)
CC	0.96
RMS	3.13 DU
SLP	0.63 ± 0.05
mean	27.22 DU
MEDD	29.84 DU
25-75 perc. range	22.56 DU to 32.50 DU
10-90 perc. range	18.03 DU to 34.10 DU
min-max range	12.99 DU to 34.63 DU
OMI CF	39.56 %
Pandora DQ0	27.76 %

NASAHQ

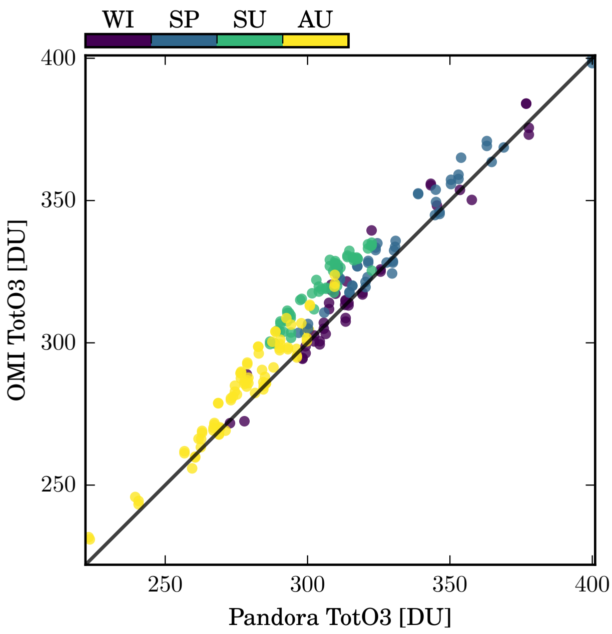

longitude, latitude	-76.8396, 38.9926
num data points	225
max Pan. (Pans.)	2 (17, 33)
CC	0.97
RMS	6.52 DU
SLP	0.98 ± 0.02
mean	7.12 DU
MEDD	7.27 DU
25-75 perc. range	1.38 DU to 12.71 DU
10-90 perc. range	-1.20 DU to 15.97 DU
min-max range	-7.46 DU to 21.33 DU
OMI CF	42.33 %
Pandora DQ0	37.15 %

NASAHQ*

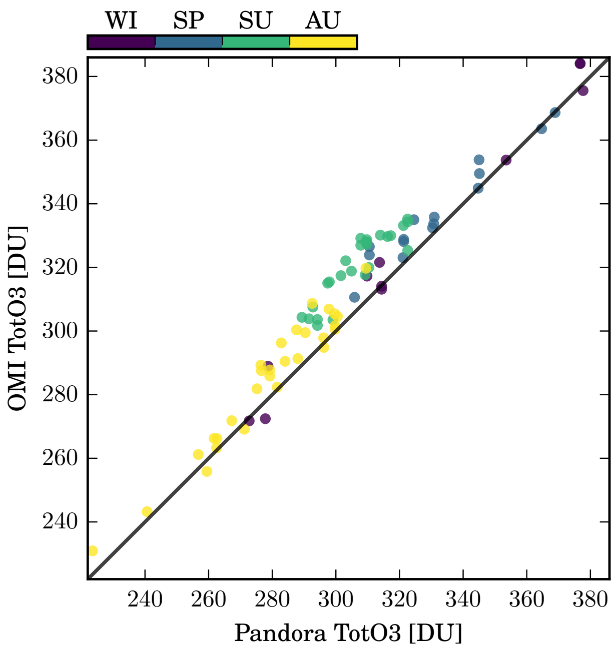

longitude, latitude	-76.8396, 38.9926
num data points	81
max Pan. (Pans.)	2 (17, 33)
CC	0.98
RMS	6.41 DU
SLP	1.00 ± 0.02
mean	7.85 DU
MEDD	7.47 DU
25-75 perc. range	2.78 DU to 12.74 DU
10-90 perc. range	-0.28 DU to 17.49 DU
min-max range	-5.39 DU to 21.33 DU
OMI CF	42.33 %
Pandora DQ0	37.15 %

NWHarris

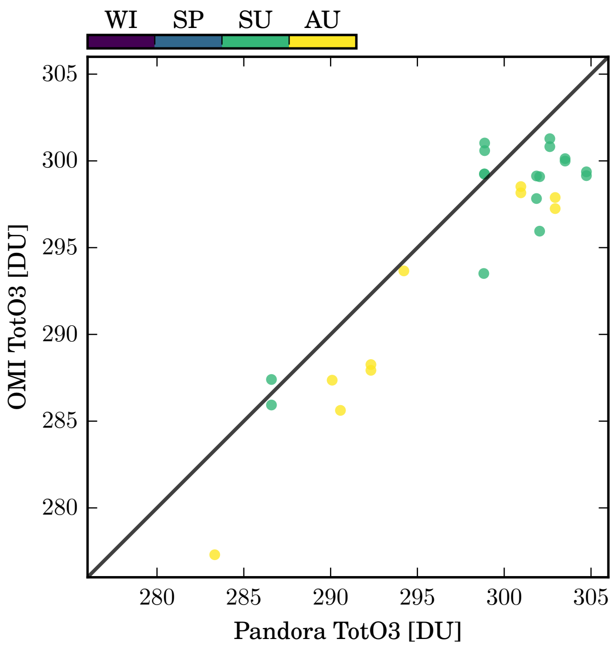

longitude, latitude	-95.6738, 30.0394
num data points	27
max Pan. (Pans.)	1 (30)
CC	0.92
RMS	2.39 DU
SLP	0.94 ± 0.08
mean	-2.82 DU
MEDD	-2.95 DU
25-75 perc. range	-5.00 DU to -1.00 DU
10-90 perc. range	-5.63 DU to 0.56 DU
min-max range	-6.09 DU to 2.16 DU
OMI CF	45.33 %
Pandora DQ0	46.10 %

NWHarris*

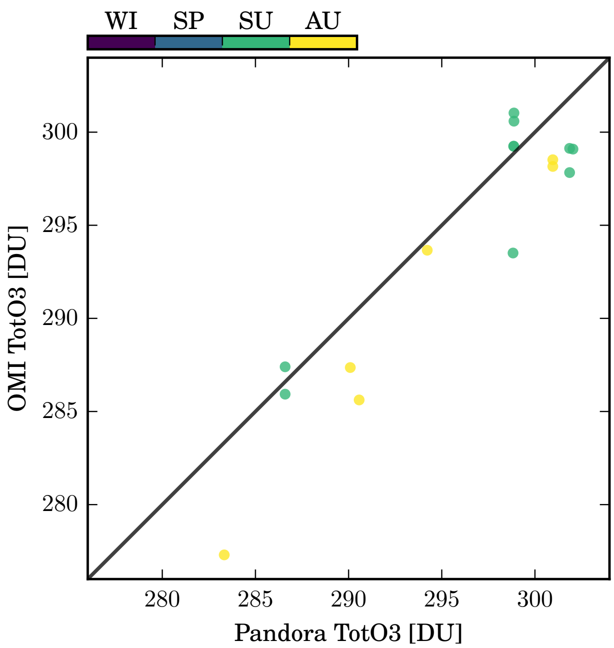

longitude, latitude	-95.6738, 30.0394
num data points	16
max Pan. (Pans.)	1 (30)
CC	0.93
RMS	2.44 DU
SLP	1.05 ± 0.11
mean	-1.86 DU
MEDD	-2.58 DU
25-75 perc. range	-3.22 DU to 0.38 DU
10-90 perc. range	-5.13 DU to 1.26 DU
min-max range	-6.03 DU to 2.16 DU
OMI CF	45.33 %
Pandora DQ0	46.10 %

Padonia

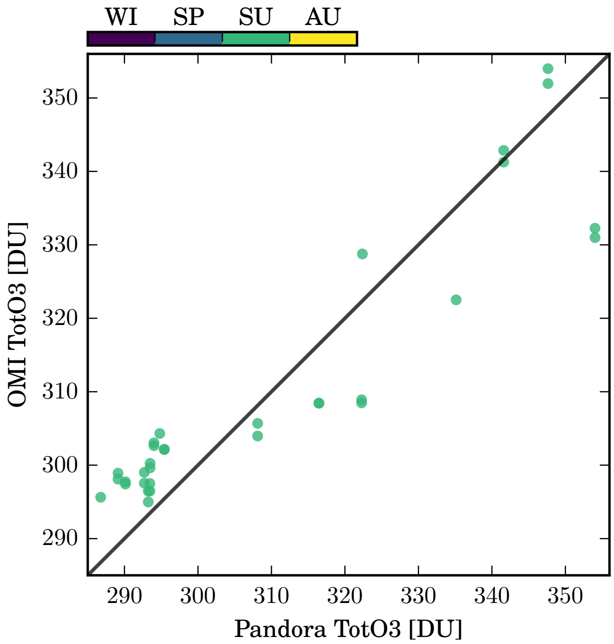

longitude, latitude	-76.631111, 39.460833
num data points	32
max Pan. (Pans.)	1 (17)
CC	0.92
RMS	6.73 DU
SLP	0.72 ± 0.06
mean	0.94 DU
MEDD	4.58 DU
25-75 perc. range	-2.86 DU to 6.90 DU
10-90 perc. range	-13.30 DU to 8.96 DU
min-max range	-23.05 DU to 9.79 DU
OMI CF	55.17 %
Pandora DQ0	62.62 %

Padonia*

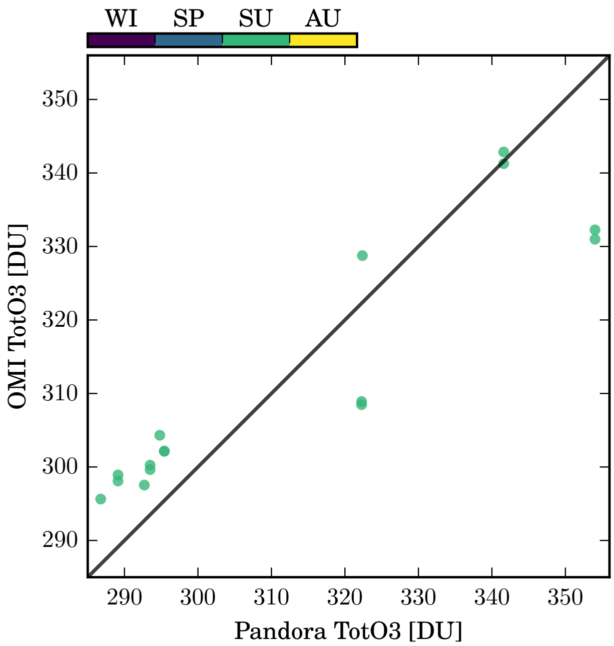

longitude, latitude	-76.631111, 39.460833
num data points	16
max Pan. (Pans.)	1 (17)
CC	0.92
RMS	6.48 DU
SLP	0.63 ± 0.07
mean	0.23 DU
MEDD	6.27 DU
25-75 perc. range	-3.59 DU to 7.29 DU
10-90 perc. range	-17.78 DU to 9.24 DU
min-max range	-23.05 DU to 9.79 DU
OMI CF	55.17 %
Pandora DQ0	62.62 %

Parlier

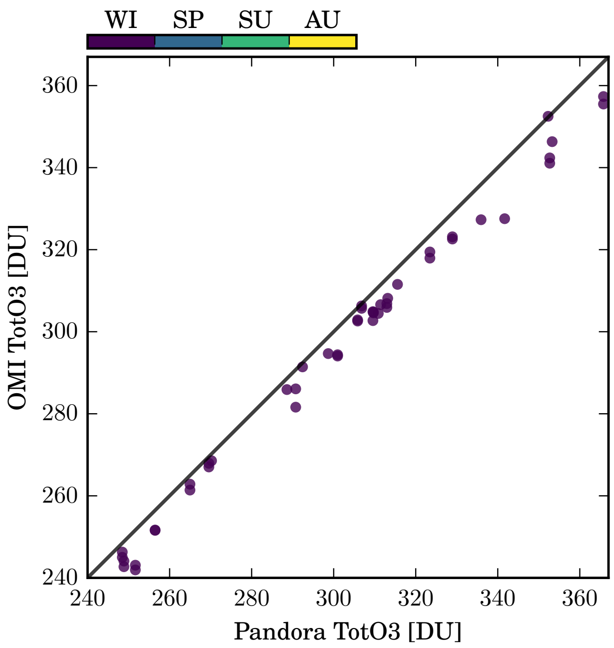

longitude, latitude	-119.5037, 36.5974
num data points	46
max Pan. (Pans.)	1 (28)
CC	1.00
RMS	2.80 DU
SLP	0.97 ± 0.01
mean	-5.34 DU
MEDD	-4.89 DU
25-75 perc. range	-6.88 DU to -3.29 DU
10-90 perc. range	-9.42 DU to -1.66 DU
min-max range	-14.13 DU to 0.23 DU
OMI CF	42.20 %
Pandora DQ0	44.04 %

Parlier*

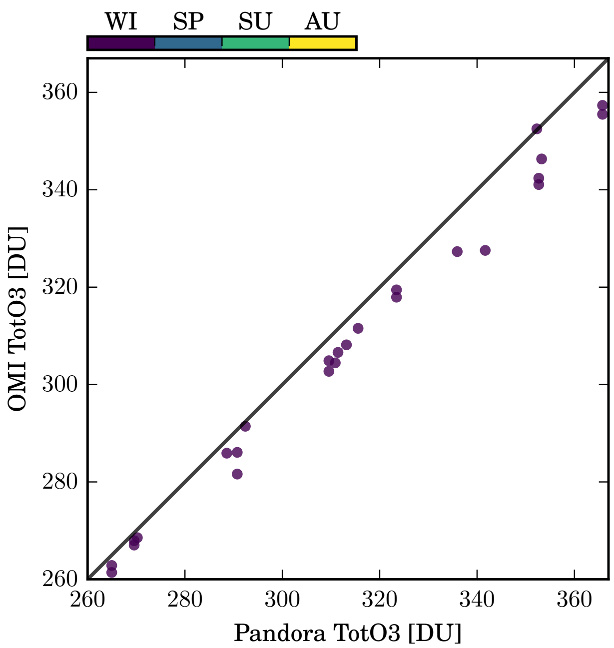

longitude, latitude	-119.5037, 36.5974
num data points	25
max Pan. (Pans.)	1 (28)
CC	1.00
RMS	2.77 DU
SLP	0.93 ± 0.02
mean	-5.62 DU
MEDD	-4.84 DU
25-75 perc. range	-8.45 DU to -2.70 DU
10-90 perc. range	-10.29 DU to -1.65 DU
min-max range	-14.13 DU to 0.23 DU
OMI CF	42.20 %
Pandora DQ0	44.04 %

Platteville

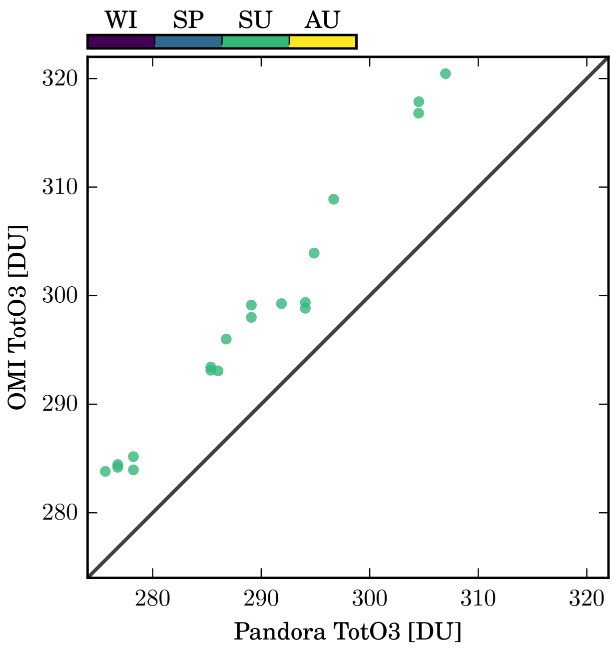

longitude, latitude	-104.726, 40.181
num data points	19
max Pan. (Pans.)	2 (30, 8)
CC	0.99
RMS	1.88 DU
SLP	1.17 ± 0.05
mean	8.67 DU
MEDD	8.06 DU
25-75 perc. range	7.22 DU to 9.63 DU
10-90 perc. range	5.64 DU to 12.51 DU
min-max range	4.78 DU to 13.47 DU
OMI CF	41.30 %
Pandora DQ0	25.85 %

Porterville

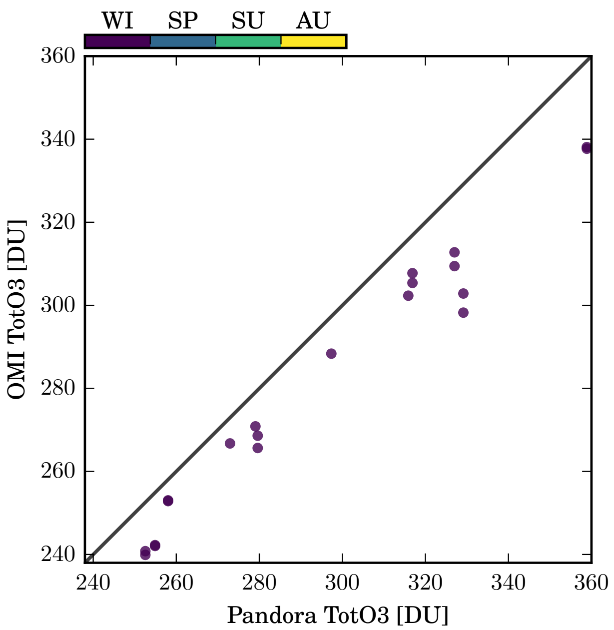

longitude, latitude	-119.055, 36.03179
num data points	20
max Pan. (Pans.)	2 (27, 8)
CC	0.99
RMS	4.97 DU
SLP	0.88 ± 0.03
mean	-13.69 DU
MEDD	-12.65 DU
25-75 perc. range	-15.08 DU to -9.11 DU
10-90 perc. range	-21.69 DU to -6.11 DU
min-max range	-30.91 DU to -5.00 DU
OMI CF	48.84 %
Pandora DQ0	31.81 %

RockyFlats

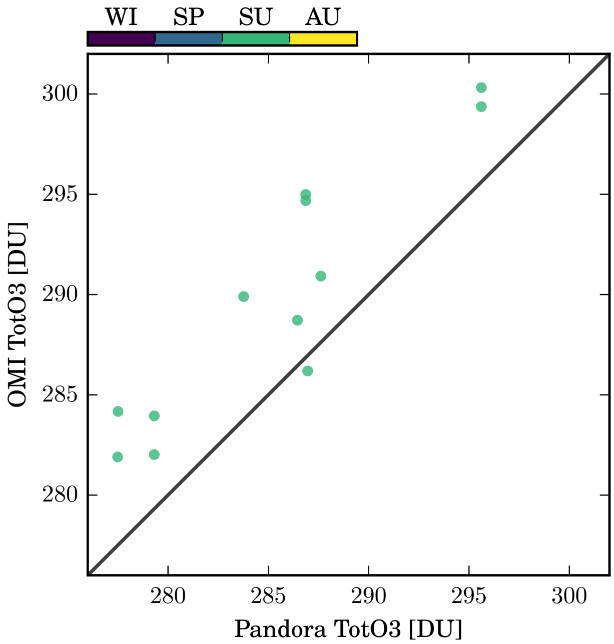

longitude, latitude	-105.19, 39.92
num data points	12
max Pan. (Pans.)	1 (31)
CC	0.92
RMS	2.39 DU
SLP	0.96 ± 0.13
mean	4.48 DU
MEDD	4.52 DU
25-75 perc. range	3.15 DU to 6.26 DU
10-90 perc. range	2.31 DU to 7.70 DU
min-max range	-0.77 DU to 8.12 DU
OMI CF	35.29 %
Pandora DQ0	18.36 %

SERC

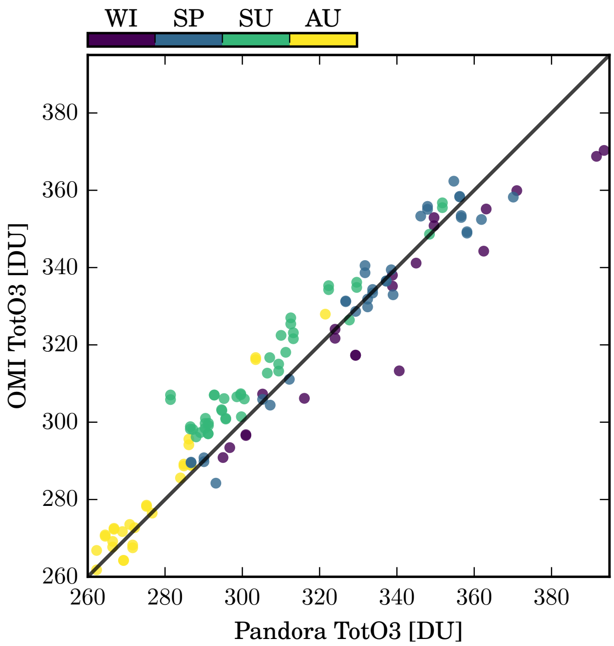

longitude, latitude	-76.55, 38.88
num data points	126
max Pan. (Pans.)	2 (24, 7)
CC	0.96
RMS	7.27 DU
SLP	0.88 ± 0.02
mean	2.47 DU
MEDD	3.17 DU
25-75 perc. range	-1.01 DU to 7.87 DU
10-90 perc. range	-8.40 DU to 11.30 DU
min-max range	-27.32 DU to 25.62 DU
OMI CF	44.64 %
Pandora DQ0	10.66 %

SERC*

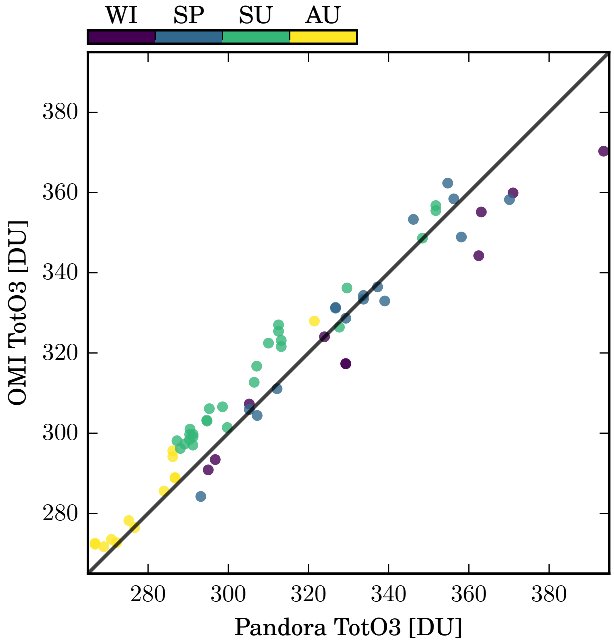

longitude, latitude	-76.55, 38.88
num data points	65
max Pan. (Pans.)	2 (24, 7)
CC	0.97
RMS	6.38 DU
SLP	0.86 ± 0.03
mean	2.28 DU
MEDD	3.01 DU
25-75 perc. range	-0.66 DU to 8.08 DU
10-90 perc. range	-9.11 DU to 9.81 DU
min-max range	-23.29 DU to 14.47 DU
OMI CF	44.64 %
Pandora DQ0	10.66 %

Seabrook

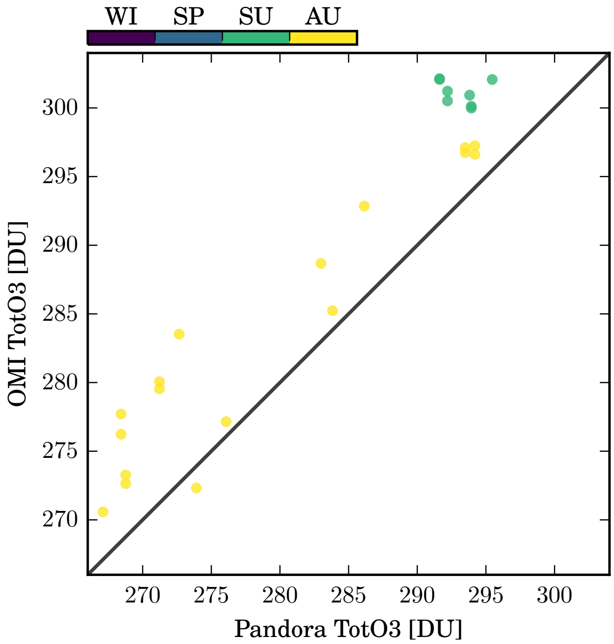

longitude, latitude	-95.3261, 29.9010
num data points	25
max Pan. (Pans.)	1 (27)
CC	0.96
RMS	3.21 DU
SLP	1.01 ± 0.06
mean	5.87 DU
MEDD	6.18 DU
25-75 perc. range	3.46 DU to 8.32 DU
10-90 perc. range	1.81 DU to 9.98 DU
min-max range	-1.59 DU to 10.87 DU
OMI CF	44.68 %
Pandora DQ0	27.56 %

Seabrook*

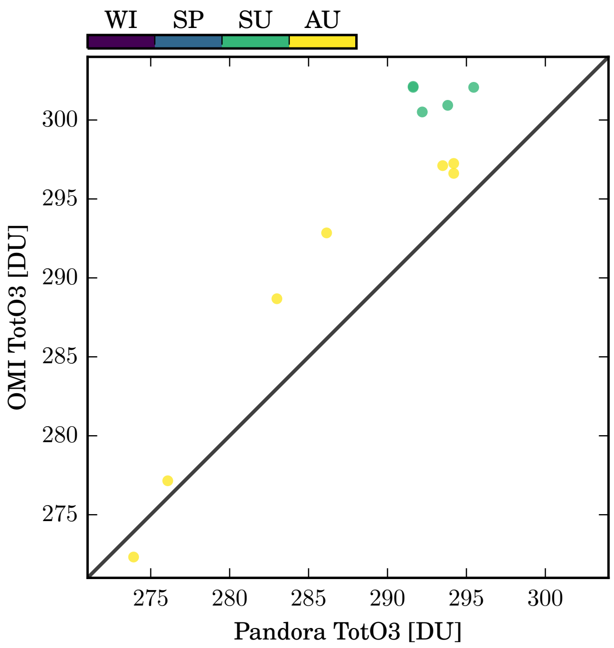

longitude, latitude	-95.3261, 29.9010
num data points	12
max Pan. (Pans.)	1 (27)
CC	0.95
RMS	2.92 DU
SLP	1.29 ± 0.13
mean	5.33 DU
MEDD	6.15 DU
25-75 perc. range	2.90 DU to 7.41 DU
10-90 perc. range	1.21 DU to 10.23 DU
min-max range	-1.59 DU to 10.50 DU
OMI CF	44.68 %
Pandora DQ0	27.56 %

Seoul

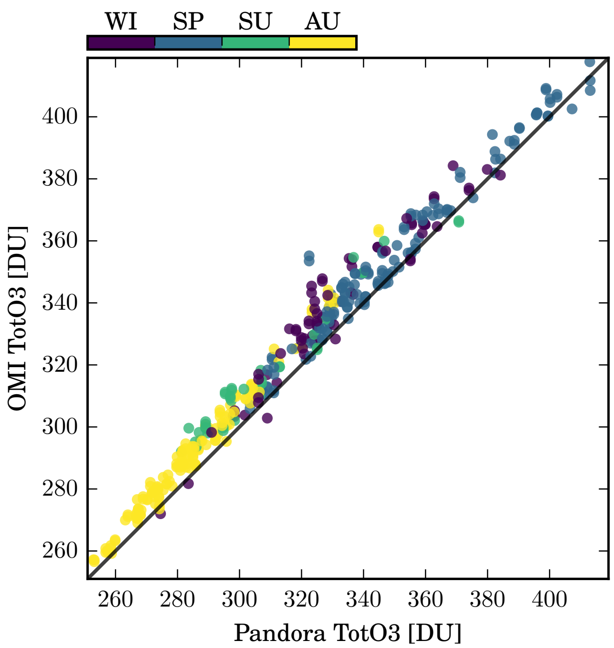

longitude, latitude	126.934, 37.5644
num data points	391
max Pan. (Pans.)	2 (17, 19)
CC	0.99
RMS	4.91 DU
SLP	0.99 ± 0.01
mean	6.78 DU
MEDD	6.39 DU
25-75 perc. range	3.58 DU to 9.69 DU
10-90 perc. range	0.90 DU to 12.66 DU
min-max range	-6.12 DU to 32.72 DU
OMI CF	42.13 %
Pandora DQ0	46.83 %

Seoul*

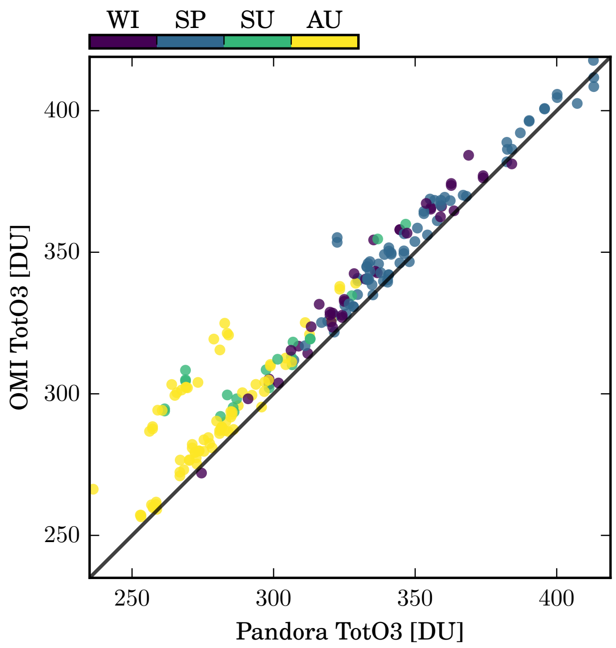

longitude, latitude	126.934, 37.5644
num data points	214
max Pan. (Pans.)	3 (17, 19, 29)
CC	0.97
RMS	9.14 DU
SLP	0.90 ± 0.02
mean	9.98 DU
MEDD	7.07 DU
25-75 perc. range	4.27 DU to 10.95 DU
10-90 perc. range	2.12 DU to 30.95 DU
min-max range	-4.71 DU to 42.20 DU
OMI CF	40.76 %
Pandora DQ0	45.24 %

Smithpoint

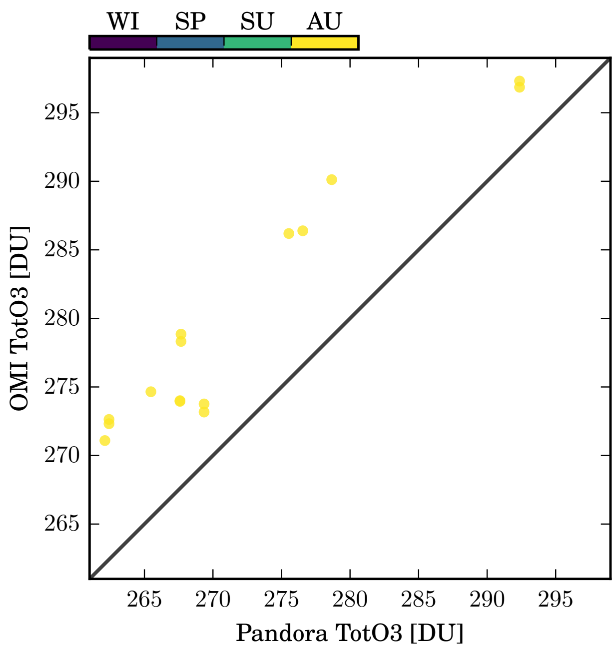

longitude, latitude	-94.7869, 29.5462
num data points	15
max Pan. (Pans.)	3 (29, 36, 8)
CC	0.96
RMS	2.48 DU
SLP	0.89 ± 0.07
mean	8.16 DU
MEDD	9.18 DU
25-75 perc. range	5.65 DU to 10.43 DU
10-90 perc. range	4.44 DU to 10.97 DU
min-max range	3.82 DU to 11.46 DU
OMI CF	40.48 %
Pandora DQ0	38.87 %

Tranquility

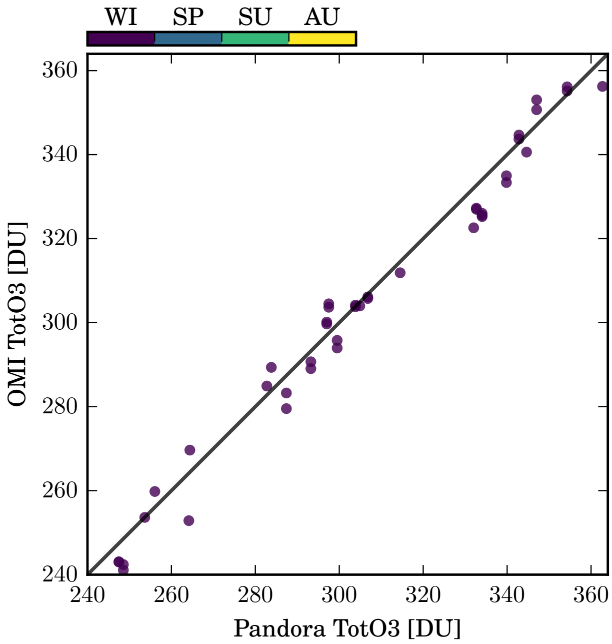

longitude, latitude	-120.3824, 36.6341
num data points	42
max Pan. (Pans.)	1 (26)
CC	0.99
RMS	4.82 DU
SLP	1.00 ± 0.02
mean	-2.00 DU
MEDD	-2.60 DU
25-75 perc. range	-5.65 DU to 1.84 DU
10-90 perc. range	-8.01 DU to 5.10 DU
min-max range	-11.29 DU to 6.98 DU
OMI CF	61.62 %
Pandora DQ0	31.49 %

Tranquility*

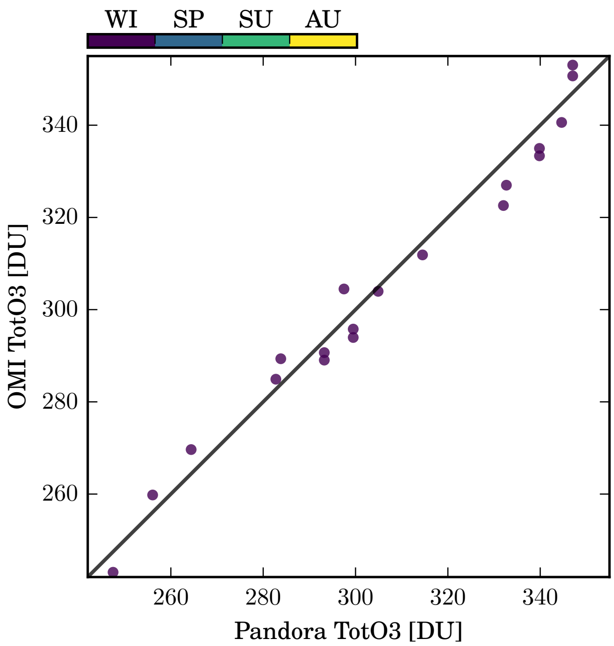

longitude, latitude	-120.3824, 36.6341
num data points	19
max Pan. (Pans.)	1 (26)
CC	0.99
RMS	4.68 DU
SLP	0.96 ± 0.04
mean	-1.11 DU
MEDD	-2.64 DU
25-75 perc. range	-4.65 DU to 3.70 DU
10-90 perc. range	-5.84 DU to 5.63 DU
min-max range	-9.45 DU to 6.98 DU
OMI CF	61.62 %
Pandora DQ0	31.49 %

UMBC

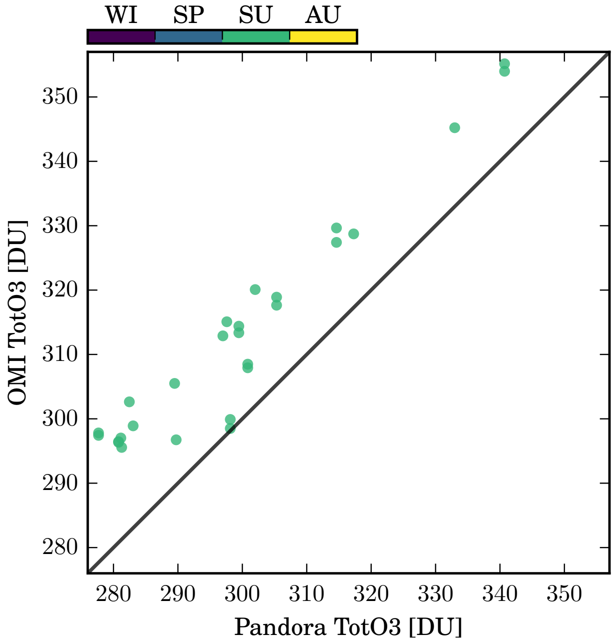

longitude, latitude	-76.709157, 39.2547
num data points	27
max Pan. (Pans.)	1 (2)
CC	0.96
RMS	4.72 DU
SLP	0.93 ± 0.05
mean	13.43 DU
MEDD	14.45 DU
25-75 perc. range	12.29 DU to 15.89 DU
10-90 perc. range	7.06 DU to 18.75 DU
min-max range	0.37 DU to 20.18 DU
OMI CF	53.73 %
Pandora DQ0	55.65 %

UMBC*

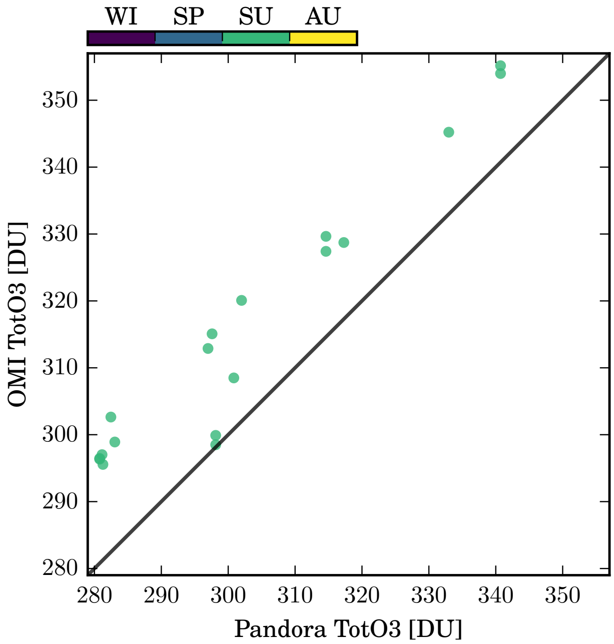

longitude, latitude	-76.709157, 39.2547
num data points	18
max Pan. (Pans.)	1 (2)
CC	0.97
RMS	4.99 DU
SLP	0.96 ± 0.06
mean	13.22 DU
MEDD	14.74 DU
25-75 perc. range	12.38 DU to 15.88 DU
10-90 perc. range	5.89 DU to 17.67 DU
min-max range	0.37 DU to 20.18 DU
OMI CF	53.73 %
Pandora DQ0	55.65 %

UMCP

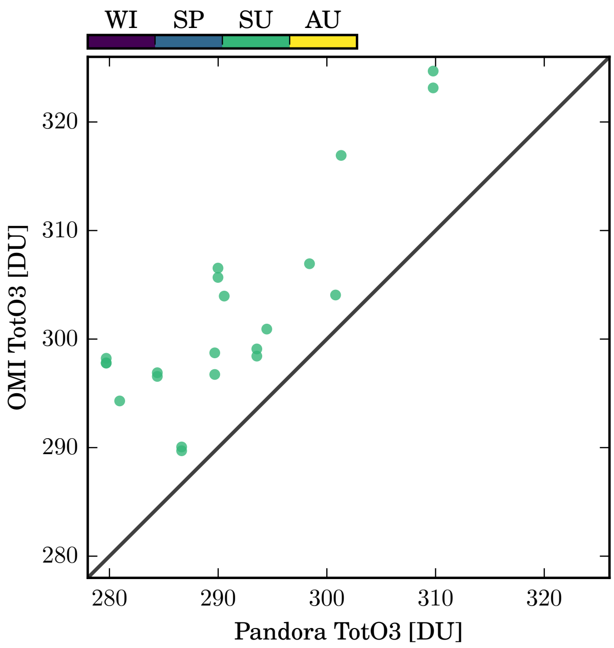

longitude, latitude	-76.942519, 38.990906
num data points	21
max Pan. (Pans.)	1 (21)
CC	0.83
RMS	5.05 DU
SLP	0.88 ± 0.13
mean	11.12 DU
MEDD	12.50 DU
25-75 perc. range	6.45 DU to 15.61 DU
10-90 perc. range	3.42 DU to 18.08 DU
min-max range	3.07 DU to 18.53 DU
OMI CF	56.00 %
Pandora DQ0	58.80 %

USNA

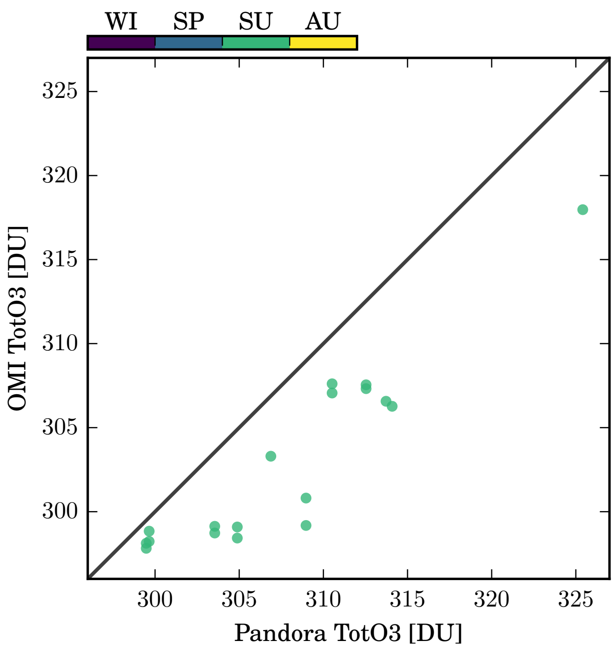

longitude, latitude	-76.479558, 38.983673
num data points	18
max Pan. (Pans.)	1 (25)
CC	0.93
RMS	1.96 DU
SLP	0.75 ± 0.07
mean	-4.85 DU
MEDD	-4.90 DU
25-75 perc. range	-6.98 DU to -3.05 DU
10-90 perc. range	-7.92 DU to -1.40 DU
min-max range	-9.79 DU to -0.81 DU
OMI CF	56.90 %
Pandora DQ0	20.05 %

Visalia

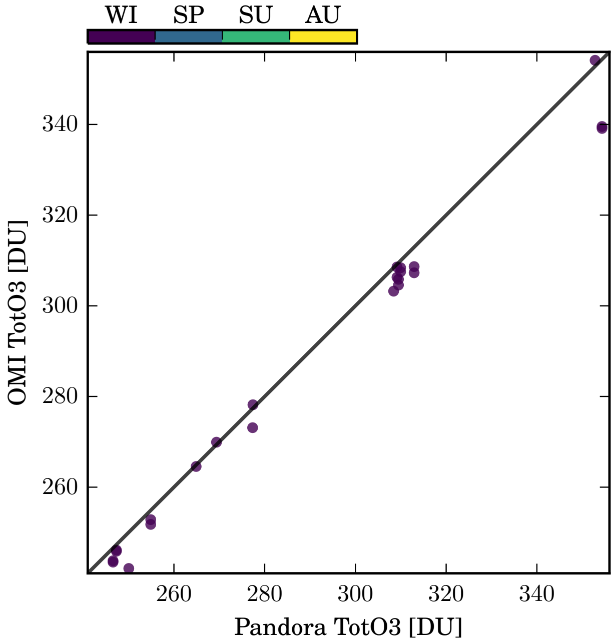

longitude, latitude	-119.3930, 36.3141
num data points	23
max Pan. (Pans.)	1 (18)
CC	0.99
RMS	3.67 DU
SLP	0.95 ± 0.02
mean	-3.69 DU
MEDD	-2.87 DU
25-75 perc. range	-4.60 DU to -1.32 DU
10-90 perc. range	-7.51 DU to 0.37 DU
min-max range	-15.24 DU to 1.32 DU
OMI CF	68.57 %
Pandora DQ0	64.00 %

Visalia*

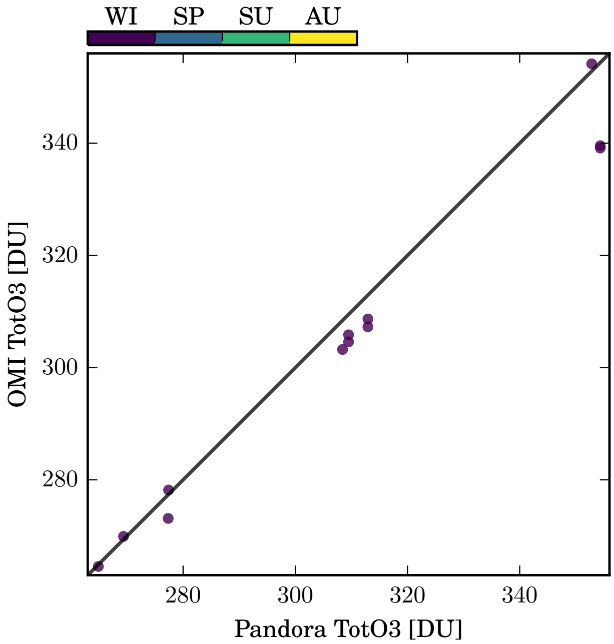

longitude, latitude	-119.3930, 36.3141
num data points	12
max Pan. (Pans.)	1 (18)
CC	0.99
RMS	3.99 DU
SLP	0.89 ± 0.04
mean	-4.64 DU
MEDD	-4.26 DU
25-75 perc. range	-5.31 DU to -0.12 DU
10-90 perc. range	-13.89 DU to 0.75 DU
min-max range	-15.24 DU to 1.32 DU
OMI CF	68.57 %
Pandora DQ0	64.00 %

WeldTower

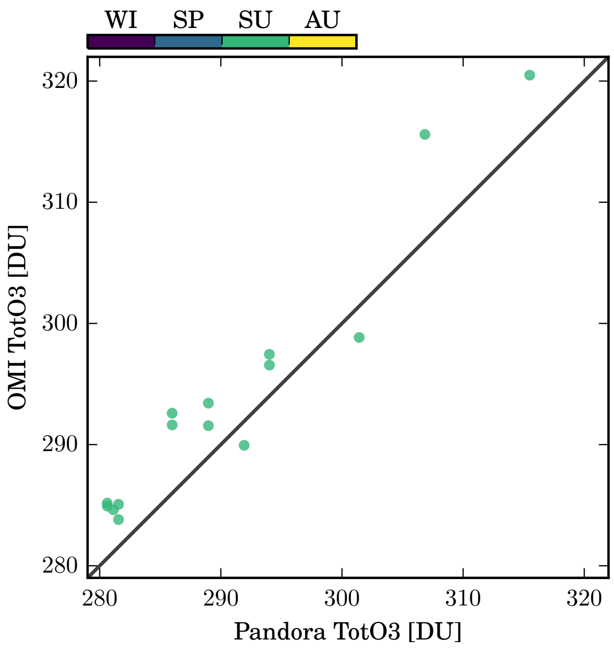

longitude, latitude	-104.73, 40.39
num data points	15
max Pan. (Pans.)	1 (21)
CC	0.96
RMS	2.79 DU
SLP	1.01 ± 0.08
mean	3.51 DU
MEDD	3.52 DU
25-75 perc. range	2.57 DU to 4.77 DU
10-90 perc. range	-0.29 DU to 6.22 DU
min-max range	-2.58 DU to 8.76 DU
OMI CF	39.13 %
Pandora DQ0	37.65 %

4.1.2 Scatter Plots: TotNO2

AMI

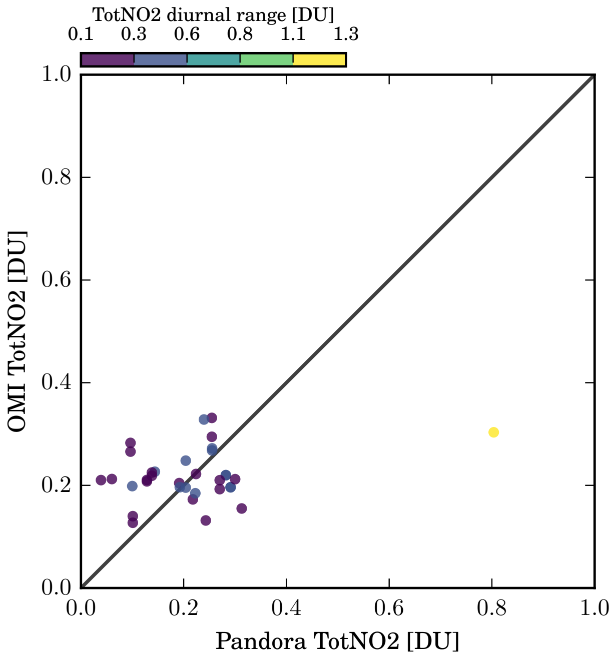

longitude, latitude	126.33, 36.538
num data points	34
max Pan. (Pans.)	1 (21)
CC	0.29
RMS	0.05 DU
SLP	0.07 ± 0.07
mean	0.00 DU
MEDD	0.01 DU
25-75 perc. range	-0.06 DU to 0.08 DU
10-90 perc. range	-0.10 DU to 0.14 DU
min-max range	-0.50 DU to 0.19 DU
OMI CF	27.27 %
Pandora DQ0	47.01 %

Aldino

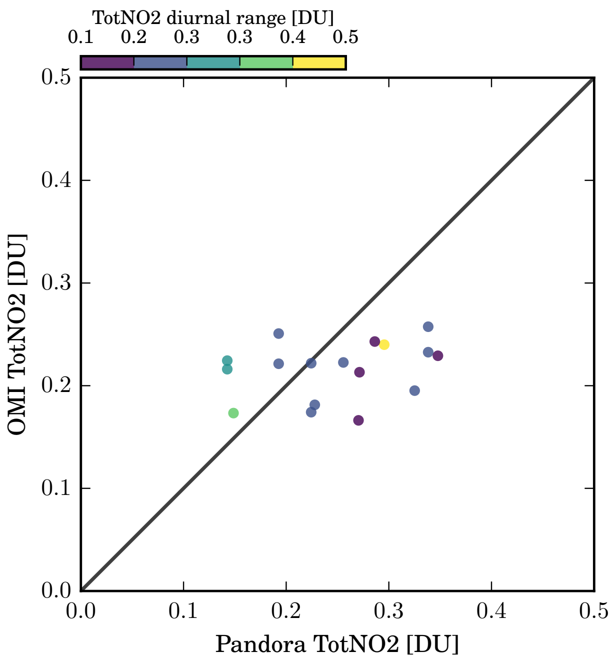

longitude, latitude	-76.203889, 39.563333
num data points	17
max Pan. (Pans.)	1 (23)
CC	0.28
RMS	0.03 DU
SLP	0.12 ± 0.20
mean	-0.03 DU
MEDD	-0.05 DU
25-75 perc. range	-0.08 DU to 0.02 DU
10-90 perc. range	-0.11 DU to 0.06 DU
min-max range	-0.13 DU to 0.08 DU
OMI CF	30.00 %
Pandora DQ0	70.55 %

Arvin

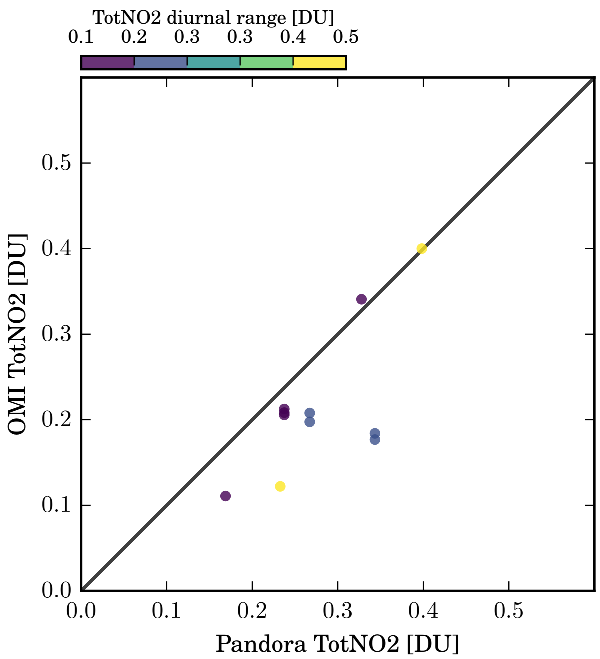

longitude, latitude	-118.7887, 35.291
num data points	11
max Pan. (Pans.)	1 (35)
CC	0.71
RMS	0.06 DU
SLP	1.00 ± 0.22
mean	-0.06 DU
MEDD	-0.06 DU
25-75 perc. range	-0.09 DU to -0.03 DU
10-90 perc. range	-0.16 DU to 0.00 DU
min-max range	-0.17 DU to 0.01 DU
OMI CF	48.18 %
Pandora DQ0	36.59 %

Baengnyeongdo

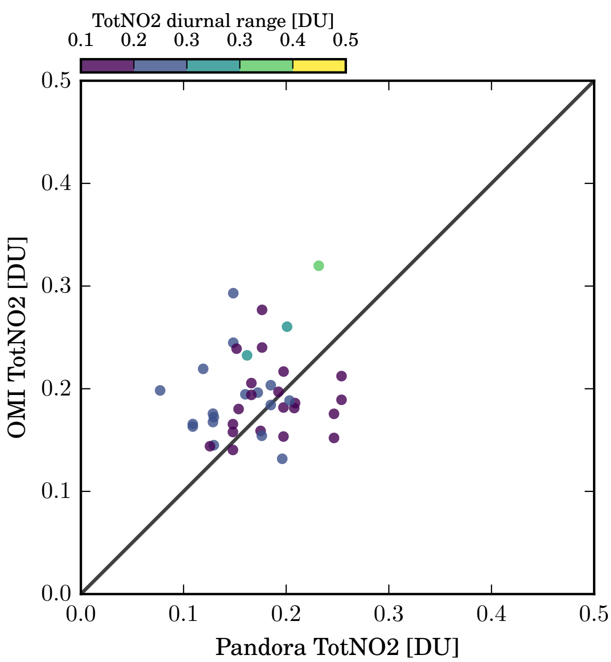

longitude, latitude	124.631, 37.965
num data points	41
max Pan. (Pans.)	1 (35)
CC	0.15
RMS	0.04 DU
SLP	0.15 ± 0.16
mean	0.02 DU
MEDD	0.02 DU
25-75 perc. range	-0.02 DU to 0.06 DU
10-90 perc. range	-0.04 DU to 0.10 DU
min-max range	-0.09 DU to 0.14 DU
OMI CF	38.62 %
Pandora DQ0	42.43 %

Bakersfield

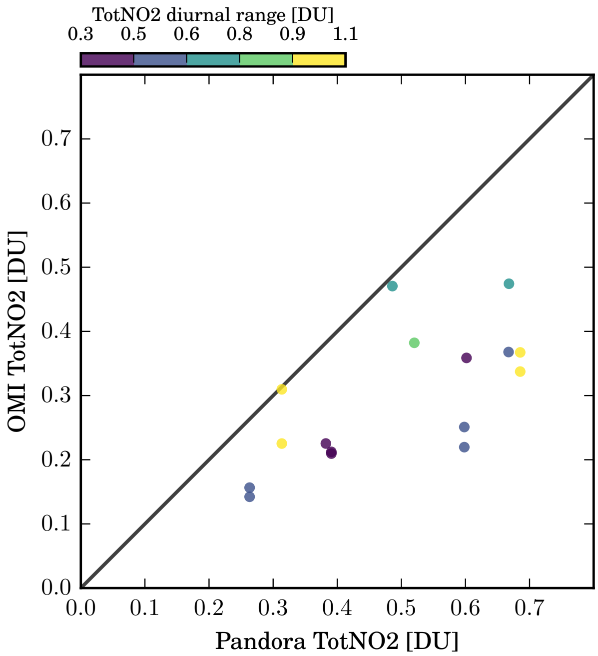

longitude, latitude	-118.9976, 35.3246
num data points	16
max Pan. (Pans.)	2 (33, 36)
CC	0.67
RMS	0.08 DU
SLP	0.42 ± 0.10
mean	-0.19 DU
MEDD	-0.18 DU
25-75 perc. range	-0.30 DU to -0.12 DU
10-90 perc. range	-0.35 DU to -0.05 DU
min-max range	-0.38 DU to -0.00 DU
OMI CF	36.36 %
Pandora DQ0	60.54 %

Beltsville

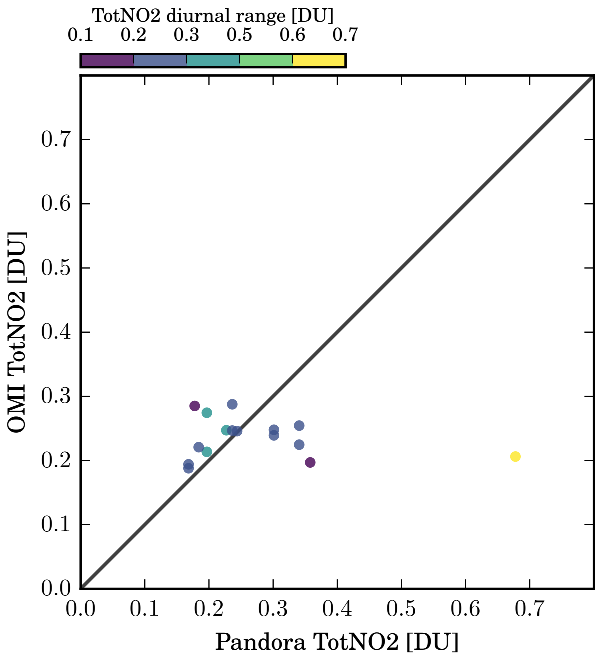

longitude, latitude	-76.878333, 39.055277
num data points	16
max Pan. (Pans.)	1 (20)
CC	-0.21
RMS	0.03 DU
SLP	-0.02 ± 0.14
mean	-0.04 DU
MEDD	0.01 DU
25-75 perc. range	-0.07 DU to 0.03 DU
10-90 perc. range	-0.14 DU to 0.06 DU
min-max range	-0.47 DU to 0.11 DU
OMI CF	33.33 %
Pandora DQ0	54.76 %

Boulder

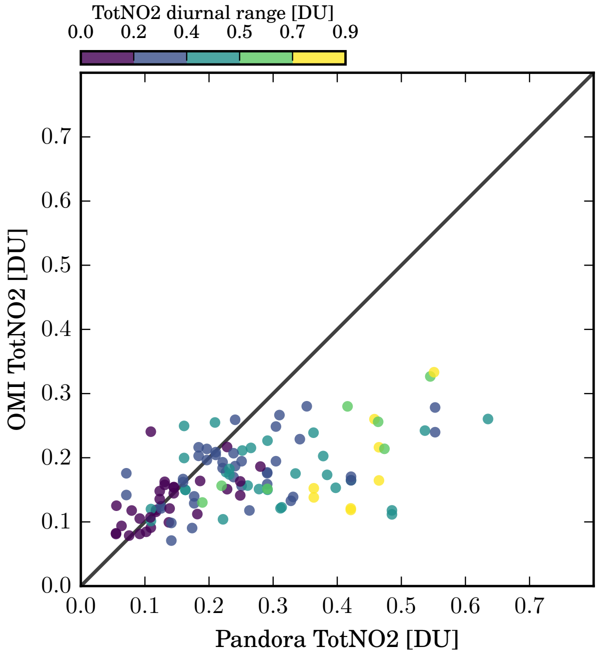

longitude, latitude	-105.26067, 39.99093
num data points	114
max Pan. (Pans.)	1 (34)
CC	0.57
RMS	0.06 DU
SLP	0.16 ± 0.01
mean	-0.08 DU
MEDD	-0.05 DU
25-75 perc. range	-0.14 DU to -0.00 DU
10-90 perc. range	-0.25 DU to 0.03 DU
min-max range	-0.37 DU to 0.13 DU
OMI CF	29.58 %
Pandora DQ0	32.57 %

Boulder*

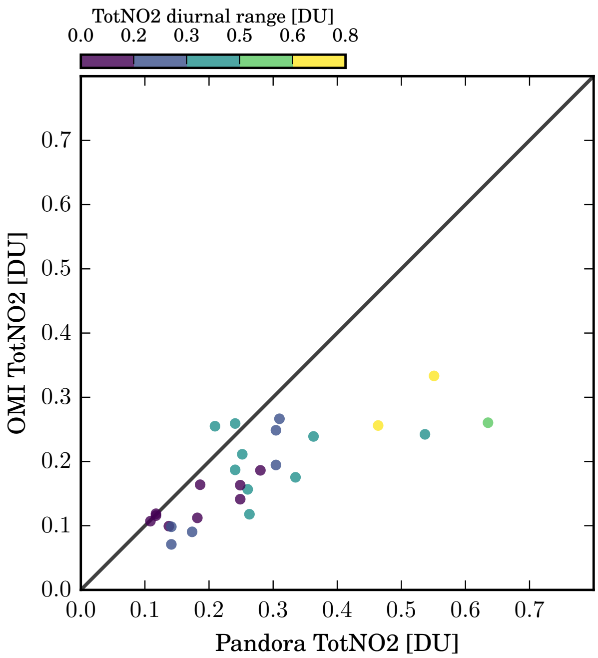

longitude, latitude	-105.26067, 39.99093
num data points	27
max Pan. (Pans.)	1 (34)
CC	0.77
RMS	0.05 DU
SLP	0.51 ± 0.05
mean	-0.09 DU
MEDD	-0.07 DU
25-75 perc. range	-0.12 DU to -0.04 DU
10-90 perc. range	-0.21 DU to -0.00 DU
min-max range	-0.37 DU to 0.05 DU
OMI CF	29.58 %
Pandora DQ0	32.57 %

Busan

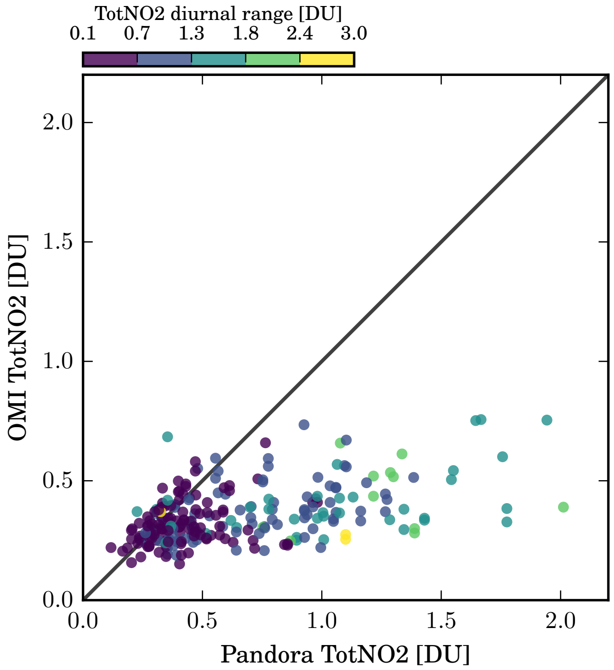

longitude, latitude	129.0825, 35.2353
num data points	249
max Pan. (Pans.)	2 (20, 36)
CC	0.47
RMS	0.11 DU
SLP	0.11 ± 0.01
mean	-0.30 DU
MEDD	-0.18 DU
25-75 perc. range	-0.55 DU to -0.03 DU
10-90 perc. range	-0.78 DU to 0.05 DU
min-max range	-1.62 DU to 0.33 DU
OMI CF	29.21 %
Pandora DQ0	62.76 %

Busan*

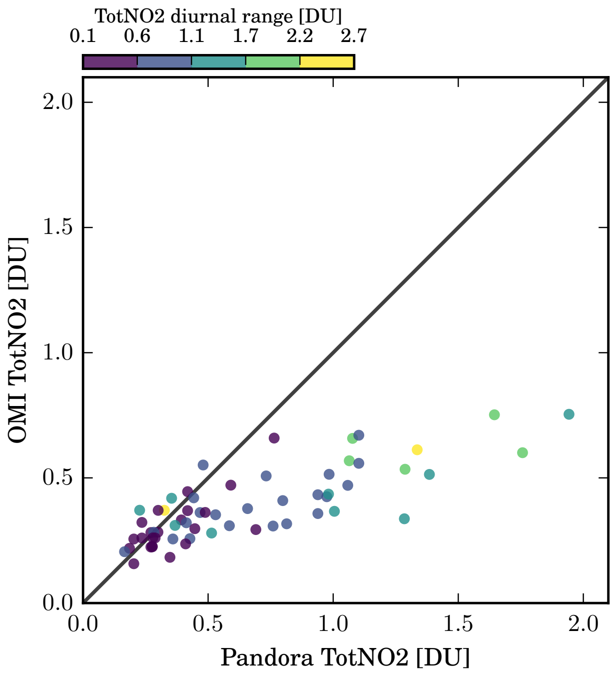

longitude, latitude	129.0825, 35.2353
num data points	61
max Pan. (Pans.)	2 (20, 36)
CC	0.80
RMS	0.09 DU
SLP	0.29 ± 0.02
mean	-0.27 DU
MEDD	-0.15 DU
25-75 perc. range	-0.50 DU to -0.02 DU
10-90 perc. range	-0.72 DU to 0.05 DU
min-max range	-1.19 DU to 0.14 DU
OMI CF	29.21 %
Pandora DQ0	62.76 %

CIAI

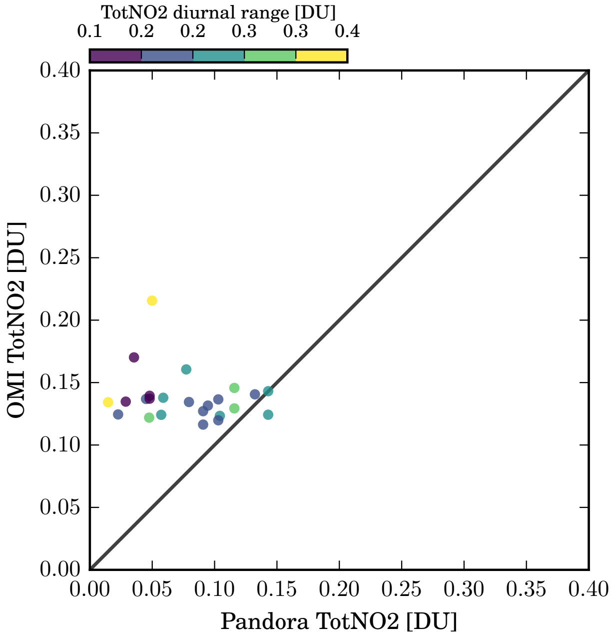

longitude, latitude	-16.4994, 28.309
num data points	24
max Pan. (Pans.)	1 (101)
CC	-0.19
RMS	0.02 DU
SLP	0.02 ± 0.12
mean	0.06 DU
MEDD	0.06 DU
25-75 perc. range	0.02 DU to 0.09 DU
10-90 perc. range	0.01 DU to 0.12 DU
min-max range	-0.02 DU to 0.17 DU
OMI CF	33.56 %
Pandora DQ0	54.18 %

Channelview

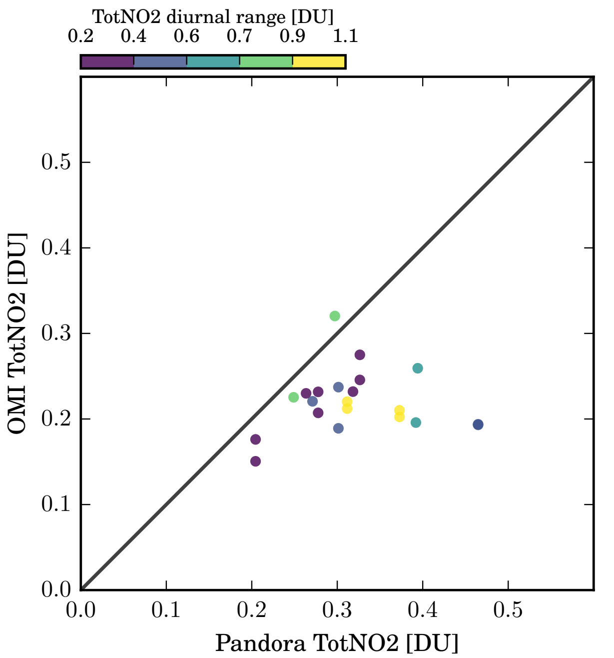

longitude, latitude	-95.1255, 29.8025
num data points	21
max Pan. (Pans.)	1 (26)
CC	0.05
RMS	0.04 DU
SLP	0.01 ± 0.10
mean	-0.10 DU
MEDD	-0.08 DU
25-75 perc. range	-0.13 DU to -0.05 DU
10-90 perc. range	-0.20 DU to -0.03 DU
min-max range	-0.27 DU to 0.02 DU
OMI CF	23.33 %
Pandora DQ0	60.88 %

Chatfield

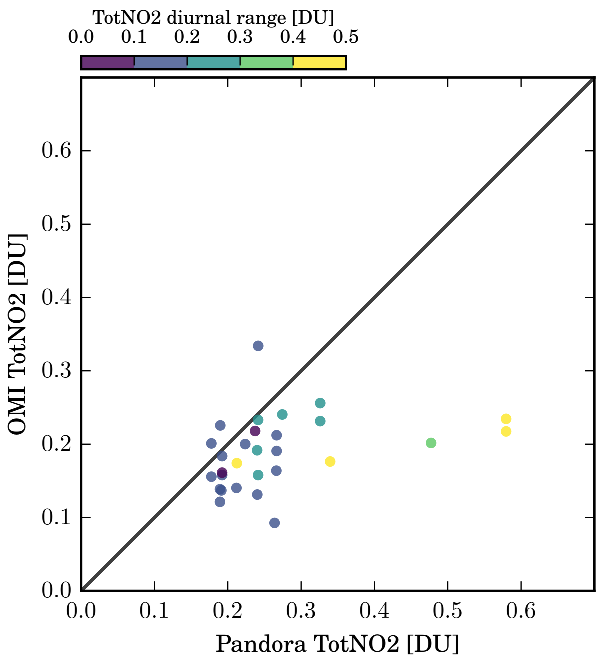

longitude, latitude	-105.07, 39.53
num data points	29
max Pan. (Pans.)	1 (26)
CC	0.33
RMS	0.05 DU
SLP	0.17 ± 0.06
mean	-0.08 DU
MEDD	-0.05 DU
25-75 perc. range	-0.09 DU to -0.02 DU
10-90 perc. range	-0.19 DU to -0.00 DU
min-max range	-0.36 DU to 0.09 DU
OMI CF	20.50 %
Pandora DQ0	55.17 %

Conroe

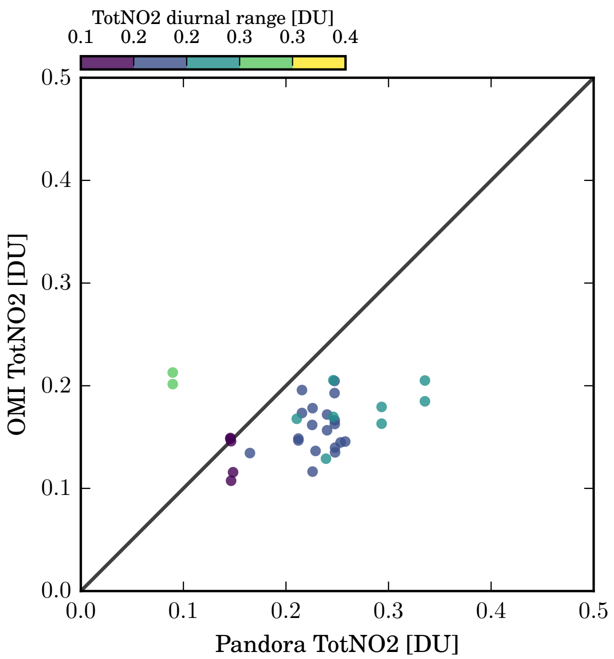

longitude, latitude	-95.425, 30.350
num data points	34
max Pan. (Pans.)	1 (31)
CC	0.17
RMS	0.03 DU
SLP	0.12 ± 0.14
mean	-0.06 DU
MEDD	-0.06 DU
25-75 perc. range	-0.11 DU to -0.04 DU
10-90 perc. range	-0.11 DU to 0.00 DU
min-max range	-0.15 DU to 0.12 DU
OMI CF	33.66 %
Pandora DQ0	59.35 %

Corcoran

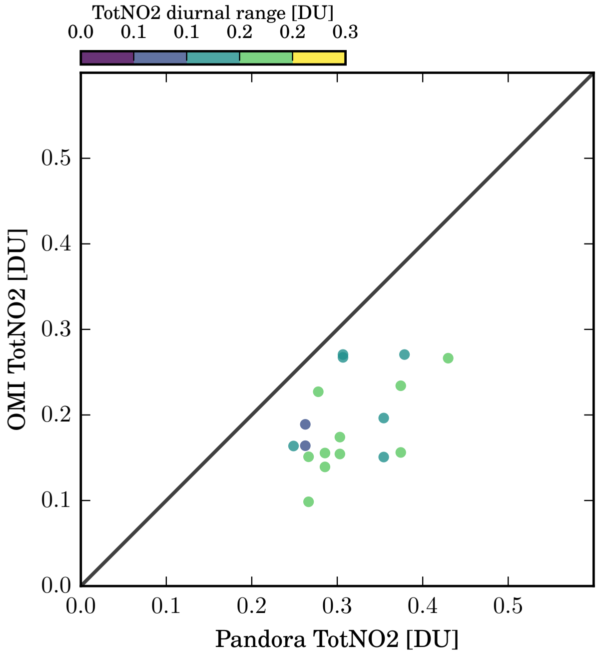

longitude, latitude	-119.5656, 36.1022
num data points	18
max Pan. (Pans.)	1 (34)
CC	0.50
RMS	0.05 DU
SLP	0.50 ± 0.21
mean	-0.12 DU
MEDD	-0.13 DU
25-75 perc. range	-0.16 DU to -0.09 DU
10-90 perc. range	-0.18 DU to -0.05 DU
min-max range	-0.22 DU to -0.04 DU
OMI CF	45.00 %
Pandora DQ0	64.51 %

DC3

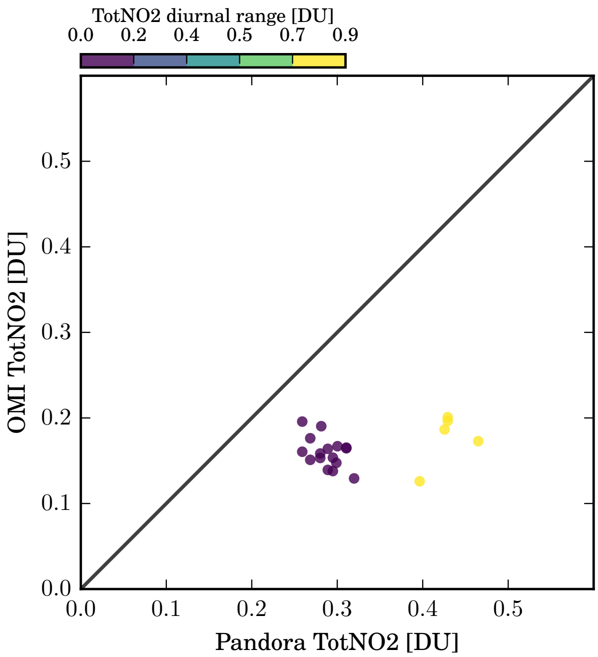

longitude, latitude	-97.3855, 38.4746
num data points	21
max Pan. (Pans.)	1 (17)
CC	0.29
RMS	0.02 DU
SLP	0.05 ± 0.14
mean	-0.16 DU
MEDD	-0.15 DU
25-75 perc. range	-0.19 DU to -0.12 DU
10-90 perc. range	-0.24 DU to -0.09 DU
min-max range	-0.29 DU to -0.06 DU
OMI CF	61.21 %
Pandora DQ0	74.80 %

Deerpark

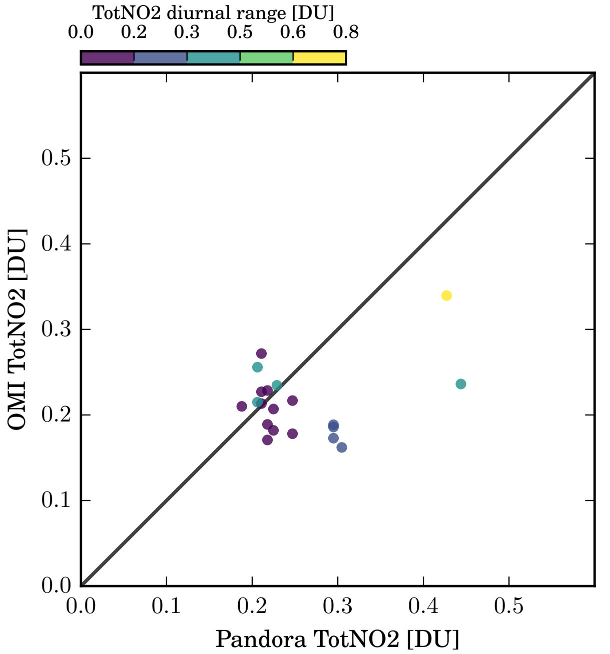

longitude, latitude	-95.1283, 29.6700
num data points	20
max Pan. (Pans.)	1 (32)
CC	0.31
RMS	0.04 DU
SLP	0.14 ± 0.22
mean	-0.04 DU
MEDD	-0.03 DU
25-75 perc. range	-0.09 DU to 0.01 DU
10-90 perc. range	-0.12 DU to 0.02 DU
min-max range	-0.21 DU to 0.06 DU
OMI CF	23.08 %
Pandora DQ0	55.08 %

DenverI25

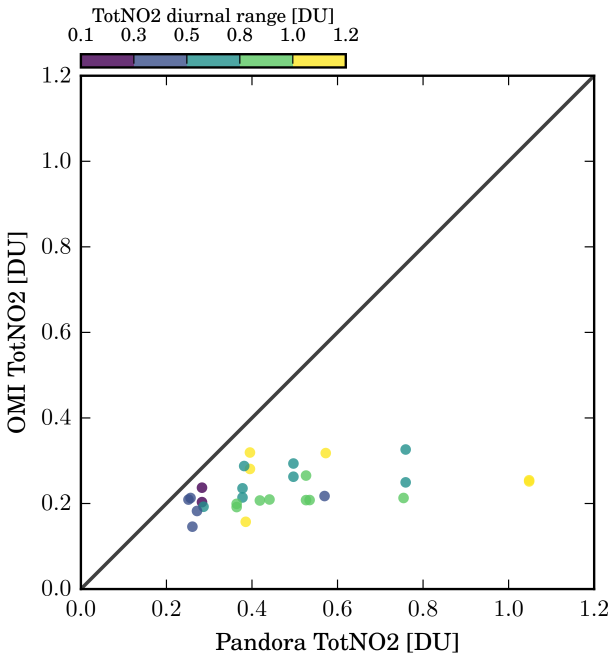

longitude, latitude	-105.015, 39.732
num data points	29
max Pan. (Pans.)	1 (27)
CC	0.39
RMS	0.05 DU
SLP	0.14 ± 0.04
mean	-0.25 DU
MEDD	-0.20 DU
25-75 perc. range	-0.32 DU to -0.09 DU
10-90 perc. range	-0.52 DU to -0.07 DU
min-max range	-0.80 DU to -0.04 DU
OMI CF	22.86 %
Pandora DQ0	59.29 %

DenverI25*

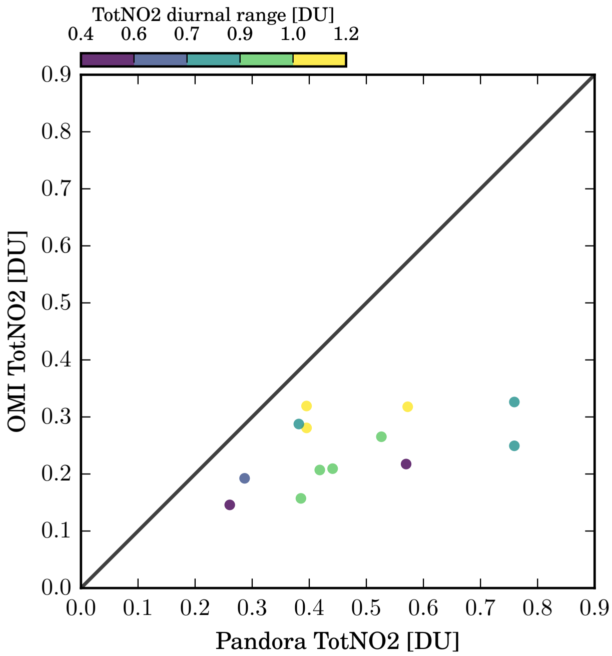

longitude, latitude	-105.015, 39.732
num data points	13
max Pan. (Pans.)	1 (27)
CC	0.52
RMS	0.06 DU
SLP	0.24 ± 0.06
mean	-0.23 DU
MEDD	-0.23 DU
25-75 perc. range	-0.26 DU to -0.11 DU
10-90 perc. range	-0.42 DU to -0.09 DU
min-max range	-0.51 DU to -0.08 DU
OMI CF	22.86 %
Pandora DQ0	59.29 %

DoiAngKhang

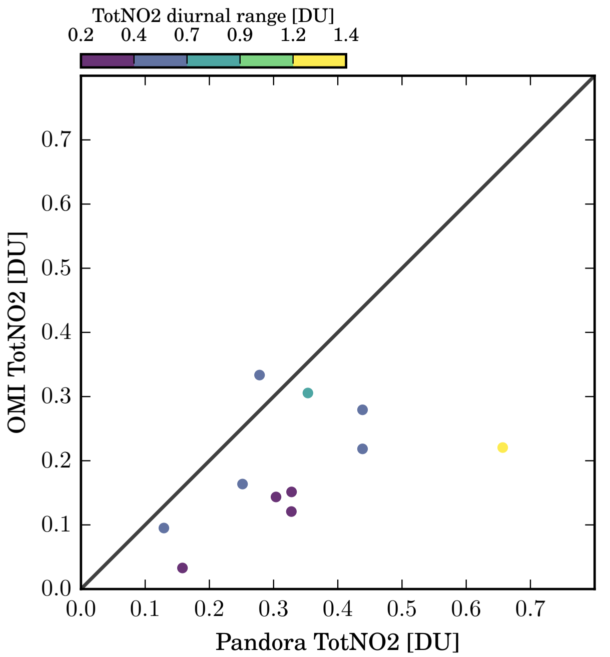

longitude, latitude	99.04526, 19.9332
num data points	12
max Pan. (Pans.)	2 (16, 42)
CC	0.58
RMS	0.09 DU
SLP	0.48 ± 0.08
mean	-0.15 DU
MEDD	-0.16 DU
25-75 perc. range	-0.19 DU to -0.08 DU
10-90 perc. range	-0.22 DU to -0.04 DU
min-max range	-0.44 DU to 0.06 DU
OMI CF	21.53 %
Pandora DQ0	70.44 %

Essex

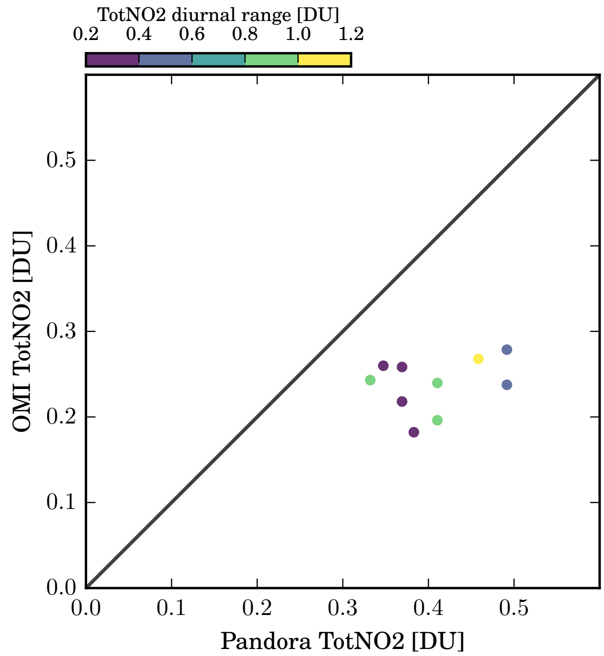

longitude, latitude	-76.474444, 39.310833
num data points	10
max Pan. (Pans.)	1 (19)
CC	0.28
RMS	0.04 DU
SLP	0.24 ± 0.35
mean	-0.17 DU
MEDD	-0.18 DU
25-75 perc. range	-0.21 DU to -0.12 DU
10-90 perc. range	-0.22 DU to -0.09 DU
min-max range	-0.25 DU to -0.09 DU
OMI CF	26.09 %
Pandora DQ0	75.65 %

FMI

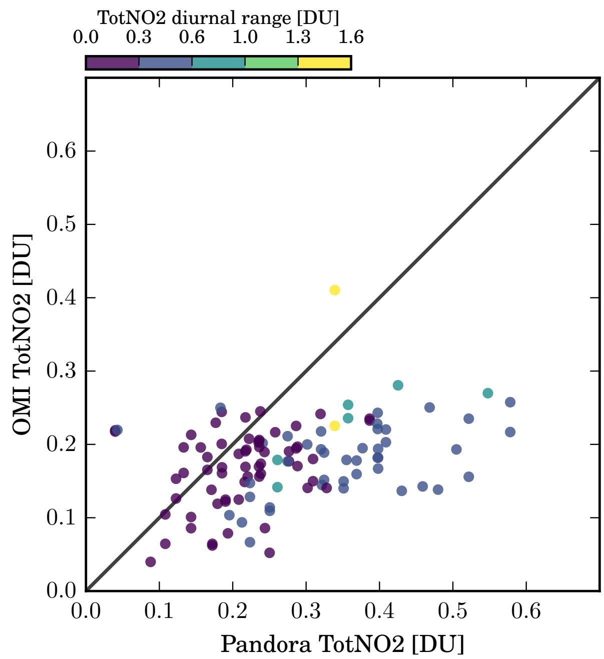

longitude, latitude	24.9612, 60.2037
num data points	113
max Pan. (Pans.)	1 (21)
CC	0.39
RMS	0.06 DU
SLP	0.21 ± 0.03
mean	-0.10 DU
MEDD	-0.09 DU
25-75 perc. range	-0.16 DU to -0.03 DU
10-90 perc. range	-0.22 DU to 0.03 DU
min-max range	-0.37 DU to 0.18 DU
OMI CF	13.54 %
Pandora DQ0	49.90 %

Fairbanks

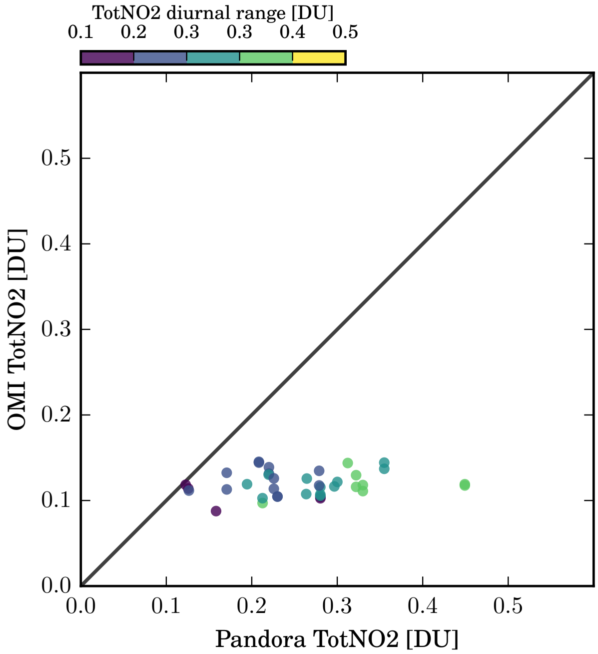

longitude, latitude	-147.85, 64.86
num data points	38
max Pan. (Pans.)	2 (2, 9)
CC	0.16
RMS	0.02 DU
SLP	0.10 ± 0.03
mean	-0.14 DU
MEDD	-0.14 DU
25-75 perc. range	-0.18 DU to -0.08 DU
10-90 perc. range	-0.21 DU to -0.05 DU
min-max range	-0.33 DU to -0.00 DU
OMI CF	39.56 %
Pandora DQ0	45.33 %

Fairhill

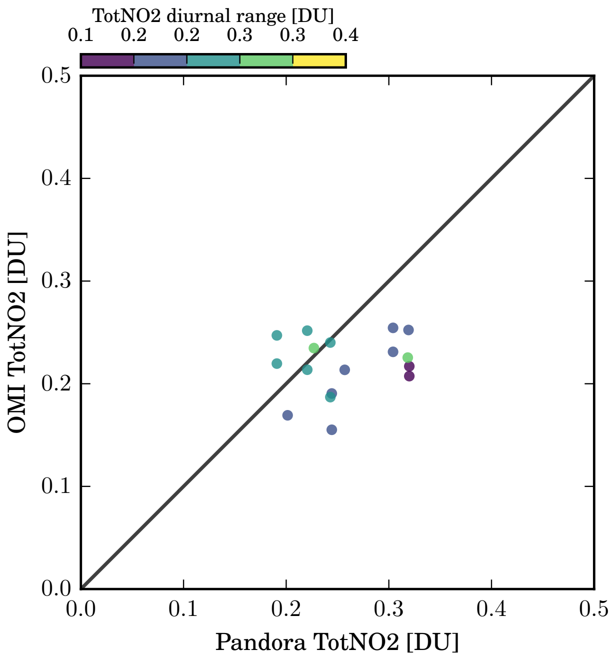

longitude, latitude	-75.868, 39.701111
num data points	17
max Pan. (Pans.)	1 (16)
CC	0.21
RMS	0.03 DU
SLP	0.22 ± 0.33
mean	-0.04 DU
MEDD	-0.05 DU
25-75 perc. range	-0.07 DU to -0.00 DU
10-90 perc. range	-0.10 DU to 0.03 DU
min-max range	-0.11 DU to 0.06 DU
OMI CF	28.12 %
Pandora DQ0	82.20 %

FortCollins

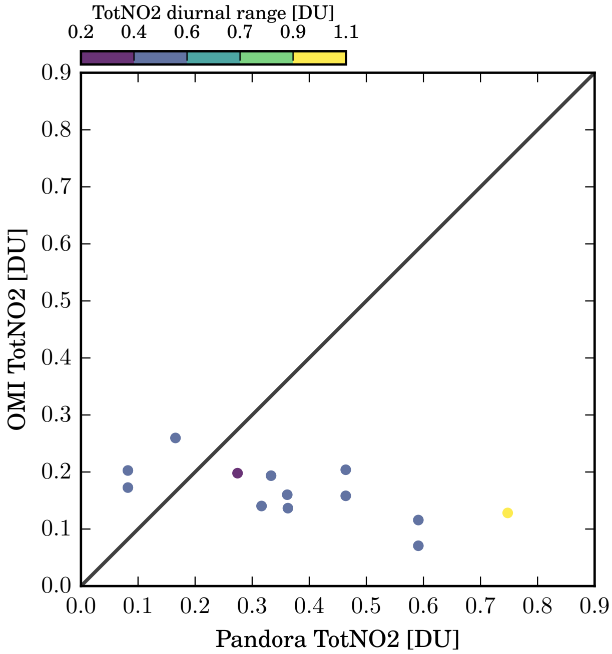

longitude, latitude	-105.129, 40.596
num data points	13
max Pan. (Pans.)	2 (17, 28)
CC	-0.67
RMS	0.04 DU
SLP	-0.10 ± 0.05
mean	-0.21 DU
MEDD	-0.20 DU
25-75 perc. range	-0.31 DU to -0.08 DU
10-90 perc. range	-0.51 DU to 0.09 DU
min-max range	-0.62 DU to 0.12 DU
OMI CF	18.60 %
Pandora DQ0	34.15 %

FourCornersNM

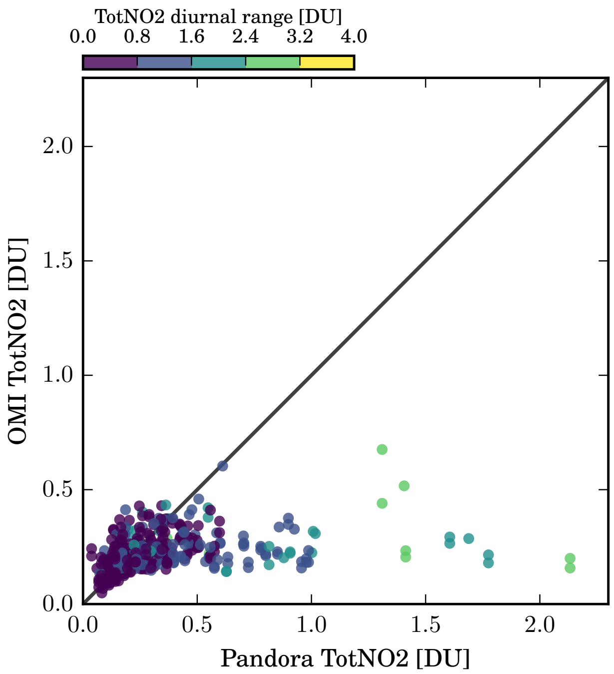

longitude, latitude	-108.480, 36.797
num data points	470
max Pan. (Pans.)	1 (23)
CC	0.33
RMS	0.08 DU
SLP	0.07 ± 0.00
mean	-0.11 DU
MEDD	-0.02 DU
25-75 perc. range	-0.13 DU to 0.02 DU
10-90 perc. range	-0.41 DU to 0.08 DU
min-max range	-1.97 DU to 0.23 DU
OMI CF	52.98 %
Pandora DQ0	58.54 %

FourCornersNM*

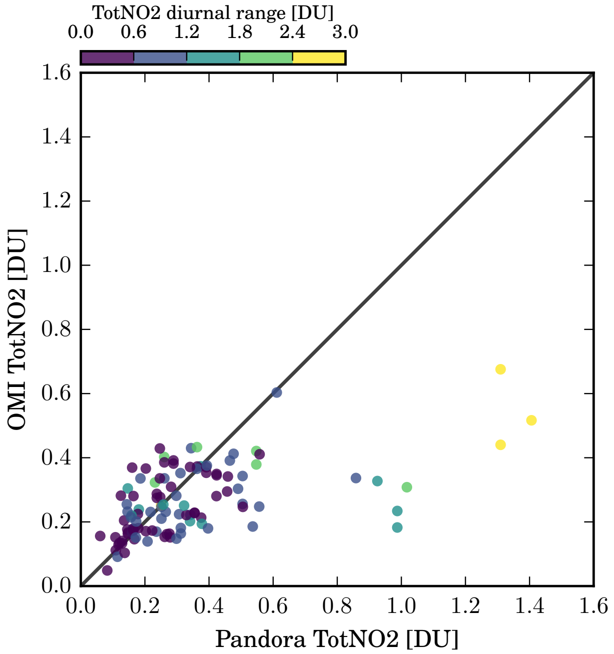

longitude, latitude	-108.480, 36.797
num data points	109
max Pan. (Pans.)	1 (23)
CC	0.56
RMS	0.10 DU
SLP	0.20 ± 0.01
mean	-0.07 DU
MEDD	-0.02 DU
25-75 perc. range	-0.13 DU to 0.04 DU
10-90 perc. range	-0.25 DU to 0.10 DU
min-max range	-0.89 DU to 0.21 DU
OMI CF	52.98 %
Pandora DQ0	58.54 %

Fresno

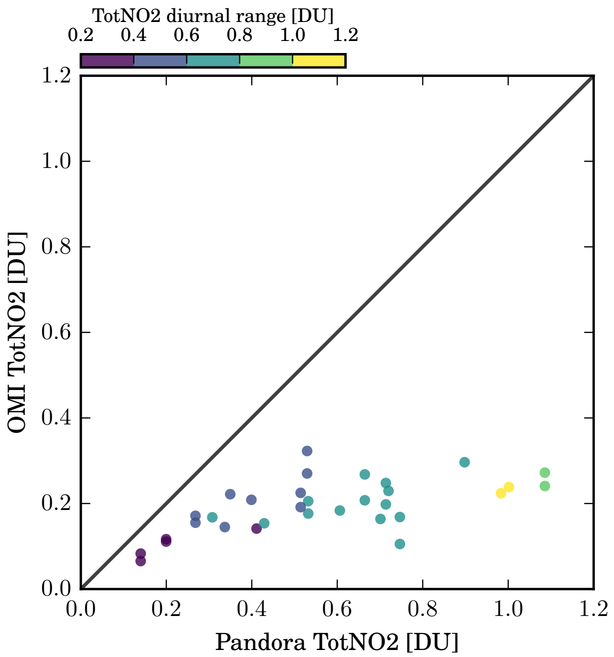

longitude, latitude	-119.7731, 36.7854
num data points	32
max Pan. (Pans.)	2 (30, 31)
CC	0.63
RMS	0.05 DU
SLP	0.16 ± 0.02
mean	-0.37 DU
MEDD	-0.32 DU
25-75 perc. range	-0.52 DU to -0.18 DU
10-90 perc. range	-0.75 DU to -0.09 DU
min-max range	-0.85 DU to -0.06 DU
OMI CF	30.77 %
Pandora DQ0	51.74 %

GIST

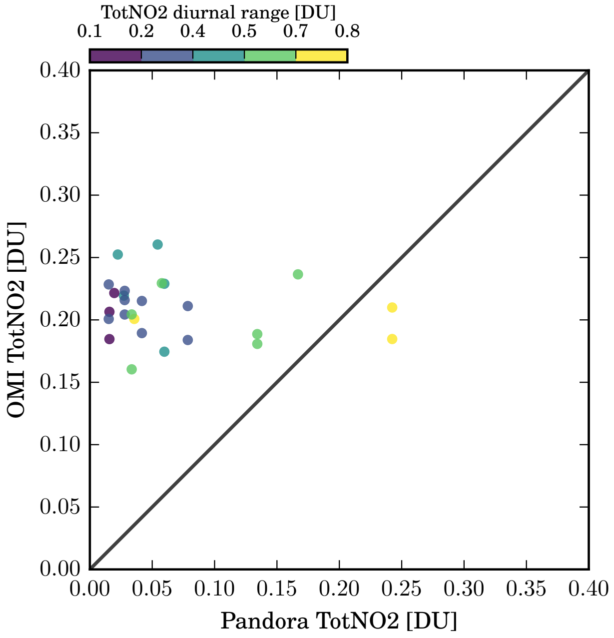

longitude, latitude	126.843, 35.226
num data points	26
max Pan. (Pans.)	1 (26)
CC	-0.16
RMS	0.02 DU
SLP	-0.03 ± 0.12
mean	0.14 DU
MEDD	0.17 DU
25-75 perc. range	0.12 DU to 0.19 DU
10-90 perc. range	0.05 DU to 0.20 DU
min-max range	-0.06 DU to 0.23 DU
OMI CF	28.19 %
Pandora DQ0	23.31 %

GSFC

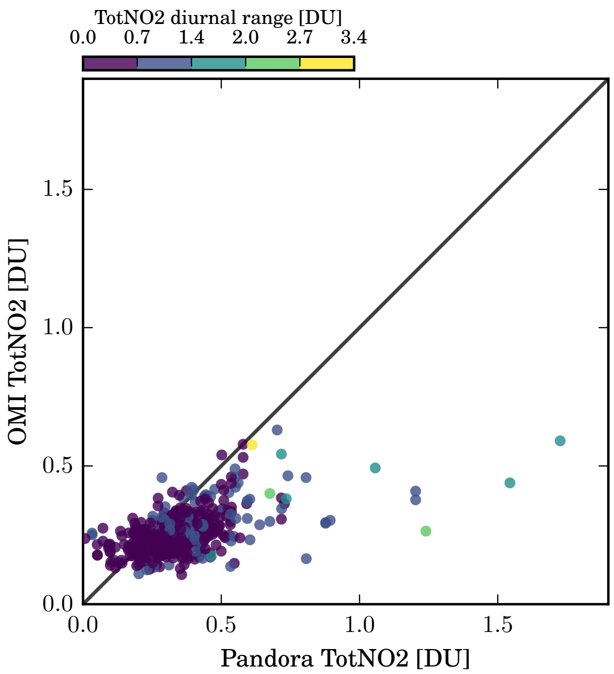

longitude, latitude	-76.8396, 38.9926
num data points	510
max Pan. (Pans.)	13 (16, 17, 18, 19, 24, 26, 27, 33, 36, 3, 41, 47, 7), not all considered!
CC	0.56
RMS	0.07 DU
SLP	0.16 ± 0.01
mean	-0.10 DU
MEDD	-0.08 DU
25-75 perc. range	-0.14 DU to -0.02 DU
10-90 perc. range	-0.22 DU to 0.04 DU
min-max range	-1.13 DU to 0.23 DU
OMI CF	29.06 %
Pandora DQ0	45.96 %

GSFC*

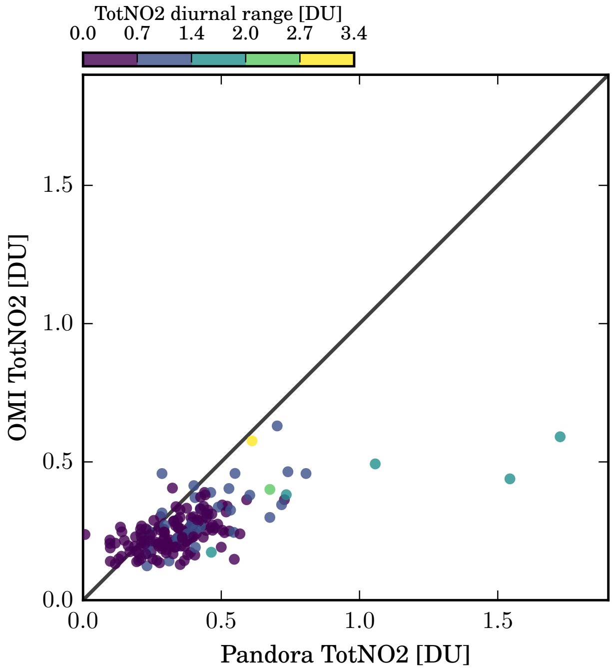

longitude, latitude	-76.8396, 38.9926
num data points	174
max Pan. (Pans.)	13 (16, 17, 18, 19, 24, 26, 27, 33, 36, 3, 41, 47, 7), not all considered!
CC	0.67
RMS	0.07 DU
SLP	0.28 ± 0.02
mean	-0.12 DU
MEDD	-0.11 DU
25-75 perc. range	-0.16 DU to -0.03 DU
10-90 perc. range	-0.25 DU to 0.03 DU
min-max range	-1.13 DU to 0.23 DU
OMI CF	29.06 %
Pandora DQ0	45.96 %

Galveston

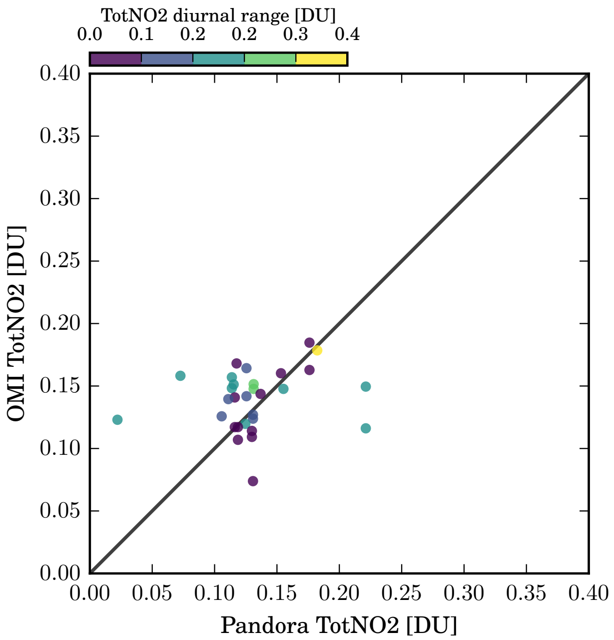

longitude, latitude	-94.8612, 29.2544
num data points	30
max Pan. (Pans.)	1 (34)
CC	0.21
RMS	0.03 DU
SLP	0.03 ± 0.10
mean	0.01 DU
MEDD	0.01 DU
25-75 perc. range	-0.01 DU to 0.03 DU
10-90 perc. range	-0.02 DU to 0.04 DU
min-max range	-0.11 DU to 0.10 DU
OMI CF	36.47 %
Pandora DQ0	62.01 %

HUFS

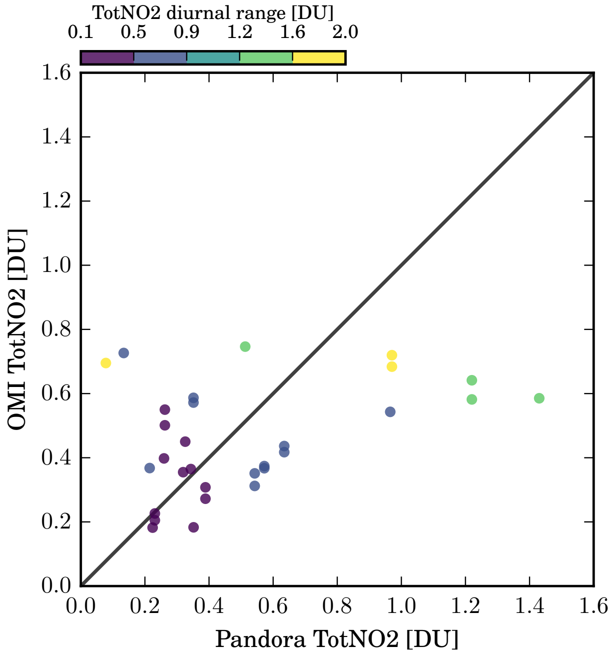

longitude, latitude	127.265, 37.338
num data points	30
max Pan. (Pans.)	1 (18)
CC	0.39
RMS	0.16 DU
SLP	0.19 ± 0.04
mean	-0.06 DU
MEDD	-0.06 DU
25-75 perc. range	-0.21 DU to 0.15 DU
10-90 perc. range	-0.44 DU to 0.24 DU
min-max range	-0.84 DU to 0.62 DU
OMI CF	21.35 %
Pandora DQ0	40.70 %

Hanford

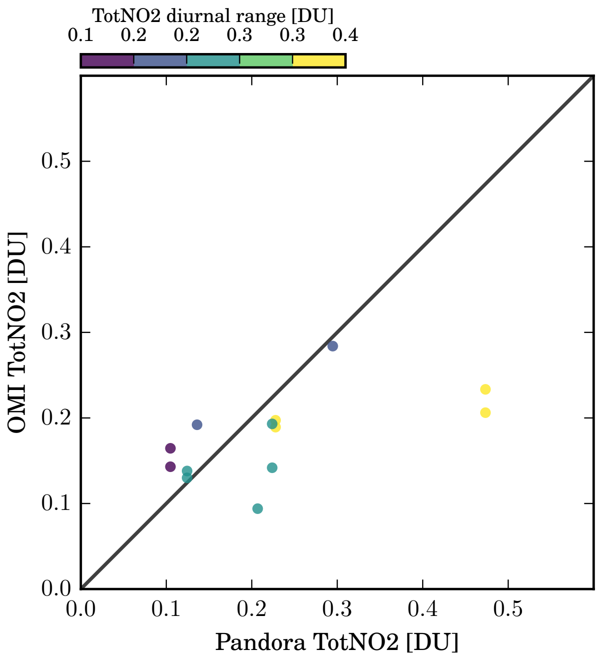

longitude, latitude	-119.6433, 36.3193
num data points	13
max Pan. (Pans.)	2 (18, 32)
CC	0.58
RMS	0.04 DU
SLP	0.24 ± 0.12
mean	-0.05 DU
MEDD	-0.03 DU
25-75 perc. range	-0.08 DU to 0.01 DU
10-90 perc. range	-0.21 DU to 0.05 DU
min-max range	-0.27 DU to 0.06 DU
OMI CF	29.79 %
Pandora DQ0	66.89 %

Harvard

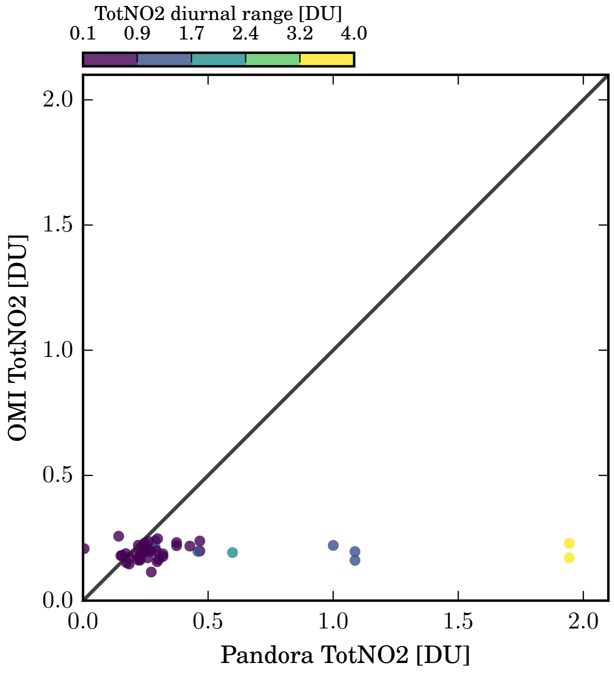

longitude, latitude	-71.116155, 42.376211
num data points	44
max Pan. (Pans.)	1 (32)
CC	0.06
RMS	0.03 DU
SLP	-0.01 ± 0.02
mean	-0.21 DU
MEDD	-0.06 DU
25-75 perc. range	-0.16 DU to -0.03 DU
10-90 perc. range	-0.67 DU to 0.01 DU
min-max range	-1.77 DU to 0.20 DU
OMI CF	23.70 %
Pandora DQ0	29.45 %

Huron

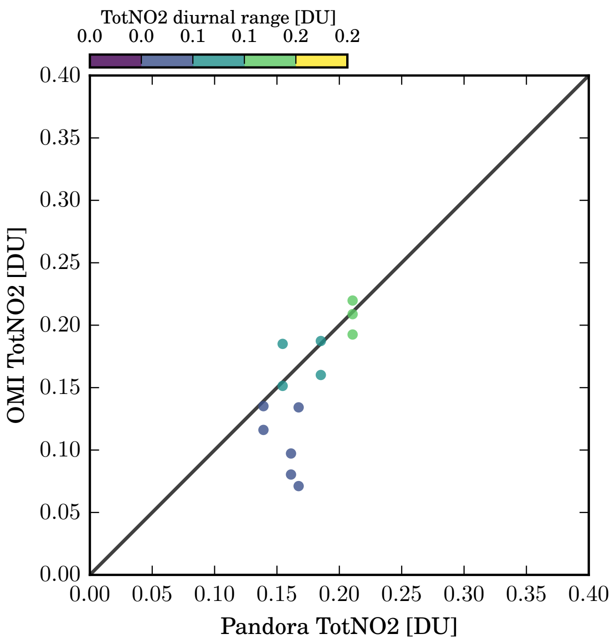

longitude, latitude	-120.105, 36.206
num data points	13
max Pan. (Pans.)	1 (2)
CC	0.67
RMS	0.04 DU
SLP	1.29 ± 0.56
mean	-0.02 DU
MEDD	-0.02 DU
25-75 perc. range	-0.03 DU to -0.00 DU
10-90 perc. range	-0.08 DU to 0.01 DU
min-max range	-0.10 DU to 0.03 DU
OMI CF	48.28 %
Pandora DQ0	81.04 %

IBK

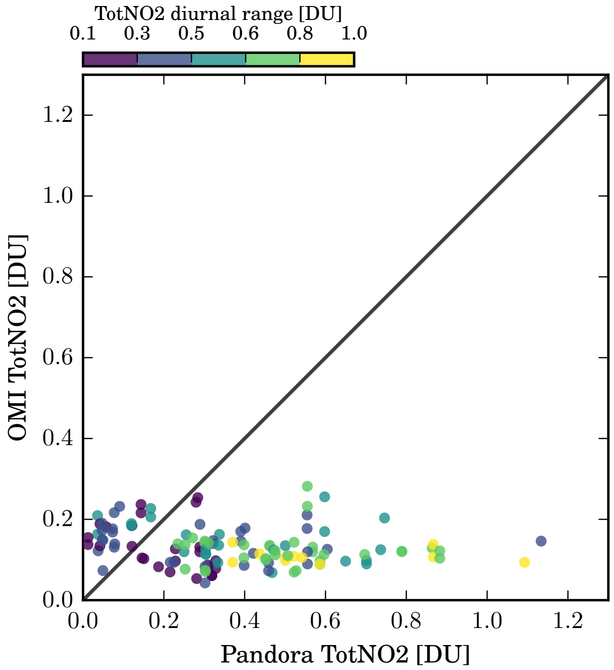

longitude, latitude	11.3852, 47.2643
num data points	128
max Pan. (Pans.)	2 (106, 110)
CC	-0.21
RMS	0.06 DU
SLP	0.02 ± 0.01
mean	-0.24 DU
MEDD	-0.23 DU
25-75 perc. range	-0.40 DU to -0.09 DU
10-90 perc. range	-0.56 DU to 0.10 DU
min-max range	-1.00 DU to 0.17 DU
OMI CF	30.19 %
Pandora DQ0	40.95 %

IBK*

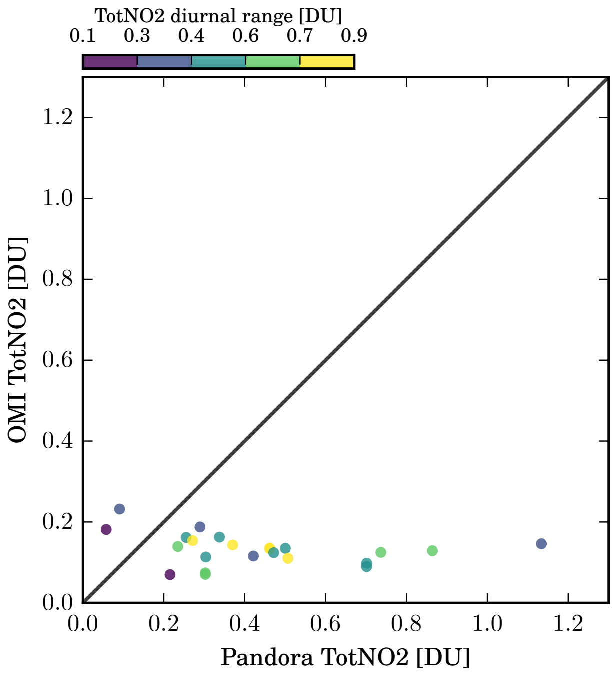

longitude, latitude	11.3852, 47.2643
num data points	23
max Pan. (Pans.)	2 (106, 110)
CC	-0.27
RMS	0.04 DU
SLP	-0.01 ± 0.02
mean	-0.30 DU
MEDD	-0.23 DU
25-75 perc. range	-0.38 DU to -0.13 DU
10-90 perc. range	-0.61 DU to -0.09 DU
min-max range	-0.99 DU to 0.14 DU
OMI CF	30.19 %
Pandora DQ0	40.95 %

IZO

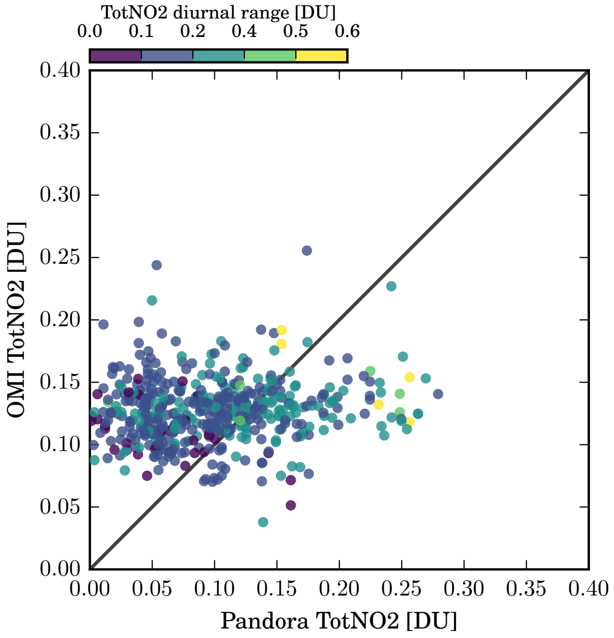

longitude, latitude	-16.4994, 28.309
num data points	497
max Pan. (Pans.)	1 (101)
CC	0.11
RMS	0.03 DU
SLP	0.04 ± 0.02
mean	0.03 DU
MEDD	0.03 DU
25-75 perc. range	-0.01 DU to 0.07 DU
10-90 perc. range	-0.06 DU to 0.10 DU
min-max range	-0.14 DU to 0.19 DU
OMI CF	33.38 %
Pandora DQ0	54.72 %

IZO*

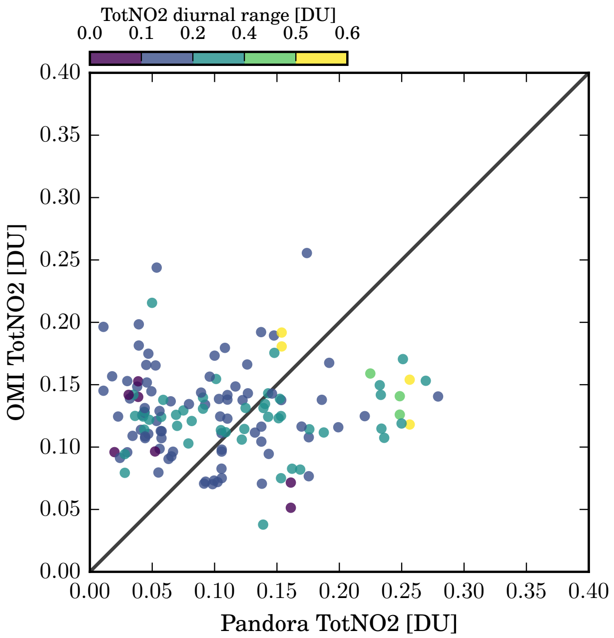

longitude, latitude	-16.4994, 28.309
num data points	138
max Pan. (Pans.)	1 (101)
CC	0.01
RMS	0.04 DU
SLP	-0.00 ± 0.03
mean	0.02 DU
MEDD	0.03 DU
25-75 perc. range	-0.03 DU to 0.07 DU
10-90 perc. range	-0.09 DU to 0.11 DU
min-max range	-0.14 DU to 0.19 DU
OMI CF	33.38 %
Pandora DQ0	54.72 %

Langley

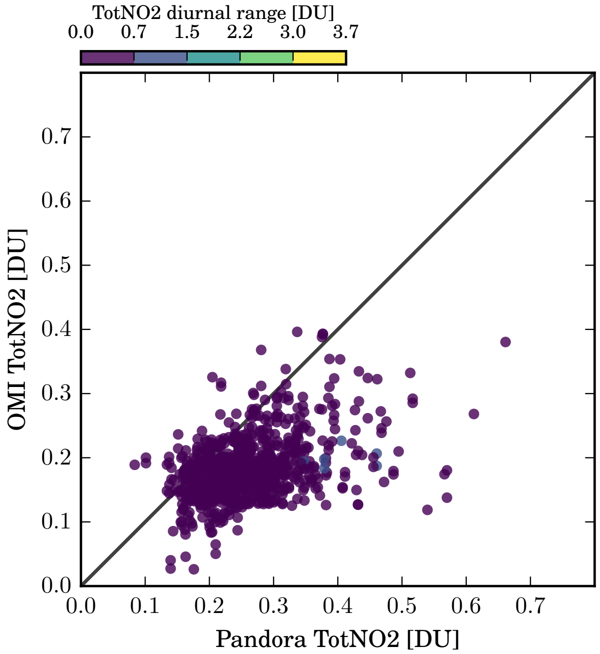

longitude, latitude	-76.3868, 37.1036
num data points	990
max Pan. (Pans.)	3 (37, 39, 6)
CC	0.42
RMS	0.04 DU
SLP	0.17 ± 0.02
mean	-0.07 DU
MEDD	-0.07 DU
25-75 perc. range	-0.11 DU to -0.03 DU
10-90 perc. range	-0.15 DU to 0.00 DU
min-max range	-0.43 DU to 0.12 DU
OMI CF	44.75 %
Pandora DQ0	51.82 %

Langley*

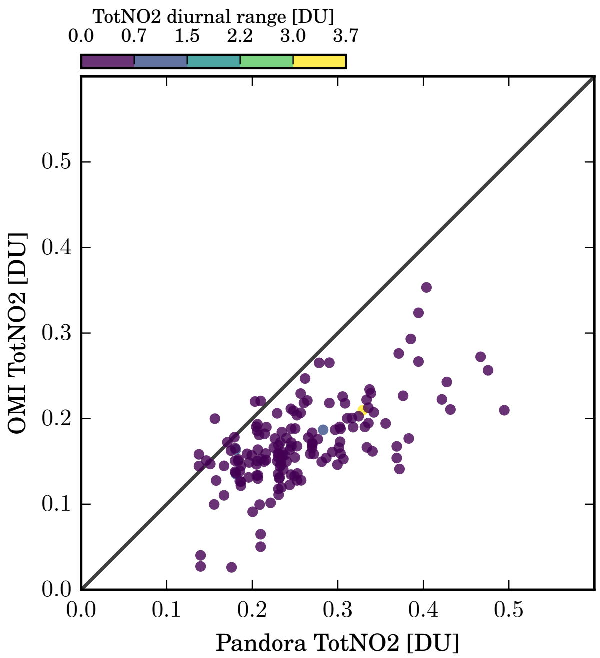

longitude, latitude	-76.3868, 37.1036
num data points	158
max Pan. (Pans.)	3 (37, 39, 6)
CC	0.64
RMS	0.04 DU
SLP	0.41 ± 0.04
mean	-0.09 DU
MEDD	-0.08 DU
25-75 perc. range	-0.12 DU to -0.05 DU
10-90 perc. range	-0.15 DU to -0.02 DU
min-max range	-0.28 DU to 0.04 DU
OMI CF	44.75 %
Pandora DQ0	51.82 %

Lauder

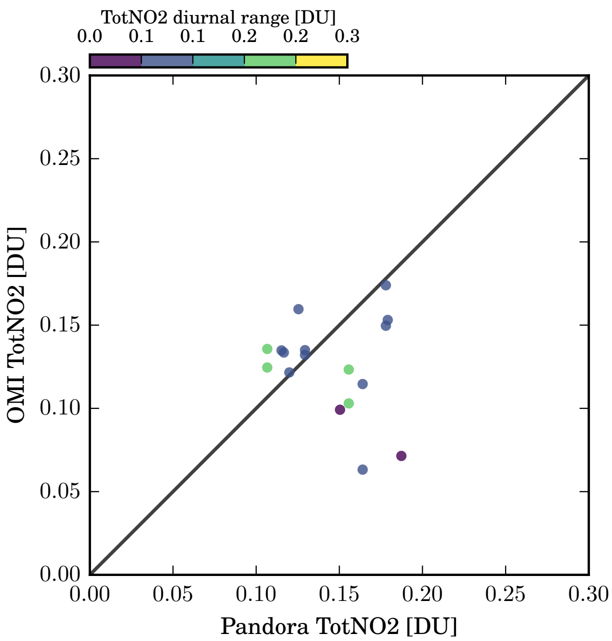

longitude, latitude	169.684, -45.038
num data points	17
max Pan. (Pans.)	1 (37)
CC	-0.19
RMS	0.03 DU
SLP	-0.35 ± 0.25
mean	-0.02 DU
MEDD	-0.00 DU
25-75 perc. range	-0.05 DU to 0.02 DU
10-90 perc. range	-0.07 DU to 0.02 DU
min-max range	-0.12 DU to 0.03 DU
OMI CF	39.53 %
Pandora DQ0	58.86 %

Madera

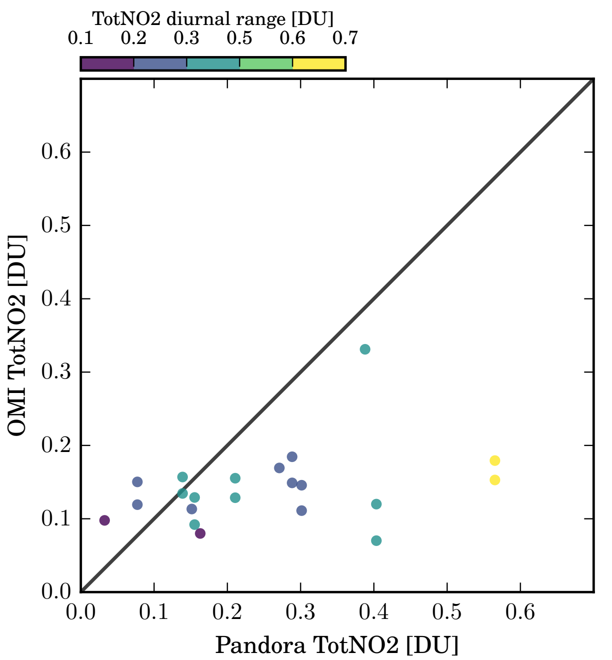

longitude, latitude	-120.0342, 36.9533
num data points	21
max Pan. (Pans.)	1 (29)
CC	0.34
RMS	0.05 DU
SLP	0.09 ± 0.06
mean	-0.11 DU
MEDD	-0.08 DU
25-75 perc. range	-0.16 DU to -0.03 DU
10-90 perc. range	-0.33 DU to 0.04 DU
min-max range	-0.41 DU to 0.07 DU
OMI CF	36.46 %
Pandora DQ0	56.83 %

Manvelcroix

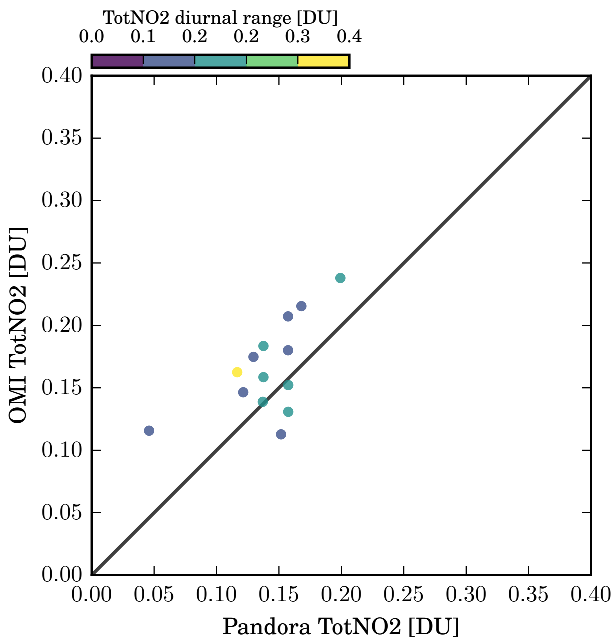

longitude, latitude	-95.392, 29.520
num data points	14
max Pan. (Pans.)	1 (33)
CC	0.62
RMS	0.03 DU
SLP	0.42 ± 0.22
mean	0.02 DU
MEDD	0.03 DU
25-75 perc. range	0.01 DU to 0.05 DU
10-90 perc. range	-0.02 DU to 0.05 DU
min-max range	-0.04 DU to 0.07 DU
OMI CF	20.65 %
Pandora DQ0	61.36 %

MaunaLoa

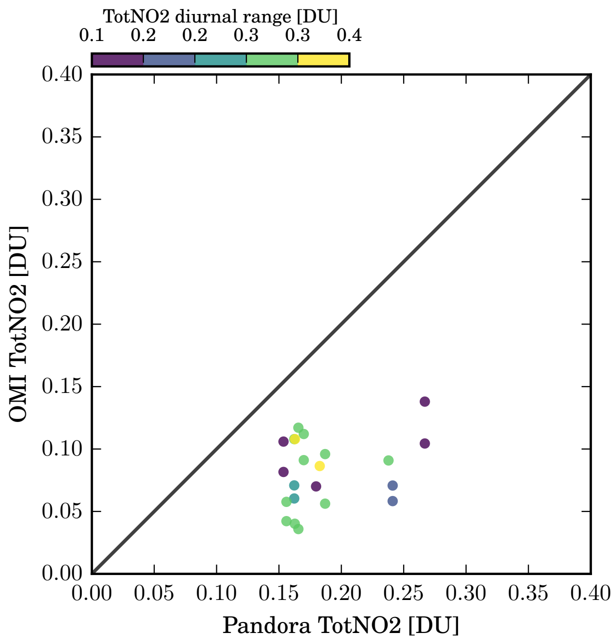

longitude, latitude	-155.6027, 19.4795
num data points	22
max Pan. (Pans.)	1 (31)
CC	0.28
RMS	0.03 DU
SLP	0.17 ± 0.18
mean	-0.10 DU
MEDD	-0.10 DU
25-75 perc. range	-0.13 DU to -0.07 DU
10-90 perc. range	-0.16 DU to -0.05 DU
min-max range	-0.18 DU to -0.05 DU
OMI CF	13.13 %
Pandora DQ0	77.51 %

Moodytower

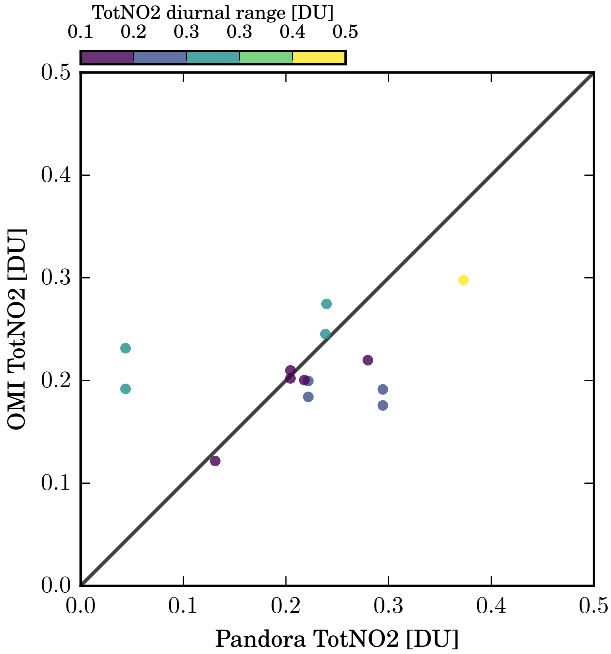

longitude, latitude	-95.3413, 29.7175
num data points	14
max Pan. (Pans.)	1 (35)
CC	0.38
RMS	0.05 DU
SLP	0.42 ± 0.15
mean	-0.00 DU
MEDD	-0.01 DU
25-75 perc. range	-0.05 DU to 0.01 DU
10-90 perc. range	-0.09 DU to 0.11 DU
min-max range	-0.12 DU to 0.19 DU
OMI CF	17.58 %
Pandora DQ0	53.97 %

NASAHQ

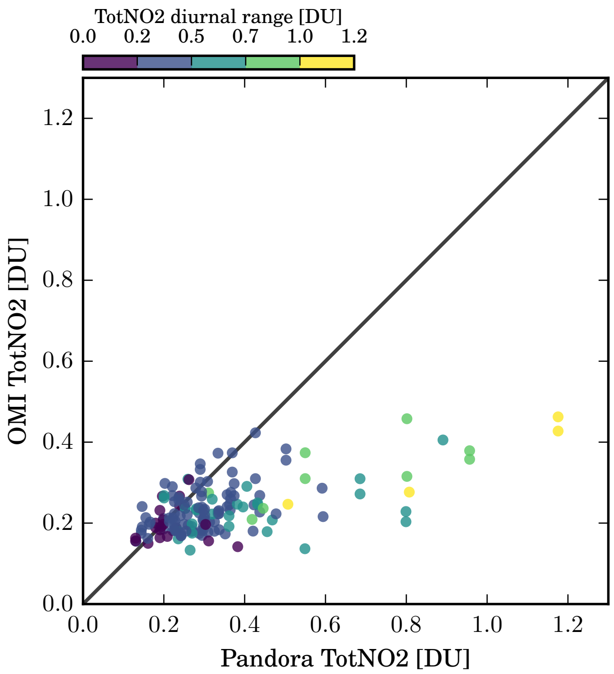

longitude, latitude	-76.8396, 38.9926
num data points	156
max Pan. (Pans.)	2 (17, 33)
CC	0.61
RMS	0.06 DU
SLP	0.12 ± 0.02
mean	-0.10 DU
MEDD	-0.07 DU
25-75 perc. range	-0.13 DU to -0.00 DU
10-90 perc. range	-0.27 DU to 0.04 DU
min-max range	-0.75 DU to 0.10 DU
OMI CF	29.29 %
Pandora DQ0	47.66 %

NASAHQ*

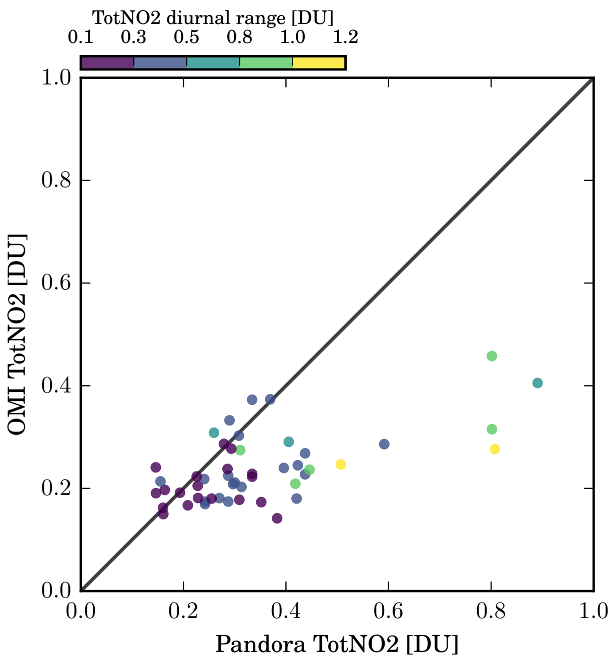

longitude, latitude	-76.8396, 38.9926
num data points	49
max Pan. (Pans.)	2 (17, 33)
CC	0.61
RMS	0.06 DU
SLP	0.19 ± 0.05
mean	-0.11 DU
MEDD	-0.07 DU
25-75 perc. range	-0.18 DU to -0.01 DU
10-90 perc. range	-0.27 DU to 0.04 DU
min-max range	-0.53 DU to 0.09 DU
OMI CF	29.29 %
Pandora DQ0	47.66 %

NWHarris

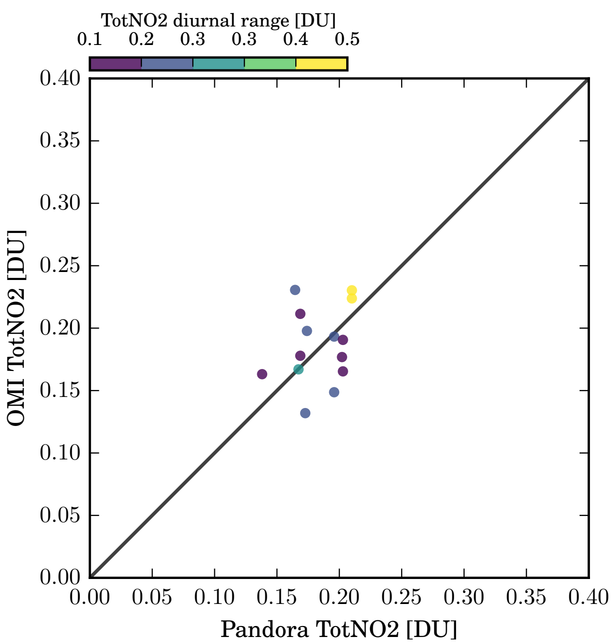

longitude, latitude	-95.6738, 30.0394
num data points	14
max Pan. (Pans.)	1 (30)
CC	0.24
RMS	0.03 DU
SLP	0.38 ± 0.62
mean	0.00 DU
MEDD	0.00 DU
25-75 perc. range	-0.02 DU to 0.02 DU
10-90 perc. range	-0.04 DU to 0.04 DU
min-max range	-0.05 DU to 0.07 DU
OMI CF	30.00 %
Pandora DQ0	59.96 %

Niwot

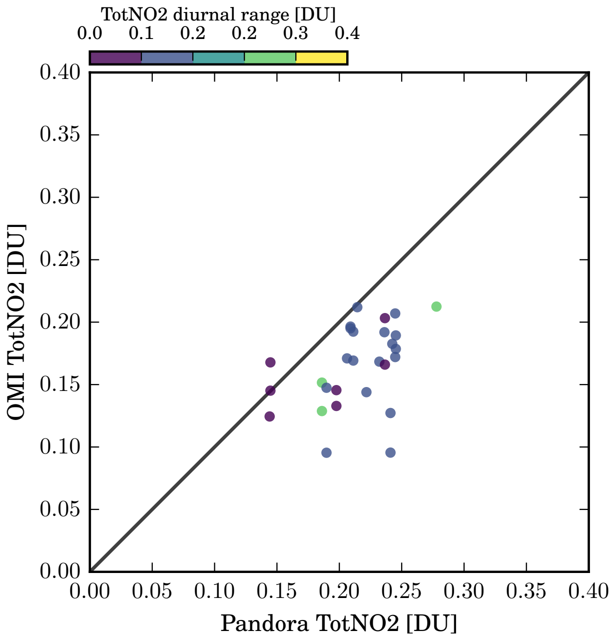

longitude, latitude	-105.5334, 40.0318
num data points	28
max Pan. (Pans.)	1 (29)
CC	0.43
RMS	0.03 DU
SLP	0.24 ± 0.17
mean	-0.05 DU
MEDD	-0.05 DU
25-75 perc. range	-0.07 DU to -0.03 DU
10-90 perc. range	-0.08 DU to -0.01 DU
min-max range	-0.15 DU to 0.02 DU
OMI CF	20.89 %
Pandora DQ0	50.01 %

PSU

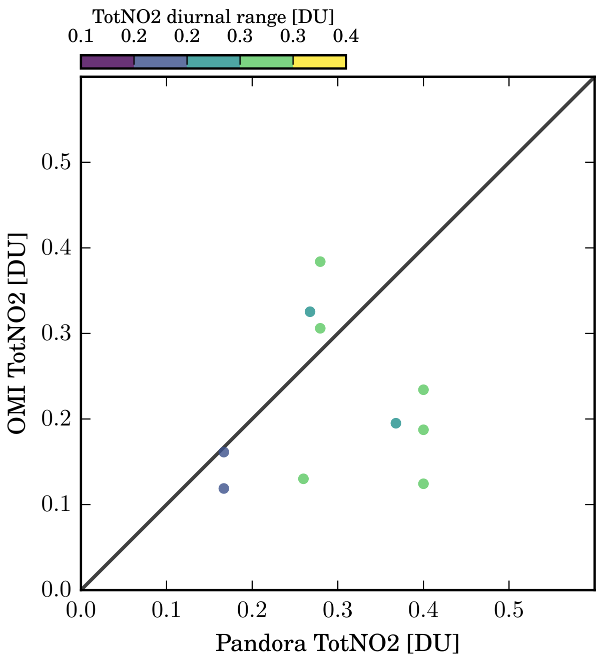

longitude, latitude	-77.86677, 40.793171
num data points	10
max Pan. (Pans.)	1 (8)
CC	0.04
RMS	0.09 DU
SLP	-0.10 ± 0.25
mean	-0.08 DU
MEDD	-0.09 DU
25-75 perc. range	-0.17 DU to 0.02 DU
10-90 perc. range	-0.22 DU to 0.06 DU
min-max range	-0.28 DU to 0.10 DU
OMI CF	16.99 %
Pandora DQ0	51.24 %

Padonia

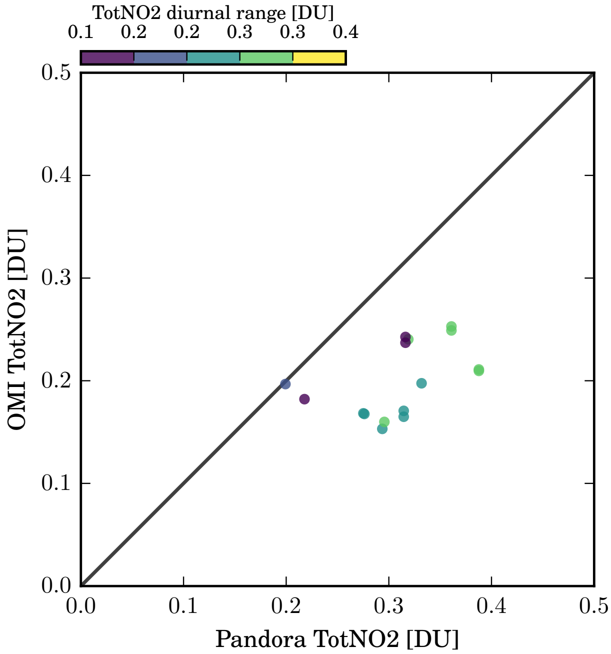

longitude, latitude	-76.631111, 39.460833
num data points	16
max Pan. (Pans.)	1 (17)
CC	0.46
RMS	0.03 DU
SLP	0.49 ± 0.26
mean	-0.11 DU
MEDD	-0.11 DU
25-75 perc. range	-0.14 DU to -0.08 DU
10-90 perc. range	-0.16 DU to -0.05 DU
min-max range	-0.18 DU to -0.00 DU
OMI CF	31.37 %
Pandora DQ0	80.93 %

Parlier

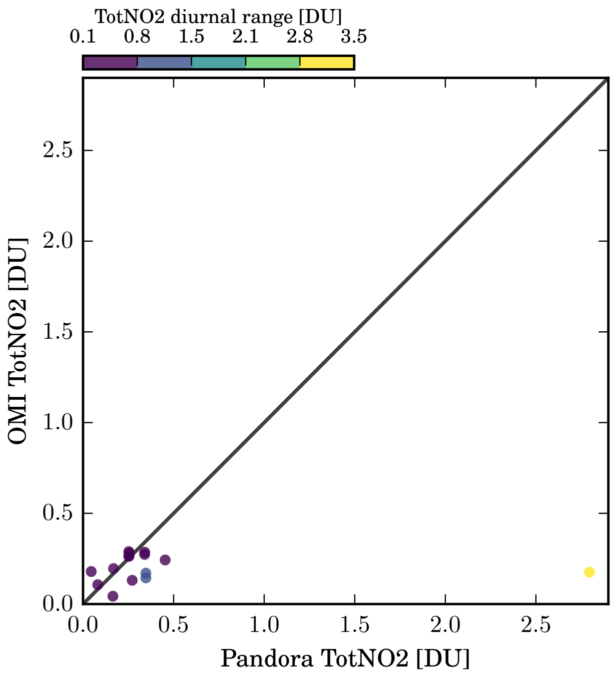

longitude, latitude	-119.5037, 36.5974
num data points	15
max Pan. (Pans.)	1 (28)
CC	-0.03
RMS	0.08 DU
SLP	0.01 ± 0.01
mean	-0.22 DU
MEDD	-0.05 DU
25-75 perc. range	-0.16 DU to 0.03 DU
10-90 perc. range	-0.21 DU to 0.03 DU
min-max range	-2.62 DU to 0.13 DU
OMI CF	24.24 %
Pandora DQ0	16.42 %

Platteville

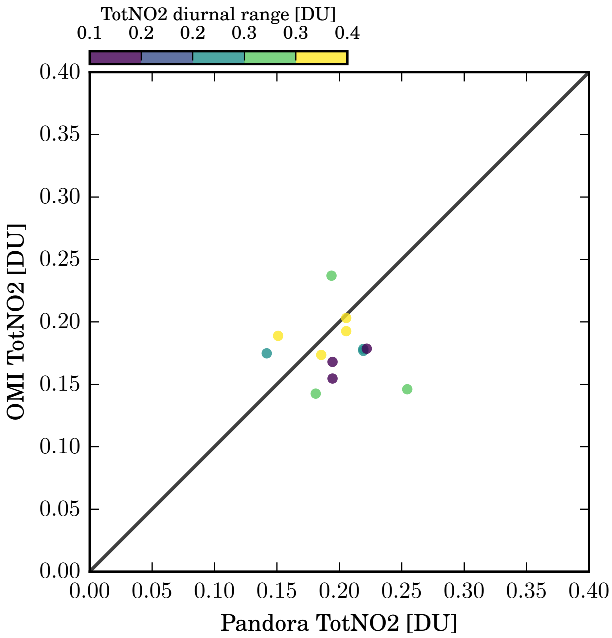

longitude, latitude	-104.726, 40.181
num data points	13
max Pan. (Pans.)	2 (30, 8)
CC	-0.15
RMS	0.02 DU
SLP	-0.05 ± 0.37
mean	-0.02 DU
MEDD	-0.03 DU
25-75 perc. range	-0.04 DU to -0.00 DU
10-90 perc. range	-0.04 DU to 0.04 DU
min-max range	-0.11 DU to 0.04 DU
OMI CF	28.26 %
Pandora DQ0	56.33 %

Porterville

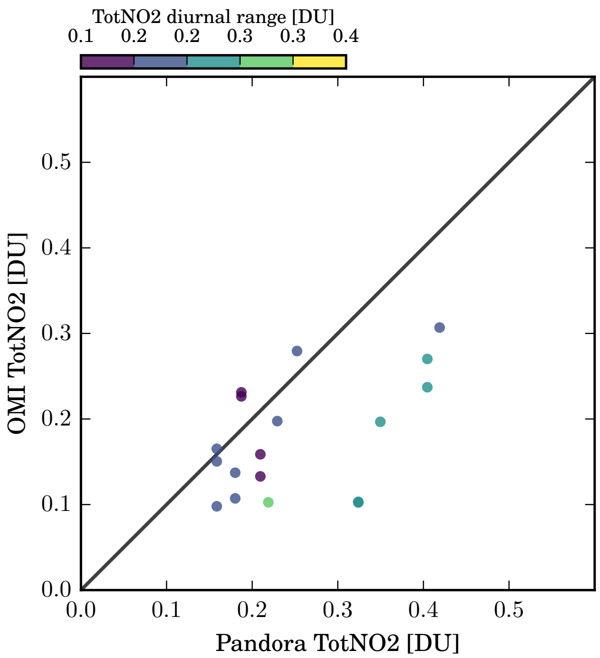

longitude, latitude	-119.055, 36.03179
num data points	18
max Pan. (Pans.)	2 (27, 8)
CC	0.50
RMS	0.09 DU
SLP	-0.12 ± 0.10
mean	-0.08 DU
MEDD	-0.07 DU
25-75 perc. range	-0.13 DU to -0.01 DU
10-90 perc. range	-0.18 DU to 0.03 DU
min-max range	-0.22 DU to 0.04 DU
OMI CF	40.00 %
Pandora DQ0	60.37 %

RockyFlats

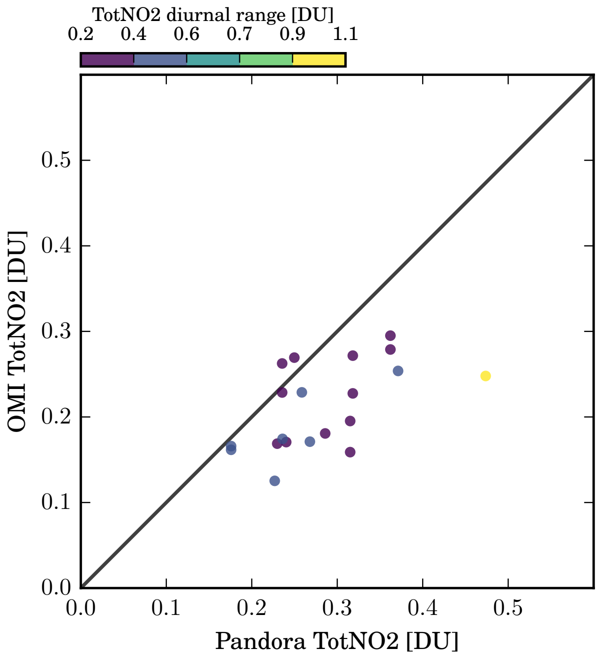

longitude, latitude	-105.19, 39.92
num data points	20
max Pan. (Pans.)	1 (31)
CC	0.56
RMS	0.04 DU
SLP	0.41 ± 0.11
mean	-0.07 DU
MEDD	-0.07 DU
25-75 perc. range	-0.10 DU to -0.03 DU
10-90 perc. range	-0.12 DU to -0.00 DU
min-max range	-0.23 DU to 0.03 DU
OMI CF	23.91 %
Pandora DQ0	59.14 %

SERC

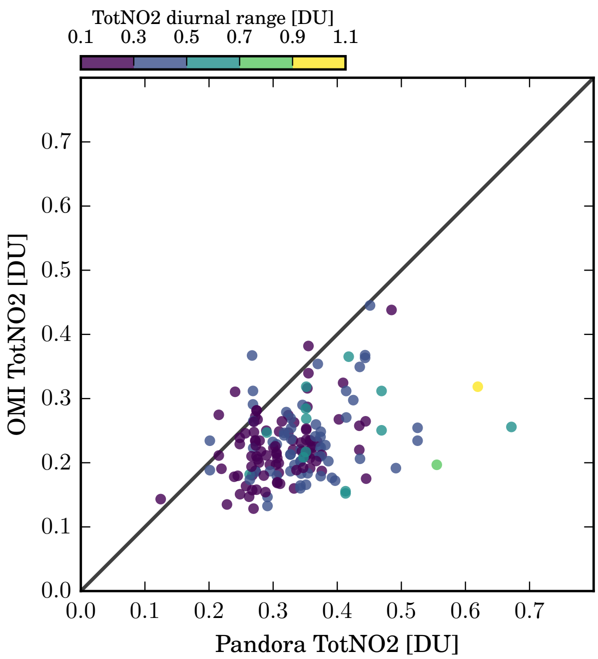

longitude, latitude	-76.55, 38.88
num data points	163
max Pan. (Pans.)	2 (24, 7)
CC	0.34
RMS	0.06 DU
SLP	0.19 ± 0.05
mean	-0.11 DU
MEDD	-0.10 DU
25-75 perc. range	-0.14 DU to -0.06 DU
10-90 perc. range	-0.19 DU to -0.01 DU
min-max range	-0.42 DU to 0.10 DU
OMI CF	31.03 %
Pandora DQ0	44.09 %

SERC*

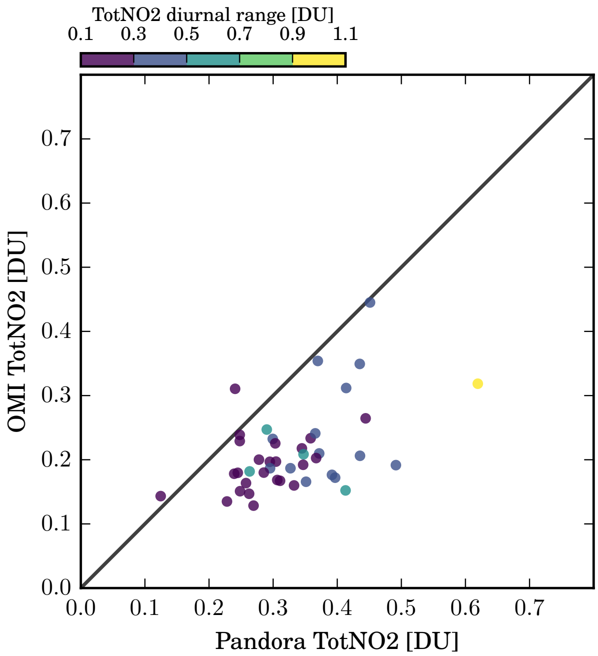

longitude, latitude	-76.55, 38.88
num data points	43
max Pan. (Pans.)	2 (24, 7)
CC	0.49
RMS	0.06 DU
SLP	0.33 $\pm$ 0.10
mean	-0.12 DU
MEDD	-0.11 DU
25-75 perc. range	-0.16 DU to -0.08 DU
10-90 perc. range	-0.22 DU to -0.02 DU
min-max range	-0.30 DU to 0.07 DU
OMI CF	31.03 %
Pandora DQ0	44.09 %

Seabrook

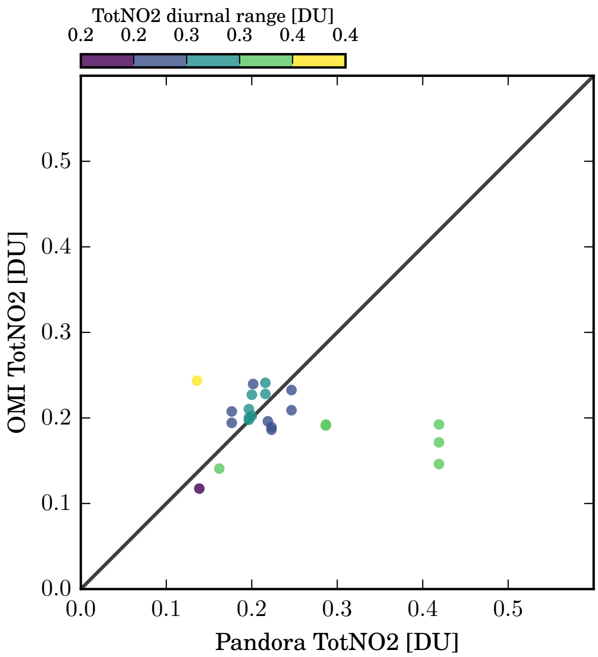

longitude, latitude	-95.3261, 29.9010
num data points	23
max Pan. (Pans.)	1 (27)
CC	-0.22
RMS	0.03 DU
SLP	-0.01 $\pm$ 0.09
mean	-0.04 DU
MEDD	-0.01 DU
25-75 perc. range	-0.04 DU to 0.02 DU
10-90 perc. range	-0.20 DU to 0.03 DU
min-max range	-0.27 DU to 0.11 DU
OMI CF	25.00 %
Pandora DQ0	48.52 %

Seoul

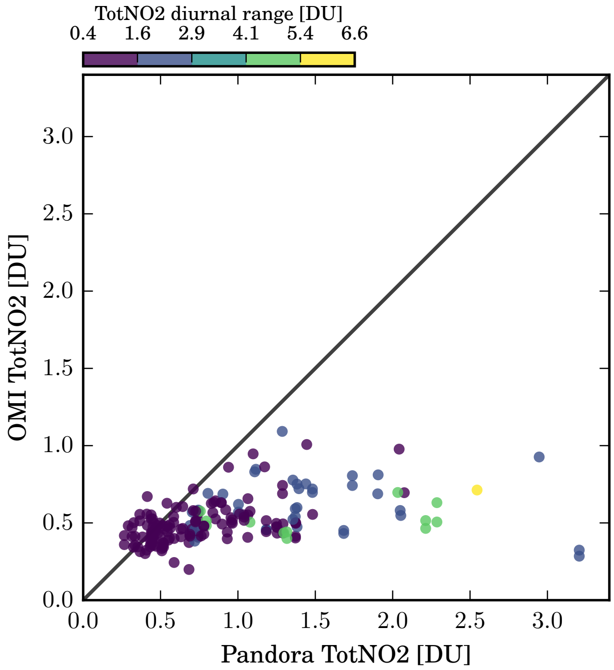

longitude, latitude	126.934, 37.5644
num data points	183
max Pan. (Pans.)	3 (17, 19, 29)
CC	0.41
RMS	0.17 DU
SLP	-0.01 ± 0.00
mean	-0.42 DU
MEDD	-0.26 DU
25-75 perc. range	-0.66 DU to -0.08 DU
10-90 perc. range	-0.97 DU to 0.02 DU
min-max range	-2.92 DU to 0.26 DU
OMI CF	23.44 %
Pandora DQ0	70.78 %

Seoul*

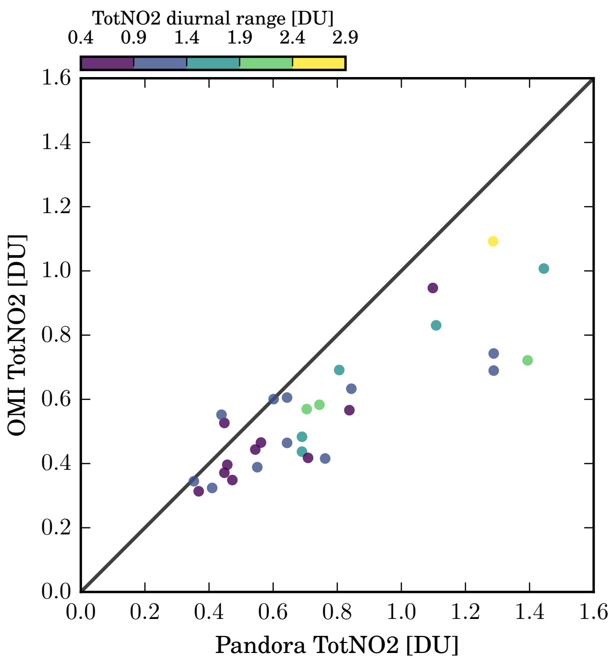

longitude, latitude	126.934, 37.5644
num data points	30
max Pan. (Pans.)	3 (17, 19, 29)
CC	0.85
RMS	0.11 DU
SLP	0.54 ± 0.04
mean	-0.19 DU
MEDD	-0.16 DU
25-75 perc. range	-0.27 DU to -0.08 DU
10-90 perc. range	-0.45 DU to -0.01 DU
min-max range	-0.67 DU to 0.11 DU
OMI CF	23.44 %
Pandora DQ0	70.78 %

Smithpoint

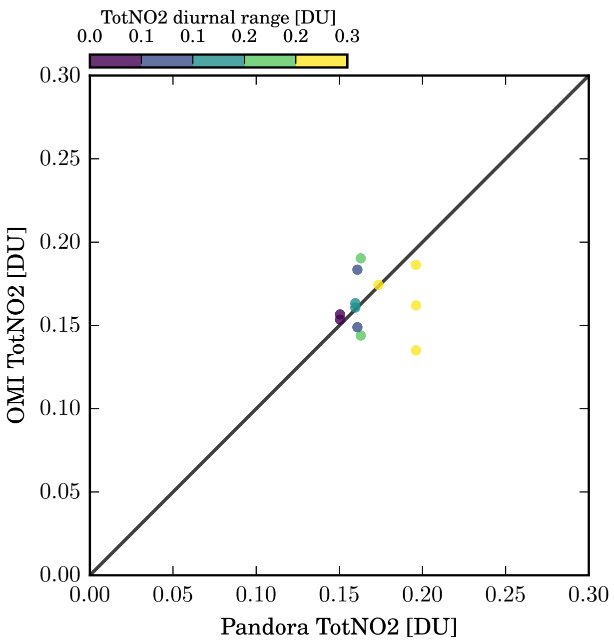

longitude, latitude	-94.7869, 29.5462
num data points	12
max Pan. (Pans.)	3 (29, 36, 8)
CC	0.03
RMS	0.02 DU
SLP	-0.30 ± 0.51
mean	-0.01 DU
MEDD	0.00 DU
25-75 perc. range	-0.01 DU to 0.00 DU
10-90 perc. range	-0.03 DU to 0.02 DU
min-max range	-0.06 DU to 0.03 DU
OMI CF	24.00 %
Pandora DQ0	65.97 %

Tranquility

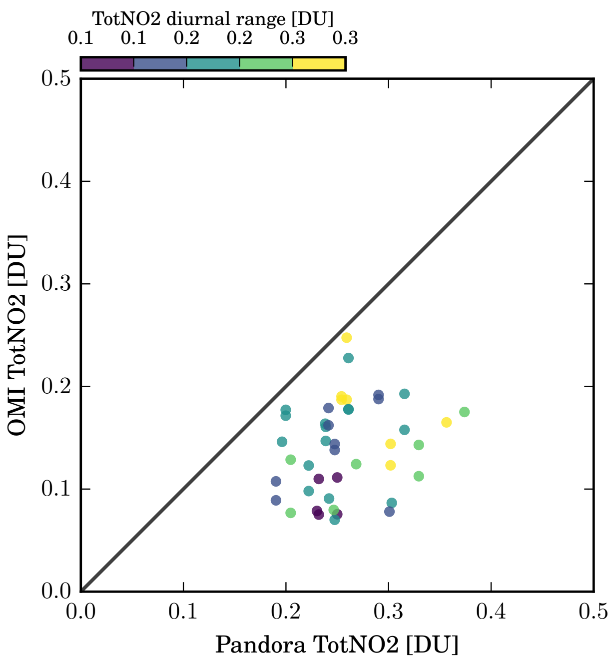

longitude, latitude	-120.3824, 36.6341
num data points	44
max Pan. (Pans.)	1 (26)
CC	0.22
RMS	0.04 DU
SLP	0.25 ± 0.13
mean	-0.12 DU
MEDD	-0.11 DU
25-75 perc. range	-0.16 DU to -0.08 DU
10-90 perc. range	-0.19 DU to -0.05 DU
min-max range	-0.22 DU to -0.01 DU
OMI CF	43.69 %
Pandora DQ0	52.60 %

UMBC

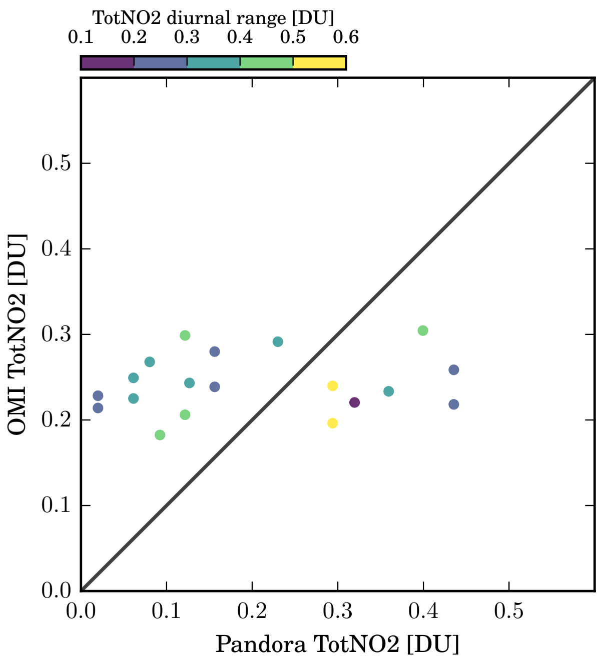

longitude, latitude	-76.709157, 39.2547
num data points	19
max Pan. (Pans.)	1 (2)
CC	0.15
RMS	0.04 DU
SLP	0.03 ± 0.09
mean	0.04 DU
MEDD	0.08 DU
25-75 perc. range	-0.10 DU to 0.17 DU
10-90 perc. range	-0.14 DU to 0.19 DU
min-max range	-0.22 DU to 0.21 DU
OMI CF	37.93 %
Pandora DQ0	68.79 %

Visalia

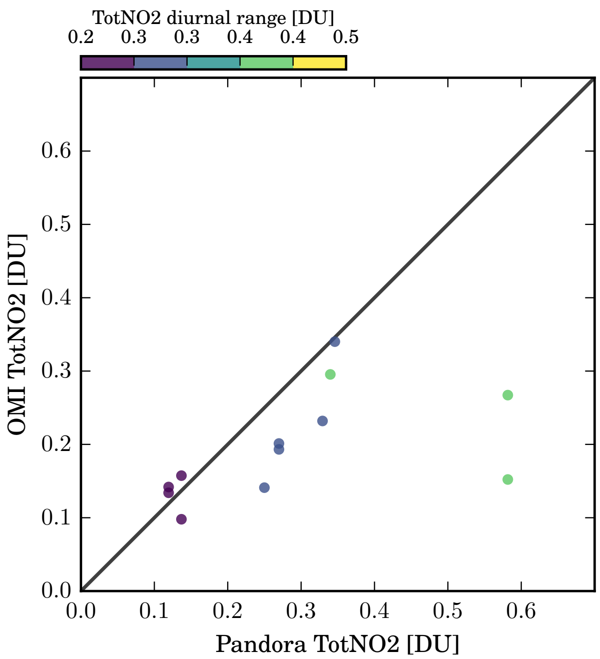

longitude, latitude	-119.3930, 36.3141
num data points	12
max Pan. (Pans.)	1 (18)
CC	0.50
RMS	0.06 DU
SLP	0.24 ± 0.09
mean	-0.09 DU
MEDD	-0.06 DU
25-75 perc. range	-0.10 DU to -0.00 DU
10-90 perc. range	-0.29 DU to 0.02 DU
min-max range	-0.43 DU to 0.02 DU
OMI CF	39.39 %
Pandora DQ0	78.80 %

4.2 Long Term Stability

In the following pages we present the long term stability of TotO3 on scenario E1 C0 G0 and E1 C0 G1 (marked with an asterisk) (section 4.2.1) and TotNO2 based on scenario E1 C1 G0 and E1 C1 G1 (marked with an asterisk) (section 4.2.2) by considering $\Delta\mathrm{TotGAS} = \mathrm{TotGAS}_{\mathrm{OMI}} - \mathrm{TotGAS}_{\mathrm{Pandora}}$ as a function of time.

The stability test is based on a Mann-Kendall test (MKT), capable of finding monotonic trends [7]. MKT is a non-parametric test, meaning no normal distribution of the data has to be assumed. Further, the trend does not have to be linear, only monotonically increasing or decreasing. In the following we avoid the terminus "trend" to not tempt to think in terms of O_3 or NO_2 trends. Instead we refer to "changes".

A ground-based instrument is considered stable, when MKT reveals no significant change assuming a 5 % significance level. Basically there can be three reasons for a change to be significant. First, the change is based on drifting data, e.g. due to aging effects of the optical parts in the ground instrument. Second, the change is triggered by a jump in the data. Usually this can be remedied by recalibration of the respective time period. Third, the change is based on a change in the satellite data. Here we would expect to see this in all ValSites simultaneously.

MKT is, however, not capable to deal with seasonal dependencies. This means to analyze ΔTotO3 we have to "remove" the seasonality first (as mentioned in section 2.1, seasonality is introduced by Pandora not considering variable TempO3). As a first order this can be done by assuming the seasonality to be sin shaped like

$$\Delta\mathrm{TotO3}_{\mathrm{seas}} = a \cdot \sin\left(2 \cdot \pi \cdot \omega \cdot t + b\right) + c, \tag{1}$$

where the frequency ω is assumed to be unity and t is the time in years. a, b and c are estimated from a least squares fit. Seasonality cleared data can be obtained by subtracting $\Delta\mathrm{TotO3}_{\mathrm{seas}}$ from the original data.

Although, as mentioned, the trend has not to be linear, we estimate only a linear change represented by its slope. A representative slope is calculated using the Theil-Senn approach, which is the median m of all slopes $(y_i - y_j)/(x_i - x_j)$ for all pairs of sample points (x_i, y_i). By this means, this method is very robust against outliers. A regression line can than be drawn by defining the intercept d the median over all $y_i - m \cdot x_i$.

We studiously avoided sophisticated time series analysis techniques for this report (an overview is given in e.g. *Cryer and Chan* [6]), since overall the time series are still to short to reliably fit multi-parameter models into the data.

Sections 4.2.1 and 4.2.2 show the stability figures for all long term stations with continuous time series longer than 1 year for TotO3 and TotNO2 respectively. The TotO3 figures are split in two panels. The top panel shows the original data with the fitted seasonal cycle in gray. The color coding further highlights the seasonality. The bottom panel shows the deseasonalized data plus the Theil-Senn regression as solid line for significant changes and as dashed line for not significant changes. The TotNO2 figures have one panel only, since we have not observed a seasonal cycle. Here the color coding depicts the diurnal NO_2 range within ± 4 hours of the OMI overpass time.

It can be seen that strong "outliers" in the TotNO2 difference between ground and satellite are always negative, i.e. the satellite strongly underestimates TotNO2 measured from the ground. In these situations the ground value is always a local TotNO2 hot spot. This is strongly reduced for the satellite, which averages over a large area on the ground.

Short Description	Long Description
longitude, latitude	ground geolocation of the Pandora unit (not its effective location)
num data points	number of data points passing the filter criteria
max Pan. (Pans.)	maximum number of Pandora units involved (Pandora ID(s) operating at this location)
change	can either be increasing, decreasing or not significant. Estimated based on MKT (explanation in the text).
slope of change	estimated from Theil-Senn approach, assuming a linear change (explanation also in the text) and given in DU per year.
significance level	probability of rejecting the null hypothesis given that it is true.
p values of significance test	probability of obtaining at least as extreme results given that the null hypothesis is true.
amplitude of seasonality	is the fitted parameter a from equation (1).

Table 10: Description on the additional information and statistics given for each ValSite.

4.2.1 Long Term Stability: TotO3

Boulder

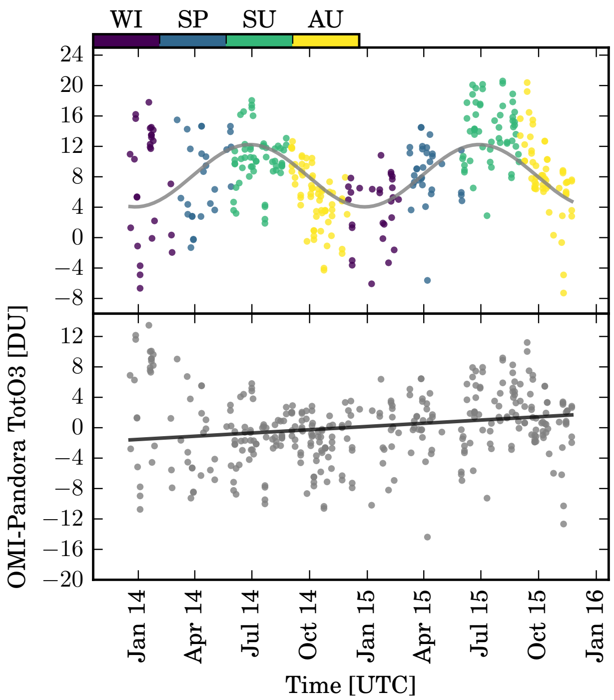

longitude, latitude	-105.26067, 39.99093
num data points	346
max Pan. (Pans.)	1 (34)
change	increasing
slope of change	1.70 $\frac{\mathrm{DU}}{\mathrm{a}}$
significance level	0.05
p value of significance test	0.00
amplitude of seasonality	4.10 DU

Boulder*

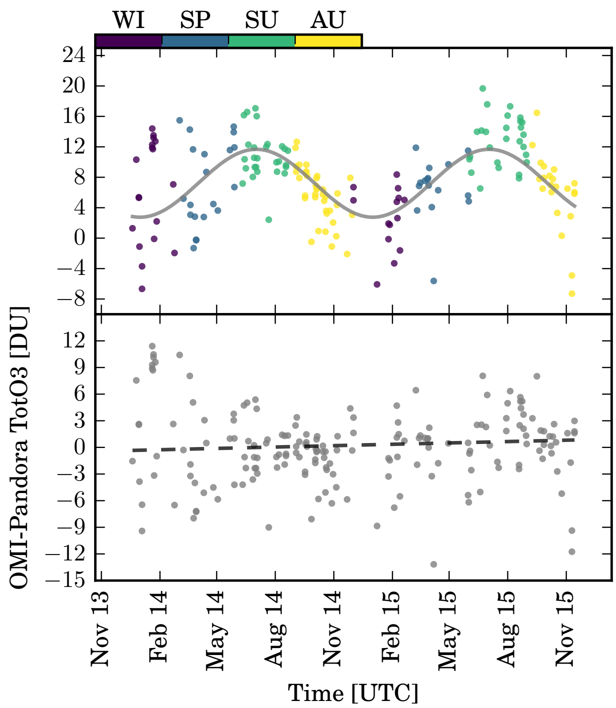

longitude, latitude	-105.26067, 39.99093
num data points	181
max Pan. (Pans.)	1 (34)
change	not significant
slope of change	0.62 $\frac{\text{DU}}{\text{a}}$
significance level	0.05
p value of significance test	0.31
amplitude of seasonality	4.47 DU

Busan

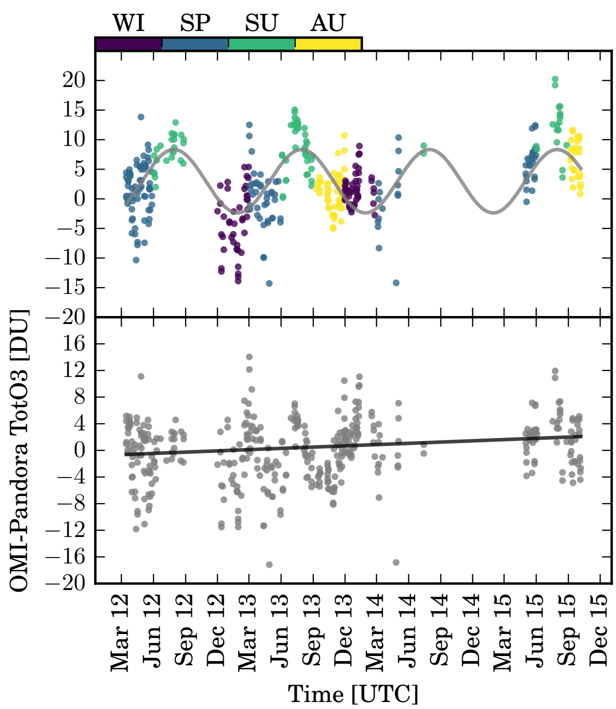

longitude, latitude	129.0825, 35.2353
num data points	394
max Pan. (Pans.)	2 (20, 36)
change	increasing
slope of change	0.76 $\frac{\text{DU}}{\text{a}}$
significance level	0.05
p value of significance test	0.00
amplitude of seasonality	5.36 DU

Busan*

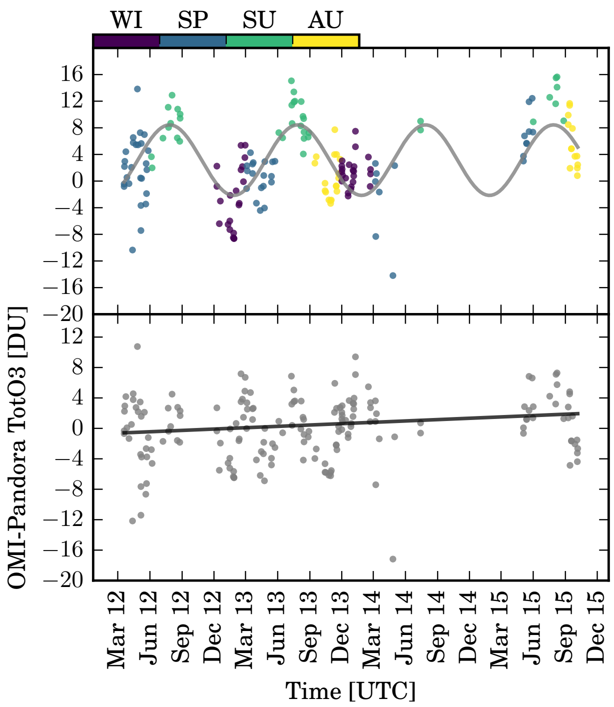

longitude, latitude	129.0825, 35.2353
num data points	173
max Pan. (Pans.)	2 (20, 36)
change	increasing
slope of change	0.71 $\frac{\text{DU}}{\text{a}}$
significance level	0.05
p value of significance test	0.02
amplitude of seasonality	5.30 DU

FourCornersNM

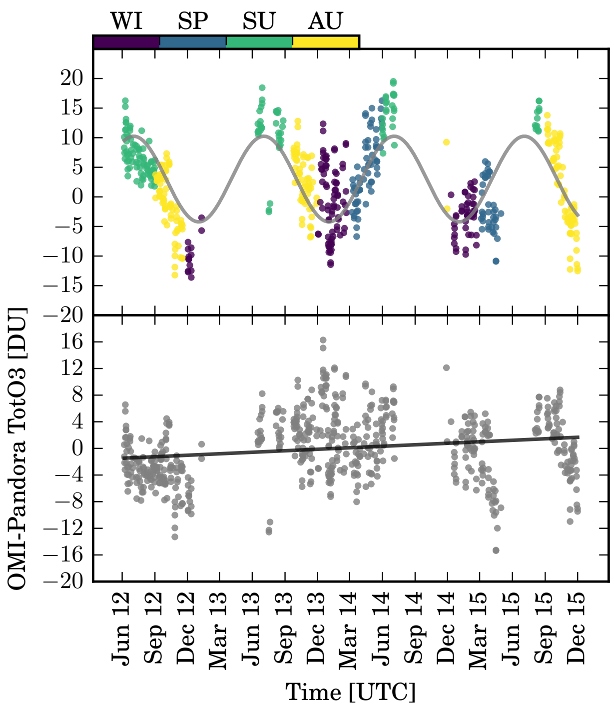

longitude, latitude	-108.480, 36.797
num data points	597
max Pan. (Pans.)	1 (23)
change	increasing
slope of change	0.90 $\frac{\text{DU}}{\text{a}}$
significance level	0.05
p value of significance test	0.00
amplitude of seasonality	7.24 DU

FourCornersNM*

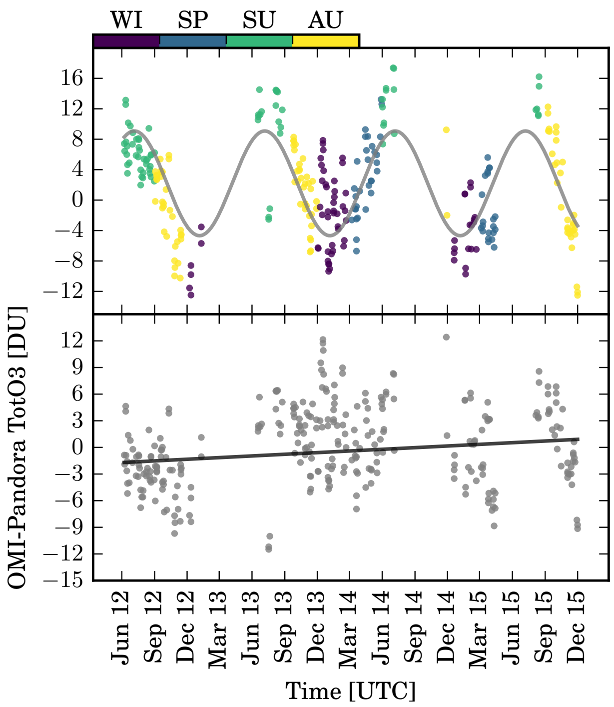

longitude, latitude	-108.480, 36.797
num data points	290
max Pan. (Pans.)	1 (23)
change	increasing
slope of change	0.75 $\frac{DU}{a}$
significance level	0.05
p value of significance test	0.00
amplitude of seasonality	6.88 DU

GSFC

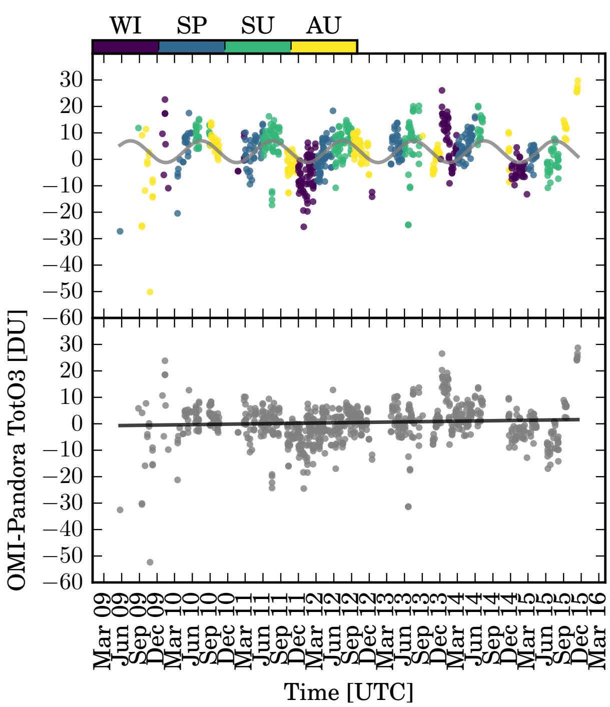

longitude, latitude	-76.8396, 38.9926
num data points	867
max Pan. (Pans.)	11 (18, 19, 21, 25, 26, 28, 2, 3, 43, 7, 9), not all considered!
change	increasing
slope of change	1.71 $\frac{DU}{a}$
significance level	0.05
p value of significance test	0.00
amplitude of seasonality	4.30 DU

GSFC*

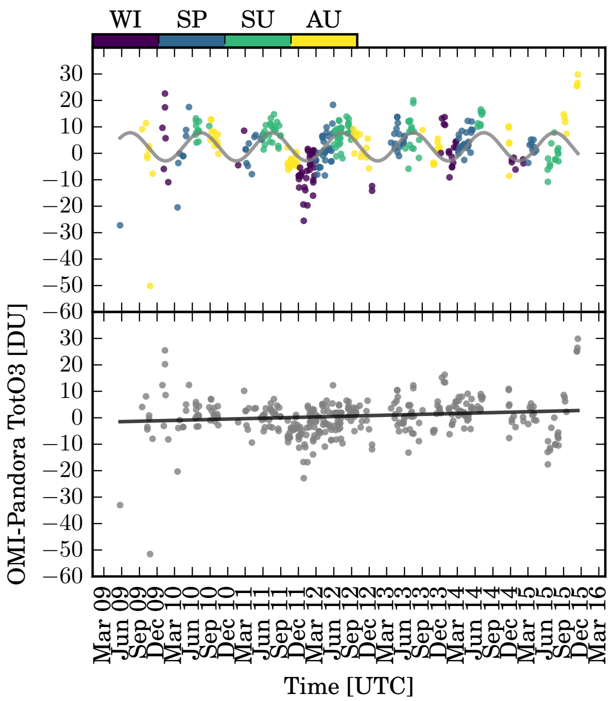

longitude, latitude	-76.8396, 38.9926
num data points	378
max Pan. (Pans.)	11 (18, 19, 21, 25, 26, 28, 2, 3, 43, 7, 9), not all considered!
change	increasing
slope of change	1.62 $\frac{DU}{a}$
significance level	0.05
p value of significance test	0.00
amplitude of seasonality	5.51 DU

IZO

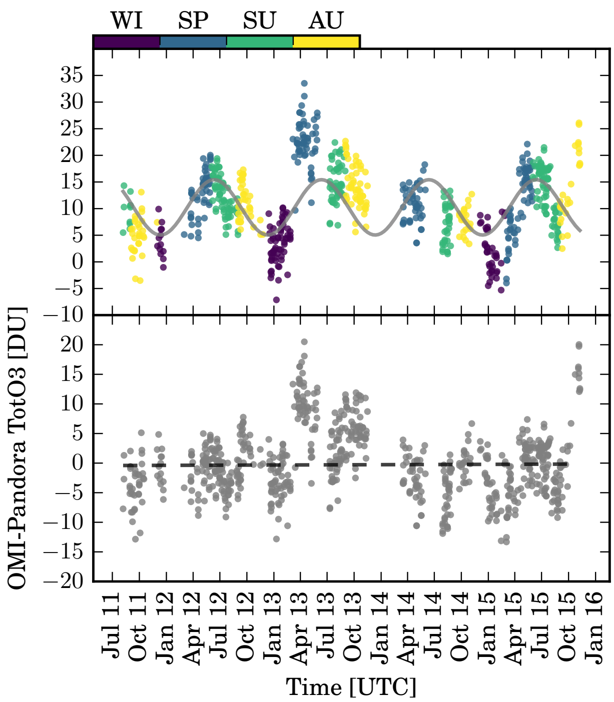

longitude, latitude	-16.4994, 28.309
num data points	744
max Pan. (Pans.)	1 (101)
change	not significant
slope of change	0.06 $\frac{DU}{a}$
significance level	0.05
p value of significance test	0.73
amplitude of seasonality	5.19 DU

IZO*

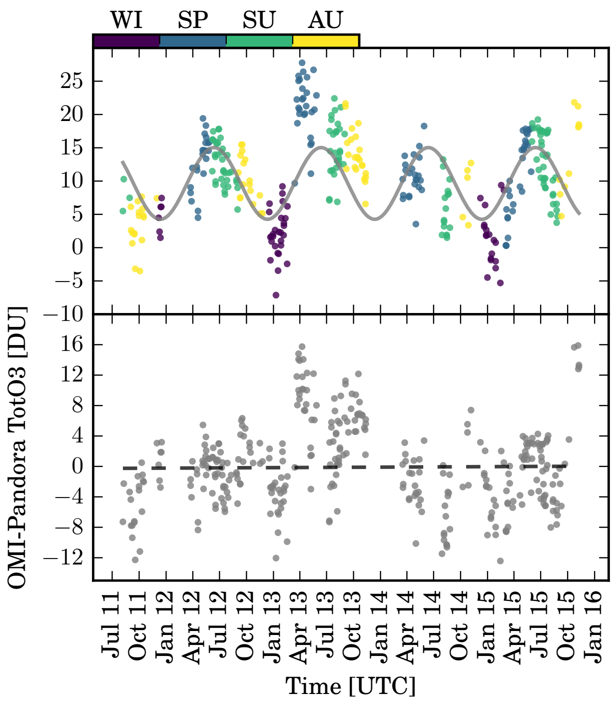

longitude, latitude	-16.4994, 28.309
num data points	348
max Pan. (Pans.)	1 (101)
change	not significant
slope of change	0.06 $\frac{\mathrm{DU}}{\mathrm{a}}$
significance level	0.05
p value of significance test	0.77
amplitude of seasonality	5.39 DU

Langley

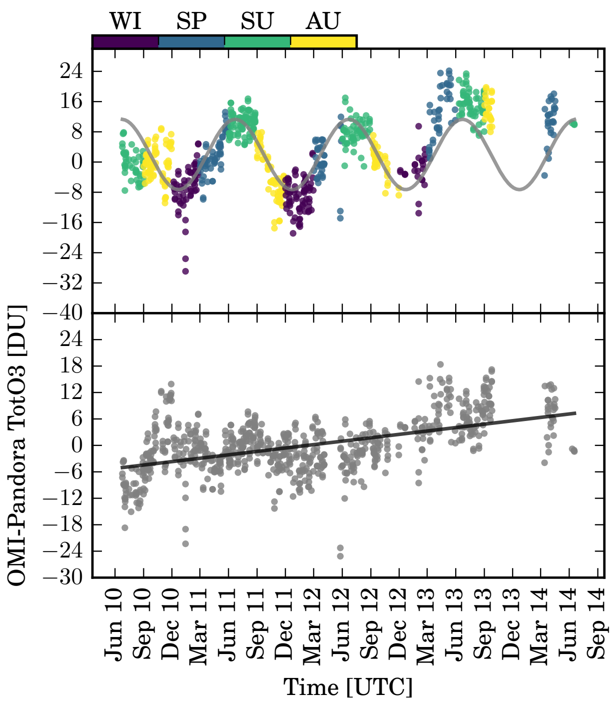

longitude, latitude	-76.3868, 37.1036
num data points	754
max Pan. (Pans.)	3 (37, 39, 6)
change	increasing
slope of change	3.09 $\frac{\mathrm{DU}}{\mathrm{a}}$
significance level	0.05
p value of significance test	0.00
amplitude of seasonality	9.30 DU

Langley*

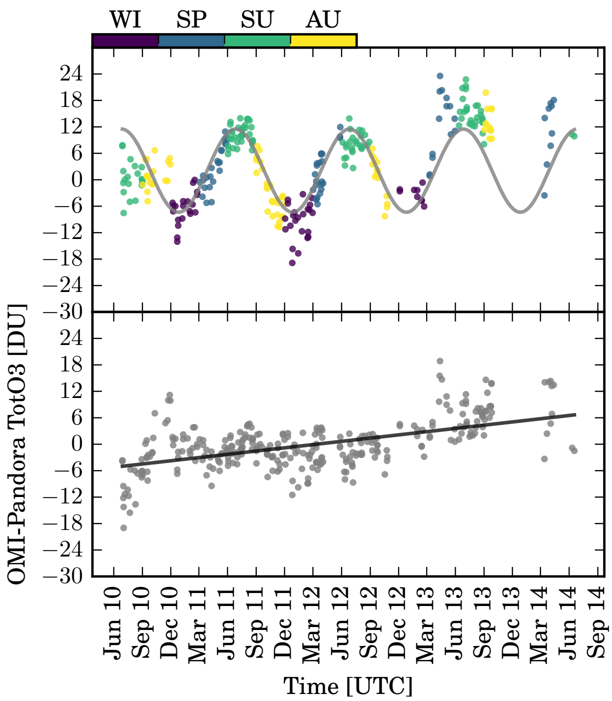

longitude, latitude	-76.3868, 37.1036
num data points	307
max Pan. (Pans.)	3 (37, 39, 6)
change	increasing
slope of change	2.94 $\frac{DU}{a}$
significance level	0.05
p value of significance test	0.00
amplitude of seasonality	9.43 DU

Seoul

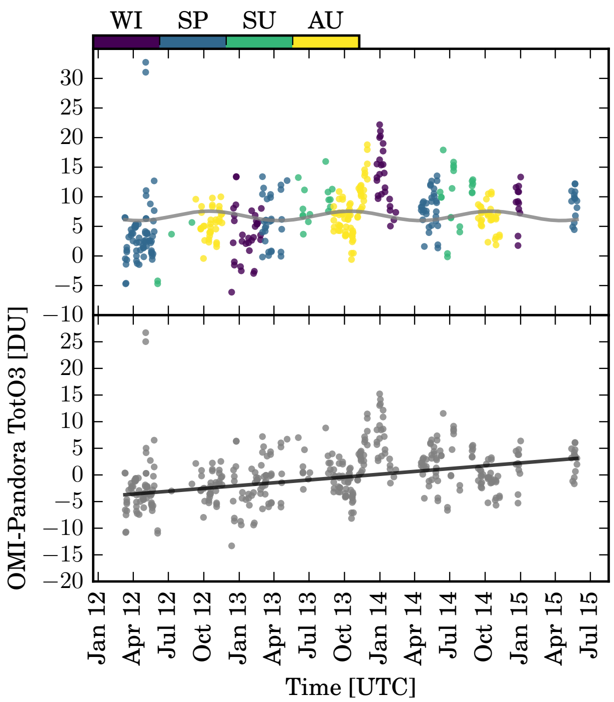

longitude, latitude	126.934, 37.5644
num data points	391
max Pan. (Pans.)	2 (17, 19)
change	increasing
slope of change	2.13 $\frac{DU}{a}$
significance level	0.05
p value of significance test	0.00
amplitude of seasonality	-0.80 DU

Seoul*

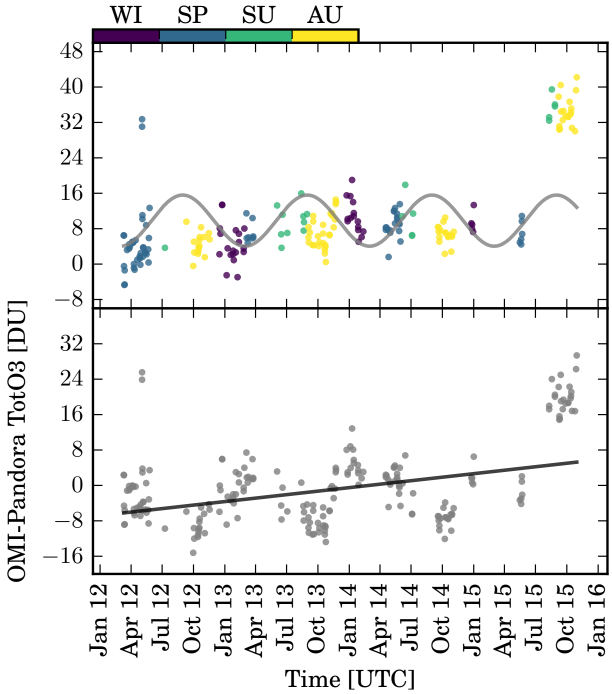

longitude, latitude	126.934, 37.5644
num data points	214
max Pan. (Pans.)	3 (17, 19, 29)
change	increasing
slope of change	3.16 $\frac{DU}{a}$
significance level	0.05
p value of significance test	0.00
amplitude of seasonality	-5.78 DU

4.2.2 Long Term Stability: TotNO2

Busan

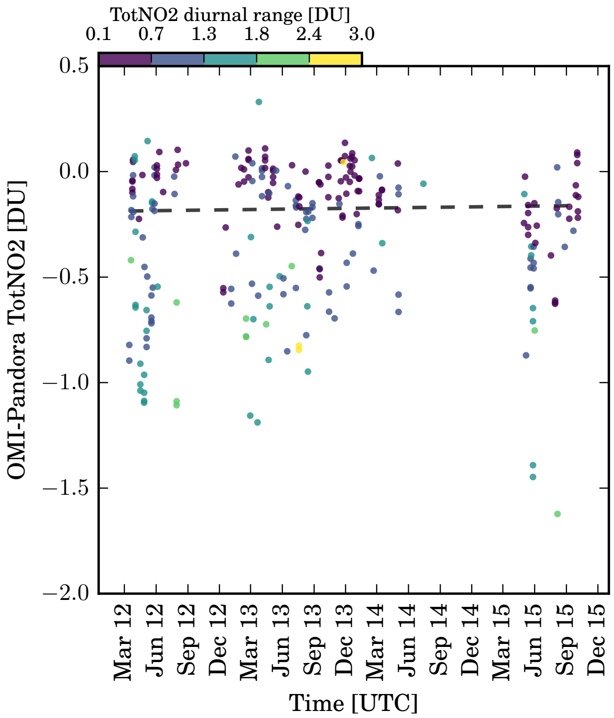

longitude, latitude	129.0825, 35.2353
num data points	249
max Pan. (Pans.)	2 (20, 36)
change	not significant
slope of change	0.01 $\frac{DU}{a}$
significance level	0.05
p value of significance test	0.70

Busan*

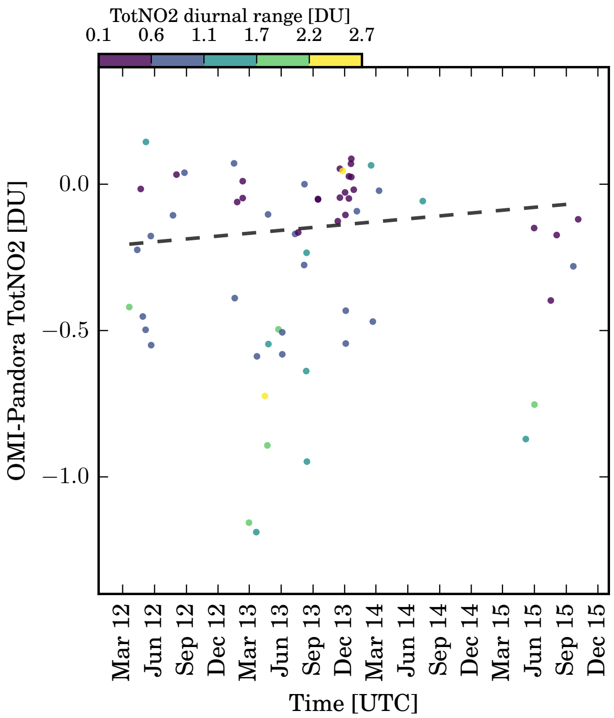

longitude, latitude	129.0825, 35.2353
num data points	61
max Pan. (Pans.)	2 (20, 36)
change	not significant
slope of change	0.04 $\frac{DU}{a}$
significance level	0.05
p value of significance test	0.39

FourCornersNM

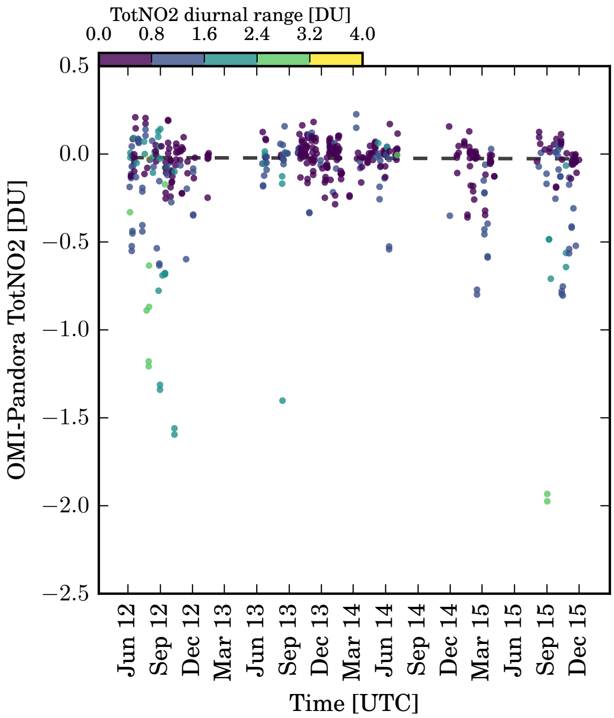

longitude, latitude	-108.480, 36.797
num data points	470
max Pan. (Pans.)	1 (23)
change	not significant
slope of change	-0.00 $\frac{DU}{a}$
significance level	0.05
p value of significance test	0.70

FourCornersNM*

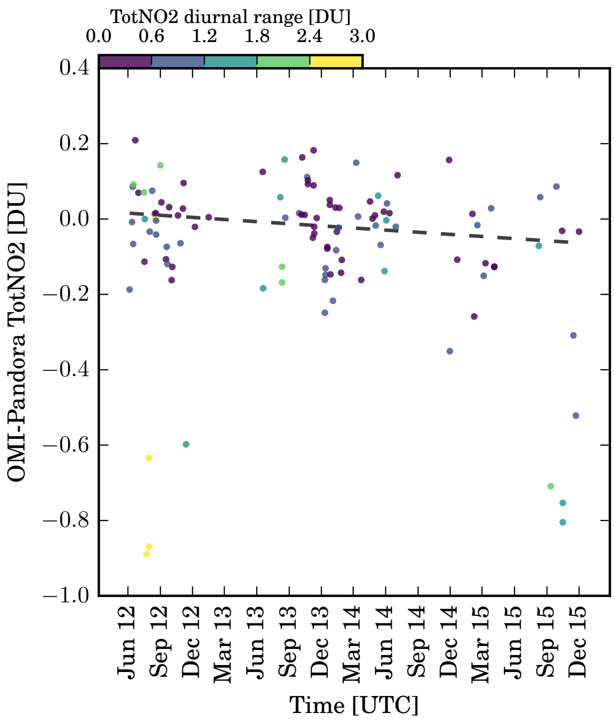

longitude, latitude	-108.480, 36.797
num data points	109
max Pan. (Pans.)	1 (23)
change	not significant
slope of change	-0.02 $\frac{DU}{a}$
significance level	0.05
p value of significance test	0.08

GSFC

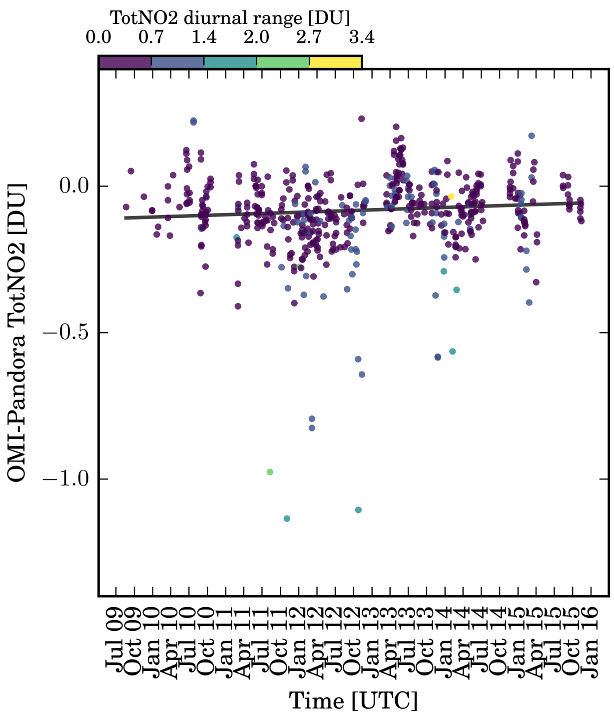

longitude, latitude	-76.8396, 38.9926
num data points	510
max Pan. (Pans.)	13 (16, 17, 18, 19, 24, 26, 27, 33, 36, 3, 41, 47, 7), not all considered!
change	increasing
slope of change	0.01 $\frac{DU}{a}$
significance level	0.05
p value of significance test	0.01

GSFC*

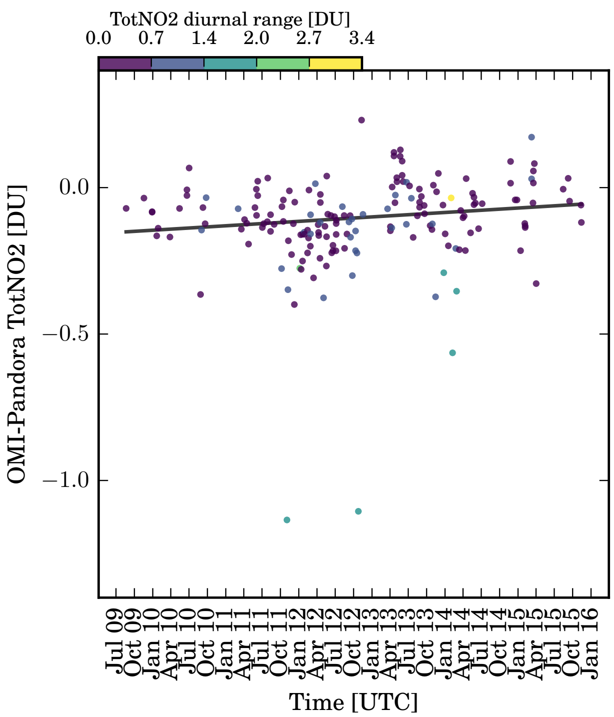

longitude, latitude	-76.8396, 38.9926
num data points	174
max Pan. (Pans.)	13 (16, 17, 18, 19, 24, 26, 27, 33, 36, 3, 41, 47, 7), not all considered!
change	increasing
slope of change	0.02 $\frac{DU}{a}$
significance level	0.05
p value of significance test	0.01

IZO

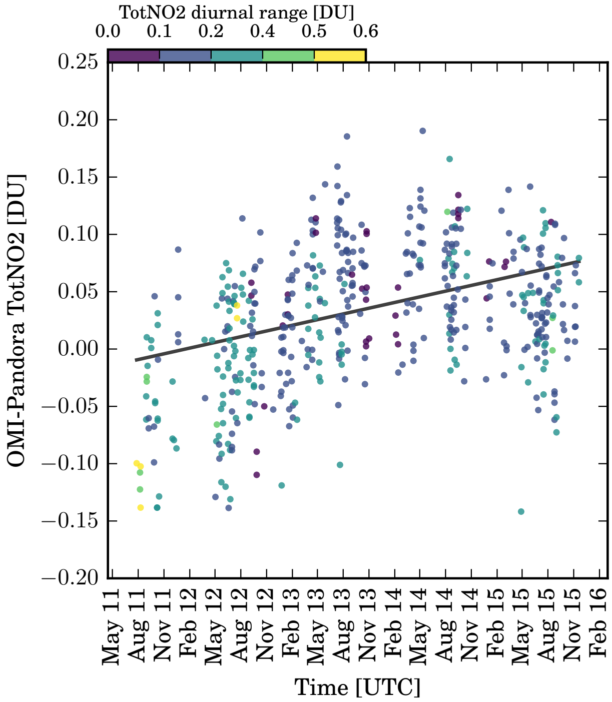

longitude, latitude	-16.4994, 28.309
num data points	497
max Pan. (Pans.)	1 (101)
change	increasing
slope of change	0.02 $\frac{DU}{a}$
significance level	0.05
p value of significance test	0.00

IZO*

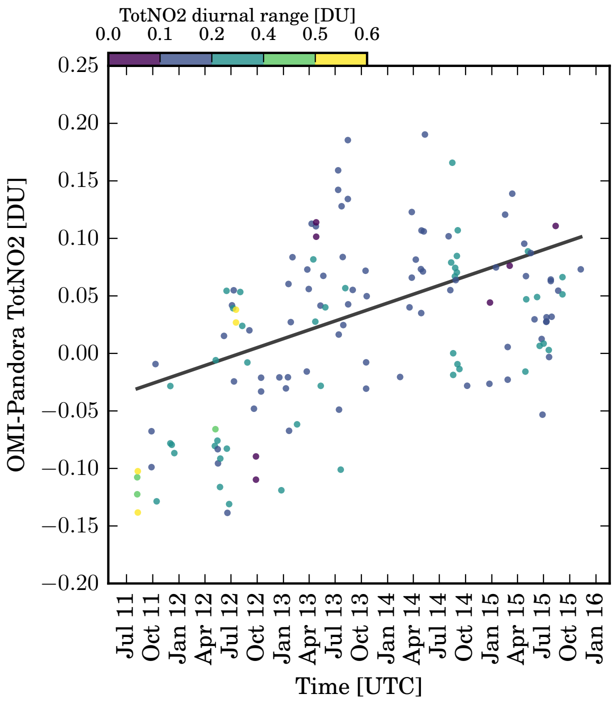

longitude, latitude	-16.4994, 28.309
num data points	138
max Pan. (Pans.)	1 (101)
change	increasing
slope of change	0.03 $\frac{DU}{a}$
significance level	0.05
p value of significance test	0.00

Langley

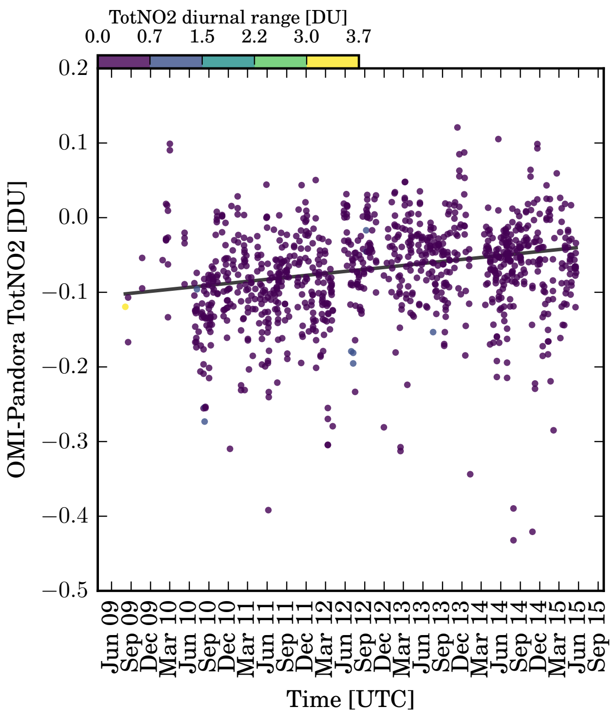

longitude, latitude	-76.3868, 37.1036
num data points	990
max Pan. (Pans.)	3 (37, 39, 6)
change	increasing
slope of change	0.01 $\frac{DU}{a}$
significance level	0.05
p value of significance test	0.00

Langley*

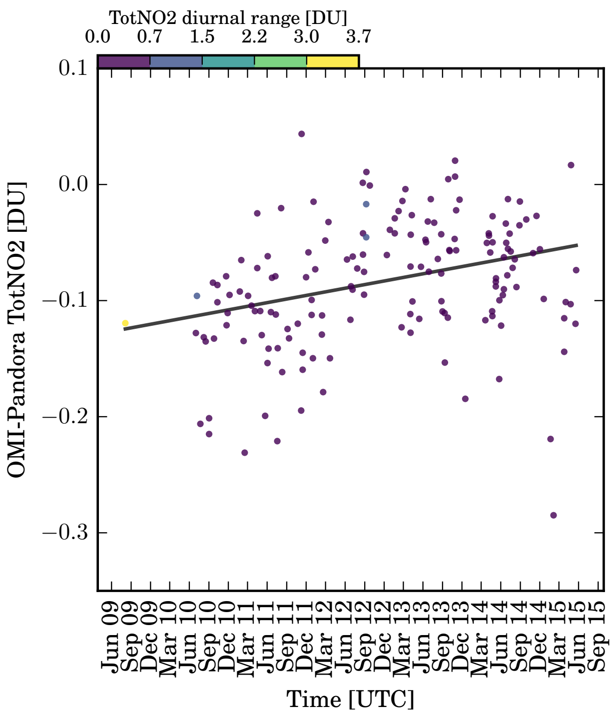

longitude, latitude	-76.3868, 37.1036
num data points	158
max Pan. (Pans.)	3 (37, 39, 6)
change	increasing
slope of change	0.01 $\frac{DU}{a}$
significance level	0.05
p value of significance test	0.00

Seoul

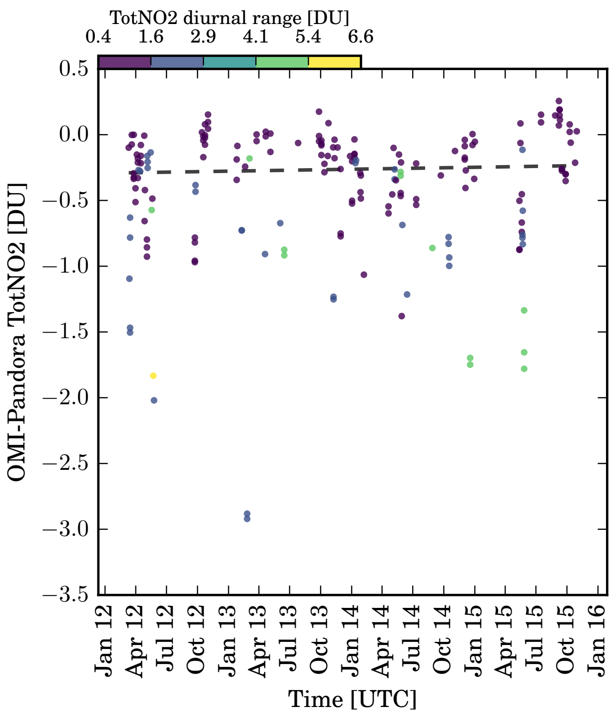

longitude, latitude	126.934, 37.5644
num data points	183
max Pan. (Pans.)	3 (17, 19, 29)
change	not significant
slope of change	0.01 $\frac{DU}{a}$
significance level	0.05
p value of significance test	0.54

Seoul*

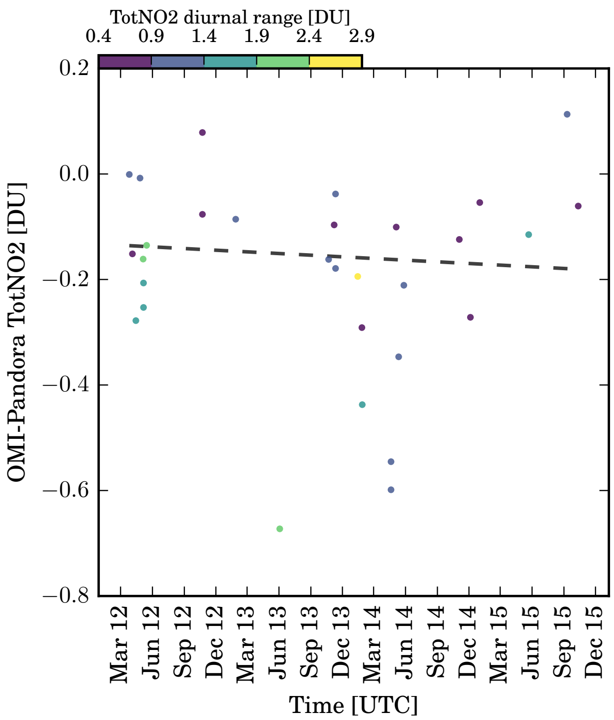

longitude, latitude	126.934, 37.5644
num data points	30
max Pan. (Pans.)	3 (17, 19, 29)
change	not significant
slope of change	-0.01 $\frac{DU}{a}$
significance level	0.05
p value of significance test	0.69